Development and Analysis of a bio-inspired tactile sensor

Entwicklung und Auswertung
eines taktilen Sensors nach biologischem Vorbild

eingereichte
MASTER-THESIS
von

Dipl.-Ing.(FH) Michael Strohmayr

Lehrstuhl für Medizintechnik
mit Schwerpunkt biokompatible Werkstoffe und Prozesstechnik
Technische Universität München

Prof. Dr. med. Dr.-Ing. habil. Erich Wintermantel

Betreuer:	Dr. Patrick van der Smagt, DLR Oberpfaffenhofen
	Dipl.-Ing. Erhard Krampe, Lehrstuhl für Medizintechnik TU München
Beginn:	01.10.2006
Abgabe:	30.04.2007

Everything should be made as simple as possible,
but not simpler.

Albert Einstein

To my parents

Acknowledgments

I want to thank all who have given time, assistance and patience so generously.

My special thanks goes to Univ. Prof. Dr. med. Dr.-Ing. habil. Erich Wintermantel, Ordinarius of the Department and Chair for Medical Engineering at TU München for the supervision of my thesis and for the opportunity to realize my ideas in the lab at Medtech.

Many thanks to Prof. Dr.-Ing. Gerd Hirzinger for the opportunity to accomplish this thesis at the Institute of Robotics and Mechatronics.

My deepest thanks to Dr. Patrick van der Smagt for your consistent trust and support on my way to this thesis.

Sincere thanks to Dipl.-Ing Erhard Krampe for the great supervision.

Thanks to Michael Stöver from ITEM GmbH - The Biotooling Company, for the SEM analysis.

Thanks to the mechanics and electronics teams at DLR for the support of the realization of the testbed.

Many thanks to the whole bionics team:

Thank you Holger for the great support with the many struggles concerning software and drivers. Thanks Nadine for the help regarding data evaluation and thanks Abhijit for the great help with the simulation.

Erklärung:

Ich versichere, dass ich die Arbeit selbständig verfasst und keine anderen als die angegebenen Hilfsmittel und Quellen verwendet habe.

München, den 30 April 2007

Michael Strohmayr

Contents

Abstract

Recent advances in robotics and mechatronics enable the design of robotic devices with an increasing market potential, but the introduction to man's everyday environment is still a long way to go. Following this path, currently an anthropomorphic Hand-Arm system is developed at DLR. Its desired small size and the mechatronic integration result in little designed space, preventing the application of "classical" sensor systems such as 6DoF load cells. Following the anthropomorphic design approach pursued in the design of the Hand-Arm system, a bio-inspired sensor setup is desired. Therefore this study aims at the development of a suitable sensor setup.

As a result of the literature research on dextrous manipulation, robotic hand-hardware and tactile sensors, piezoresistivity has been chosen as transduction principle.

For the derivation of the bio-inspired sensor setup the general requirements for valuable tactile sensors and the special requirements resulting form the anthropomorphic design approach are assessed. Hence a consistency matrix is applied to evaluate the requirements and to identify possible conflicts of goals between the requirements. To solve the conflicts of goals, the following bionic method is applied: First the the technical challenge is abstracted, secondly the equivalent functionality in human tactile perception is analyzed and the functional principle, i.e., nature's strategy is abstracted. Where applicable, the functional principle is propagated to a technical system. Following possible technical approaches are derived. Finally, the proposed approaches are assessed using a rating matrix. Thus the the most promising approaches are identified and combined to a bio-inspired sensor setup.

The proposed bio-inspired sensor setup consists of a "dermal" and a superficial sensor which are arranged in different layers of an artificial skin. While the "dermal" sensor is based on metal readout wires cast into a compliant piezoresisitive material, the superficial sensor is designed as a strain sensitive layer covering the "dermal" sensor. For the investigation of the proposed sensor principles a modu-

lar testbed has been designed and realized within this study. In its current version the testbed allows for automated testing of a testpatch under a pre-set force or indentation depth. For the evaluation of different sensor materials, testpatches have been manufactured and examined on the testbed and with a tensile testing machine. Based on the results of these tests, a particularly suitable piezoresistive silicone has been selected for the further development of the tactile sensor.

During the development of the "dermal" sensor the conducted tests revealed an optimization challenge concerning good piezoresistive behavior, high compliance, and good adhesion to the cast-in metal wires. As the means of optimization are in conflict the proposed principle for the "dermal" sensor could not be proven. Although the combination with metal wires is not applicable, the evaluated silicone shows very promising properties, being well-suited for the superficial sensor. Based on the results of the experiments for the "dermal" sensor, a new transduction principle for the superficial strain sensor was developed and patented. Applying the afore investigated materials, a prototype of the superficial sensor could be realized. In a first set of tests the sensor prototype showed an exponential correlation between the applied force and the measurable resistance, and could easily be linearized with a logarithmic amplifier.

As the sensor principle for the superficial strain sensor could be proven, continuative studies will deal with the redesign of the "dermal" sensor and the propagation of the bio-inspired sensor setup to the anthropomorphic fingertip.

1 Introduction

1.1 Artificial tactile sensing

Today, more and more robotic devices are developed to support humans. While in industrial production the application of robots has become common, the deployment of robotic devices in human's everyday environment is still a few steps away. Not only poor speech interfaces prevent the introduction of robots to human environment but also safety reasons and limitations in maneuverability. The unstructured human environment is particularly uneligible for robotic devices.

Although media shows professionally staged presentations of the latest humanoid robots the overwhelming majority of the presented robots still is relatively heavy-handed. The literal heavy-handedness of those robots is not only caused by the heavy mechanical components of the hands but also by the bulky sensory systems. Especially the manipulation of objects designed for human hands is critical for robotic manipulators. Today, the simple task of making and pouring a cup of tea is among the most sophisticated tasks robots are capable to conduct autonomously. The safe gripping of a delicate object like an egg, to this day is an almost unsurmountable challenge for robotic manipulators. One of the major drawbacks is the insufficient dexterity of the robotic manipulators. Robotic hands lack sophisticated hardware and, more serious, valuable tactile sensors. According to [63] a tactile sensor is defined as "a device or system that can measure a given property of an object or contact event through physical contact between the sensor and the object".

As the demand for valuable tactile sensors, not only for robotic grippers, increases, various approaches towards artificial tactile sensing are investigated by researchers all over the world.

1.2 Motivation, Fields of application

One of the main reasons for the research in artificial tactile sensing is the broad range of possible applications. As not only robotic manipulators are hindered by the lack of tactile information, additional fields of application are possible:

- Human-Robot-Interaction
- Prosthetics
- Service-, Space- and Medical-Robotics
- Automation

1.3 Goals

This study aims toward the development of a bio-inspired tactile sensor for DLR's new Hand-Arm system. Following an anthropomorphic design approach, the sensor setup has to be designed to be applicable on the 3D surfaces of the artificial fingertips. Thus the minimization of the sensor is of particular importance as the sensor has to fit to the limited designed space of the anthropomorphic hand. To complete the proprioceptive system of the robotic hand, the sensor has to be capable to collect data regarding the stretch of the skin at the finger joints. Moreover the sensor must be suitable for laboratory and off-the-lab application, necessitating a durable sensor surface, which is capable to stand long-term wear and tear. In addition a simple and low-cost producibility of large sensor surfaces would be desirable. Moreover possible additional requirements resulting form other fields of application should be considered. For the support of the future development and to allow for repeatable tests of tactile sensors a suitable testbed has to be designed and realized. An automated testing of the skin prototypes would be desirable. Subsequently, possible sensor materials have to be evaluated and the sensor concept has to be proved. If applicable, the developed bio-inspired sensor setup should be realized in form of a prototype.

1.4 Structure

Starting from a literature research of the state of the art in robotic hands and approaches towards artificial tactile sensing, the requirements for a valuable tactile sensor are derived, see 2. Applying the results of the literature research a suitable transduction principle is selected. Following possible transduction mechanisms in pressure sensitive materials are reviewed in chapter 3. For the development of a bio-inspired sensor setup for DLR's Hand-Arm system bionics is applied as a method to derive technical approaches from nature's strategy, see chapter 4. Therefore possible conflicts between the requirements are identified and assessed. Subsequently the most critical conflicts are selected and possible approaches for the avoidance of the conflicts of goals are derived.

Using the human mechano-perceptive system as a source of inspiration the underlying strategy is identified, and propagated to a technical approach where applicable. Following the solutions for the single conflicts of goals are combined to a bio-inspired sensor setup, that is capable to avoid the conflicts of goals by its design. For the support of the development of the artificial skin a special test facility is designed and realized, see chapter 5. Therefore suitable components are selected and combined to a testbed. Following the testbed is calibrated and programmed to enable automated testing. Subsequently, existing testpatches and alternative sensor materials are evaluated on the testbed in chapter 6. Based on the results of those tests a sensor material is selected for the further development of the tactile sensor. Based on the assessment of the manufactured testpaches a prototype of the sensor is realized and evaluated on the testbed in chapter 7. Finally the results of the study are discussed and future prospects are outlined, see chapter 8 and 9.

1.5 Restrictions of this study

This study will focus on the development and the analysis of the hardware of a bio-inspired tactile sensor and will not address approaches towards further data analysis.

2 State of the Art

2.1 Dexterous Manipulation

Many everyday tasks, e.g. buttoning a shirt, do require dexterous manipulation. A definition of dexterous robotic manipulation is given in the overview presented in [79]. The authors refer to dexterous manipulation as the grasping and manipulation of an object by multiple manipulators or robotic fingers. Dexterous manipulation is characterized as object-centered, i.e., the desired motion and the forces that should be exerted to the object are defined, and then the movements of the joints of the robotic manipulators are computed to conduct the desired movement of the object. According to [6], the three main functions of the human hand are to explore, to restrain and to manipulate objects. Manipulation with fingers as compared to manipulation with robotic arms is referred to as dexterous manipulation.

To achieve dexterous manipulation of an object with robotic fingers, two requirements have to be fulfilled: (1) The grasp has to be stable for object motion, i.e., after being disturbed, the object returns to the desired position and orientation, and (2) the grasp has to be stable for fingertip contact, i.e., the fingers must not lose contact nor slip over the surface of the object. These two requirements are fulfilled if the vector of the forces, which the robotic finger applies to the object does not leave the so-called friction cone.

Fingertip sensors should be capable of providing the information whether the force vector is inside or outside the friction cone [48]. Tactile information is not only useful in robotic manipulation but also in robotic exploration. [80] present an approach towards robotic object exploration, based on controlled rolling and sliding. The exploration method is based on the cooperation of two fingers equipped with different types of sensors. One of the fingers is equipped with a soft fingertip and a force sensor, on the other finger a tactile array sensor is mounted. From the combination of the acquired sensory data the object properties are calculated. For exploration tasks a

tactile sensor array should provide easy slipping, which does not affect the data recording trough stick-slip-vibrations. But the experiments were not only restricted by the insufficient tactile sensors but also by the mechanical limitations of the robotic fingers used [80], [78]. As the challenge of insufficient robotic hand hardware has been met by various institutions, today robotic hands exist, that allow research on dexterous manipulation. Most of these hands are laboratory prototypes, which are not commercially available. The following section presents some of the most advanced robotic hands of different laboratories.

2.2 Robotic Hands

2.2.1 Gifu Hand II

The Gifu Hand II, presented in figure 1, from the Department of Mechanical and Systems Engineering, Gifu University, Japan, is an anthropomorphic robot hand with four fingers and a thumb. The fingers have four joints with three degrees of freedom (DoF) each, the thumb is equipped with four joints enabling four DoF. The servomotors

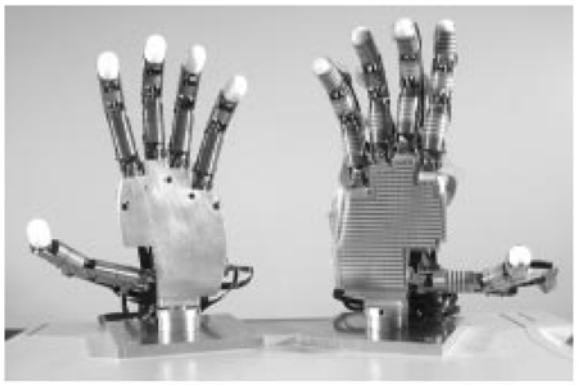

Figure 1: Gifu Hand II, taken from [53]

which are actuating fingers and thumb are integrated to the palm. According to [53] six-DoF force-torque sensors and a tactile sensor with 624 detection points can be attached to the fingertips. The maximum fingertip-force is 4.9N and the maximum output torque 3.46Nm. The total weight of the hand is approximately 1.4kg.

2.2.2 DLR Hand II

The DLR Hand II is based on four identical fingers, see figure 2. The fingers are equipped with four joints, with the last two joints mechanically coupled. As actuators

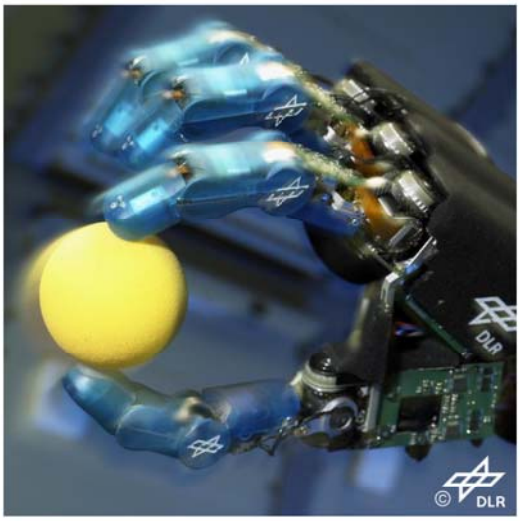

Figure 2: DLR Hand II, source: DLR

three brushless DC motors per finger are used. The motors are connected to harmonic drive gears via toothbelts. The base joints are formed by differential bevel gears. This setup allows to use the torque of both motors for flexion and extension, and allows, in spite of using very small motors, fingertip forces up to 30N. The DLR Hand II provides two possible hand configurations, power grasp and precision grasp. In power grasp configuration the three fingers are positioned parallel to each other with the thumb opponing the first finger.

For dexterous manipulation a precision grasp configuration is available. For this configuration the third finger and the thumb are rotated inwards forming a bowl-shaped palm. The DLR Hand II is approximately 1.3 times the size of a male human's hand and weighs 1.8kg. To increase the dexterity approximately 100 sensors are included. Those sensors provide information about motor-positions, joint-angles and joint-torques as well as temperature. In addition the fingertips are equipped with custom-made six-DoF force-torque sensors based on strain gauges [10].

2.2.3 DLR/HIT Hand

Figure 3 shows the DLR/HIT Hand, which it is the commercialized version of DLR Hand II. Its size is approximately 1.3 times of a human male hand. The hand is

Figure 3: DLR/HIT Hand, source: DLR

modularly built. Thus the fingers and the thumb can be interchanged. Each finger has four joints, with the last two joints mechanically coupled. The maximum fingertip-force is 8N. The DLR/HIT Hand is equipped with multiple sensors. Each finger possesses three joint position, joint torque and motor position sensors, one force-torque and two temperature sensors [26].

2.2.4 Fluidhand Karlsruhe

At Forschungszentrum Karlsruhe a lightweight prosthetic robotic hand is developed [93]. In contrast to most other robotic hands this hand is not actuated by motors and gears but via a hydraulic system, see figure 4. If the flexible fluid actuators are filled, the fingers are flexed. The extension of the fingers is powered by the restoring force of

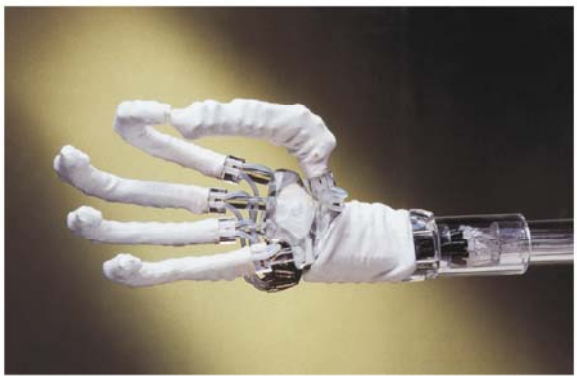

Figure 4: Fluidhand Karlsruhe, source: Forschungszentrum Karlsruhe

the flexible fluid actuators. The maximum fingertip force reaches up to 6.6N, the total weight without power supply is around 800g.

2.2.5 Robonaut Hand

For space applications NASA developed the Robonaut Hand [66]. The hand, shown in figure 5, was designed for remotely controlled teleoperation in space. The hand is

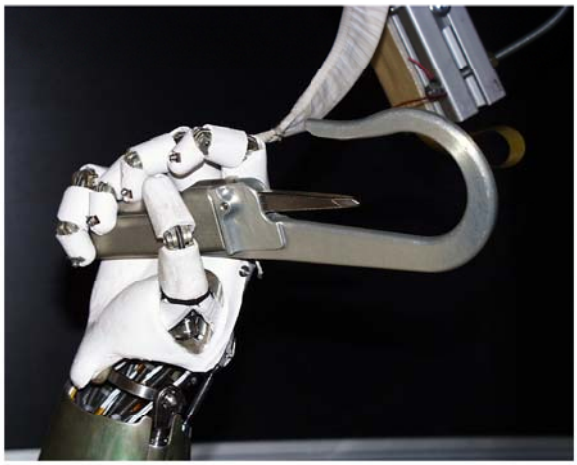

Figure 5: Robonaut Hand, source: NASA

powered by twelve brushless DC motors that actuate the tendon-driven fingers and are integrated into the forearm. The sensory system consists of joint- and motor-position sensors. The size of the hand is approximately the size of a human's hand.

2.2.6 Dextra Hand

At Rutgers University (USA) the so-called Dextra Hand is developed [14]. It provides five fingers, which are moved via tendons that are actuated by electric motors. As

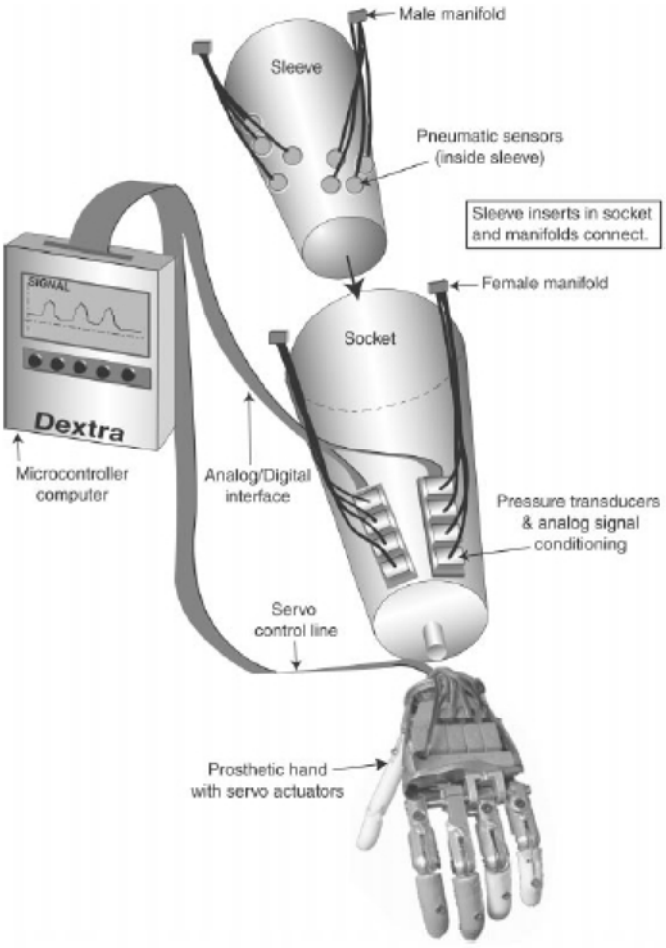

Figure 6: Dextra Hand, taken from [14]

shown in figure 6, the Dextra Hand is integrated into a prosthetic system that includes a sleeve with pneumatic sensors, a socket with pressure transducers with analog signal conditioning as well as a microcontroller computer. The pneumatic sensors in the sleeve do measures 3D forces produced by the muscles in the socket. This data is conditioned and sent to the microcontroller computer. Here the data is digitalized and commands for the prosthetic hand are calculated.

2.2.7 Discussion

Most of the presented hands do suffer either from the lack of sophisticated robotic hardware or from insufficient controllability. Even DLR's Hand II, which is capable of catching a flying ball and to unscrew a closed container, up to today, is not capable of fine dexterous manipulation as buttoning a shirt or lighting a match. One of the main reasons is, that dexterous manipulation and haptic exploration with robotic hands does not only require sophisticated robotic hand's hardware, but also a variety of information of the contact conditions between the robotic finger and the gripped object.

In humans the required information is derived from the combination of the two most prominent sensory systems, vision and tactile perception. Especially for the manipulation of small objects tactile information is crucial, e.g., it is quite easy for an adult to button a shirt with closed eyes, but almost impossible to close the buttons under sight, with the fingertips anesthetized. As the transition of the human's vision system to technical systems is quite advanced, the limiting factor for dexterous manipulation with robotic hands is the lack of sufficient tactile data. Following a small selection of the various approaches towards technical tactile sensing is presented.

2.3 Overview of technical approaches to tactile sensing

Technical tactile sensors are mainly divided into two groups, intrinsic and extrinsic sensing devices. Intrinsic devices do measure the applied forces in the skeleton of a robotic device, for example torque sensors in the joints of a robotic hand. In contrary extrinsic sensing devices measure the forces applied to or near the surface of the robot or end-effector. The following review papers deal with artificial tactile sensing, and are presented in chronological order of appearance:

The state of the art in robotic tactile sensing up to 1992 is reviewed in [37]. From an overview of human tactile sensing, lessons for robotic manipulation are drawn. Further-

more a classification for tactile sensors is presented. According to this paper, tactile sensing devices for a robotic hand can be divided into five areas: tactile array sensors, fingertip force-torque sensors (FTS), finger joint angle sensors, actuator effort sensors, and dynamic tactile sensors. Tactile array sensors are distributed devices that mimic the sensory system of human skin. They are used to collect pressure distribution over the surface of the sensor and to determine the local shape of the contacted object. Fingertip FTS are mostly multi-DoF load cells that are integrated into the mechanical structure of the robotic device.

FTS serve to measure forces and torques applied, e.g., to the robotic finger by the contacted object. FTS are unable to determine the exact contact location but serve for the calculation of the force vectors and torques applied to the whole fingertip. With the finger joint angle sensors and the kinematic model of the robot finger it is possible to determine the orientation and thereby the current position of the fingertip. This is important to identify the contact location and thus the size of an object, gripped between two fingers. If actuator effort sensors are attached to the actuators of the robot finger or hand, it is possible to quantify the motor torques and to calculate the contact forces using the kinematic model. Dynamic tactile sensors serve to detect vibration, slippage and stress changes within the sensors material. This sensor type is important for dexterous manipulation because by the detection of changes of the contact conditions it is possible to create reaction strategies, e.g., slippage detection with subsequent calculation of the readjustment of the desired contact forces. As a conclusion the experimental application of tactile sensors in manipulation is analyzed and future research directions are outlined.

[63] gives a detailed state-of-the-art survey of tactile sensing for mechatronics. The development of tactile sensing devices is compared with that of the technical analogies of the other human sensing capabilities. The following difficulties in drawing on the human tactile sense are outlined. In contrast to the other human senses, tactile sensing is not based on a discretely localized sensory organ but is formed by distributed sensor cells, which is much more complex to simulate than discrete sensing organs as the ear

or the eye. The authors state, that the transduction processes in tactile sensing are not very well understood, and argument that therefore the search of technical analogies is quite difficult. It is still unclear which are the most suitable physical quantities to be measured by a technical tactile sensing device, to generate meaningful data. They draw the conclusion, that the research interest has shifted, from the development of new transduction technologies towards the engineering of the sensors. Where a predominance of approaches using resistivity and capacity as transduction method is seen. Therein piezo-resistivity, applied in sensitive arrays, plays the most important role.

[79] survey the research in dexterous manipulation and give an overview of the ongoing research. They present accomplishments and define important areas for continuative work. Besides software and algorithms many future work is to be done concerning hardware. Fields of work are to be found in hand design, actuation, miniaturization and sensing. According to [79], sensors are essential for dexterous manipulation. Within the sensors, tactile sensors are the primary source of information. The following major problems of extrinsic tactile sensors are identified: sensitivity to noise, delicacy, poor resolution, slow data acquisition and processing, difficulties in manufacturing, large numbers of wires, and cost.

[62] gives a report of the state-of-the-art in tactile sensing and shows new directions and challenges. The authors see a major change of direction in tactile sensing. As the former vision, that tactile sensing would induce a major change in industrial robotics and automation has not proven true, the focus of research and possible applications has changed. In this paper new application areas and promising developments are defined. According to [62] new fields of application and thus new challenges for tactile sensing are most likely to be found in unstructured areas as health care, medicine, surgery, service robotics and in the automation of the handling of natural products. The application of technical tactile sensors in medicine is presented in [71]. The article reviews the possible application of artificial tactile sensing systems in minimal access surgery (MAS). While MAS offers many benefits for the patient, coverage of the whole area is at distant prospect, because it is associated with some additional challenges

for the surgeon. Of these new challenges the loss of the "sense of feel" is the severest limitation. [71] conclude, that artificial tactile sensing systems would be of great benefit to the MAS-surgeon, but the available systems do no reach, by far, the demands of the surgeons. [101] overview tactile sensing for intelligent robot manipulation. Some examples for technical tactile sensors are presented and the most common approaches with their particular advantages and disadvantages are discussed. While the authors state, that in the past progress in technical tactile sensing has been quite slow, they see very good conditions for the growth of the research field in near future.

These reviews of the state of the art in artificial tactile sensing lead to the conclusion, that the expected fields of application have shifted away from the well structured and controllable environment of industrial automation towards unstructured fields as the everyday environment of humans, space or the human body. To achieve major advances, still many work has to be done, especially in the field of reliable artificial tactile sensors. In the following, different transduction principles that are used in today's tactile sensors are presented. In this study the overview of the different transduction methods will be given according to the classification of [63]. Research has been conducted for transduction methods based on the measurement of the following quantities and effects:

- Resistance and Conductance
- Capacitance
- Piezoelectric and Pyroelectric
- Magnetic
- Optical
- Ultrasonic
- Strain gauges.

2.4 Transduction effects and sensor examples

This chapter will give a brief overview of the most common transduction effects, and shows examples of current approaches towards artificial tactile sensing.

2.4.1 Resistance and Conductance

Sensors using the measurement of resistance and conductance for data acquisition are generally based on the so-called piezoresistive effect, which can be observed in metals and semiconductors. The piezoresistive effect can be observed in materials that change their electrical resistance depending on mechanical stress applied to the material. For the application in sensors, typically silicone rubber compounds and polymers are used. As elastic materials are normally insulators, they have to be specially treated to achieve a semiconducting pressure-sensitive behavior. This is achieved via doping the insulating elastomeric matrix with conductive filler particles. There is a large variety of filler particles which are used: Most common are graphite [54] and carbon black [40], and less commonly used, carbon fibers, coated glass spheres, gold, nickel, copper and aluminium particles [88].

The transduction principle is the same for all particle-filled elastomers. Depending on the content of particles, conductive pathways between the surfaces of the elastic matrix are formed. A resistance can be measured. If the content of conductive particles is increased, more conductive pathways can be formed, the measurable resistance decreases. For the application as pressure sensor the filler content v_c of the elastomeric matrix is tuned near the so-called percolation threshold. Around the percolation threshold the resistance of the semiconducting matrix is highly dependent of the particle content, see figure 7. If the elastic matrix is pressurized with a load, the material shuns from the load. Thus the local content of conductive particles between the contact location and a reference electrode increases. An increasing number of conductive pathways can be formed. This leads to a measurable decrease of the resistance, [109]. An other sensing principle, based on the change in resistance is presented in [114]. For this approach

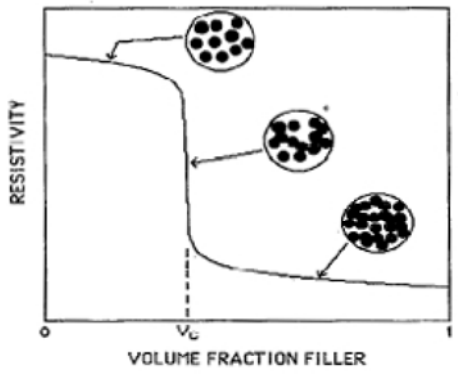

Figure 7: Percolation area, taken from [88]

not a change of resistance within a semiconducting elastomeric matrix is used, but the change of the resistance induced by the variant contact surface of hemispheric nibs. If the elastic nibs are mechanically loaded they deform. Thus the contact surface increases and the transition resistance decreases.

Various other approaches are based on the piezoresistive effect of semiconducting materials but use other setups, [53, 54, 76].

2.4.2 Capacitance

There are two transduction principles which are used for tactile sensing based on the change of capacitance. Both are based on changes in the electric field between the two electrodes of a capacitor. The following capacitance equation shows the context:

$$C = \varepsilon_0 \cdot \varepsilon_R \cdot \frac{A}{d} \tag{1}$$

where C is the ideal capacitance, ε_0 is the permittivity of free space, ε_R is the relative dielectric constant of the dielectric medium separating the capacitor's electrodes, A is the surface of the capacitor, and d is the distance between the two electrodes of a capacitor. The approach used in commercially available proximity sensors uses the disturbance of the field lines induced by objects that enter the electric field of the capacitor. A similar approach is used in [56], see figure 8. The approach used in tactile sensors is mostly based on mechanically induced altering of the distance between the

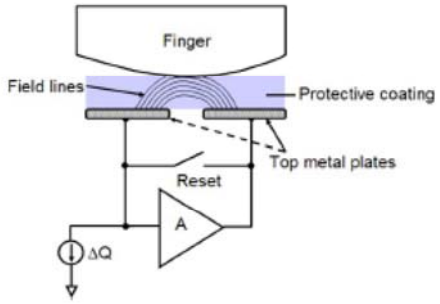

Figure 8: Capacitive pressure sensor, taken from [56]

two electrodes or the altering of the surface of the electrodes forming the capacitor, [86]. The changes of the capacitance are measurable. This enables a simple setup for a tactile sensor. The electrodes of the capacitor are separated by an elastic dielectric material. If an external mechanical load compresses the capacitor the distance d is reduced and the capacitance increases.

2.4.3 Piezoelectric and Pyroelectric

Sensors based on the so-called piezoelectric effect use materials that generate an electric potential on the surface if they are compressed. There are various approaches towards tactile sensing using the piezoelectric effect. As shown in figure 9, [57] use a piezoelectric polyvinylidene fluoride (PVDF) polymer in a parallel plate capacitor setup. If the two plates of the capacitor are mechanically compressed, an electric potential

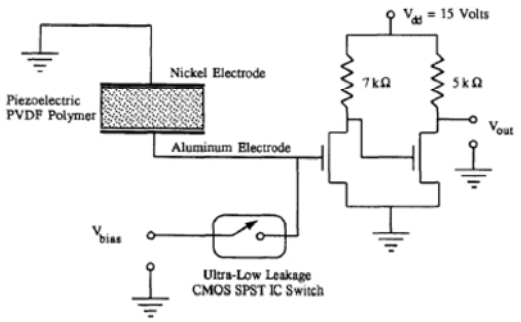

Figure 9: Piezoelectric pressure sensor, taken from [57]

is generated at the electrodes of the capacitor. This potential is used with a *in situ* amplifier to minimize signal losses. In the approach of [100], PVDF films are used in a stand alone setup and are therefore capable to sense the strain velocity. PVDF films also can serve as shockwave sensors [4] or in multimodal sensor setups to provide additional information like thermal conductance properties of the grasped object [87]. The transduction effect that can be used for thermal sensing is the so-called pyroelectric effect. Pyroelectric materials generate an electric potential if they are heated or cooled. Sensors based on pyroelectricity are specially suitable for temperature measurement. As these sensors offer only indirect tactile information, they will not be surveyed in detail within this study.

2.4.4 Magnetic and Magnetoelectric

There are different tactile sensing principles that are based on magnetism. The most common sensing principle is the measurement of the change of the magnetic field induced by an object entering or moving through the magnetic field. [13] presents a sensing principle for highly compliant objects. The effect used is the deformation of the sensor's compliant membrane by the object. A magnetic field induced from a rigid sensor array is disturbed by the deforming outer membrane, the changes in the magnetic field are measured. [33] present an approach that combines an electromagnetically actuated tactile sensing principle which is combined with a diaphragm with piezoresistive sensing elements.

2.4.5 Optical

Recently more and more researchers follow the line of optical tactile sensing. There is a large variety of different approaches mostly based on optical devices as optical waveguides or image processing systems. In the following exemplarily approaches using the most common transduction effects are presented. [48] present a fingertip-shaped tactile sensor based on an optical waveguide. The sensor is able to detect the contact

location and the surface normal of the grasped object. To enable an instant response to a contact force the waveguide is placed right below the outer membrane of the sensor. [23] propose a vision-based sensor. On the outer membrane of the transparent compliant fingertip a pattern of dark dots is painted. At the basis of the fingertip a charge coupled device (CCD) is mounted. The image of the undeformed geometrically known pattern is stored and afterwards compared to the image of the distorted pattern on the deformed membrane. From the analysis of the difference between the original image and the image of the deformed membrane the applied force and its direction is computed. A similar approach is followed in [49], see figure 10. Other than [23]

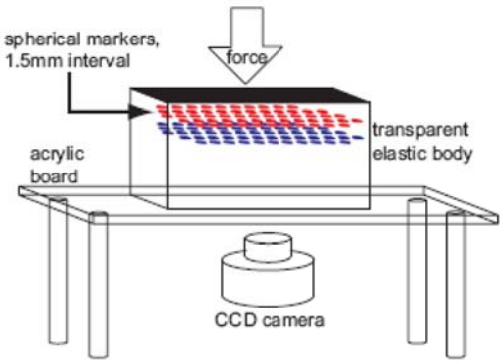

Figure 10: Vision based pressure sensor, taken from [49]

the pattern is not brought up to the surface but is included as colored markers in two layers in the transparent elastic body of the sensor. This setup enables to derive a larger variety of force vectors and therefore permits the finer discrimination of different charges, e.g. torques.

[34] follow an approach that is based on a partly translucent material that changes its optical damping properties according to the pressure applied. [115] present an optical sensor that uses wireless optical sensing chips which are attached to the outer membrane of the finger-shaped sensor. The sensor chips do analyze the signal of a light emitting diode (LED), mounted on the inner side of the nail. The information is digitalized and is sent back to a receiver via radio frequency.

2.4.6 Ultrasonic

Ultrasonic tactile sensors are mostly based on the analysis of an ultrasonic signal which is send from a transmitter through a compliant material to a receiver. If the material is deformed by external forces the ultrasonic signal changes. From the analysis of the signal that reaches the receiver the causative force can be count back. [2] propose a tactile sensor setup which is able to detect forces in all six DoFs. This approach uses PVDF films as ultrasonic transmitters and receivers, which are mounted to the basis and the top surface of a silicone rubber layer, see figure 11. According to the

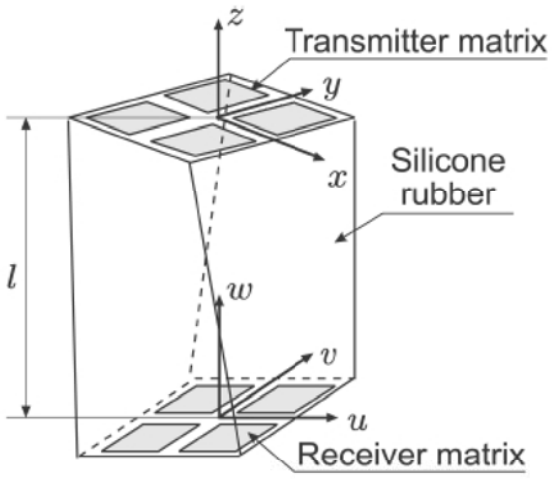

Figure 11: Ultrasonic pressure sensor, taken from [2]

deformation of the silicone rubber layer the ultrasonic signal reaching the receiver matrix alters. If the emitting mode is modulated the different force directions and torques can be calculated. [94] pursue an approach that uses air-filled cavities within an elastic material. The cavity is connected to an ultrasonic transmitter and receiver via two fine, air-filled ultrasound paths. Depending on the deformation of the cavity the backscattered ultrasonic signal changes. From these changes different load cases can be detected.

2.4.7 Strain gauges

Strain gauges are devices which transduce mechanical deformation to a change of electrical resistivity. Therefore a fine metallic structure is superimposed to a flexible carrier foil. The foil is attached to the component that should be analyzed. If the component

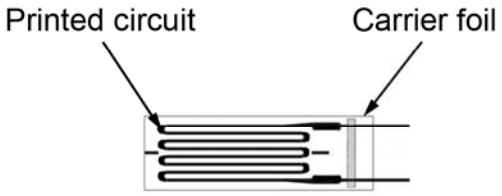

Figure 12: Strain gauge

is deformed, the foil and therefore the metallic structure is deformed. The elongation of the metallic structure causes a measurable change of its electric resistivity. As strain gauges are particularly sensitive in one specified direction they have to be arranged orthogonal in space to provide information of the deformation in all three axial directions. [11] do use this transduction principle in an approach towards an integrated fingerprint sensor. An approach to fabricate a compliant sensitive artificial fingertip is presented in [100]. In contrast to other sensor setups the sensing elements (strain gauges and PVDF films) are arranged arbitrarily. This setup necessitates an adaptable readout system. According to [100] the strain gauges provide information about the direction of slippage.

2.5 Conclusion

By now, both, advanced robotic hands and tactile sensor solutions do exist, but non of the above presented systems does offer a satisfactory combination of dexterous robotic hand-hardware and integrated tactile sensors, offering the information which is necessary for fine dexterous manipulation and haptic exploration.

2.6 General requirements for valuable technical tactile sensors

The following chapter describes which information should be provided by the tactile sensor and which requirements a valuable tactile sensor should meet.

According to [6] contacts between a robotic finger and a grasped object are commonly divided into three different forms of contact. Point contacts, frictional point contacts and soft contacts. At a frictionless contact the robotic finger is only able to transmit a force which is parallel to the common normal of the fingertip and the grasped object at the point of contact. At a frictional contact a normal force and a tangential force can be transmitted. With a soft contact also a torsional moment about the common normal can be exerted. For practical use only frictional point contacts and soft contacts are considered. For the control of dynamic grasping according to [48] the information whether the vector of the contact force is oriented within the friction cone or not is fundamental. To complete the information for dexterous manipulation, which is derived from "classical" sensors integrated to the structure and the actuators of a robotic hand, e.g. joint-position, joint-torque, motor-position sensors, etc., tactile sensors are to provide information about:

- the force vector
- shear forces
- contact location
- contact properties
- object properties

[80] states that for exploration tasks a tactile sensor array, in addition to a high resolution, should provide easy slipping over the grasped object, which does not affect the data recording through stick-slip vibrations. [62] presents a table of design criteria for an artificial skin which has first been defined in [32]:

- compliant and durable sensing surface
- $1mm$ *to* $2mm$ spatial resolution
- 1g minimum pressure sensitivity
- about $1000 : 1$ dynamic range
- monotonic output response (preferably but not necessarily linear)
- at least $100Hz$ frequency response
- good stability and repeatability
- low hysteresis

Although robotics has developed significantly since these criteria have been defined, the desired abilities are still the same and therefore the given criteria are still applicable.

2.7 DLR's new Hand-Arm system

Currently DLR is developing a new, highly integrated, biomorphic robotic Hand-Arm system, presented in figure 13. The hand will allow for fine dexterous manipulation as well as powerful performance. Therefore an anthropomorphic fingertip design, that emulates the mechanical anisotropy of the human fingertip has been developed in [82]. The hand will consist of a highly compliant, viscoelastic artificial tissue that emulates the mechanical properties of human tissue, and an endoskeleton forming the actuated scaffold of the hand.

As one of the main goals is to design a Hand-Arm system which has the same size as a male human arm and hand, miniaturization and high mechatronic integration are very important. The hand will be equipped with five fingers, each having four independent DoFs. In fingers four and five, the distal and medial interphalangeal (ip) joints will be mechanically coupled. In contrast to "classical" robotic approaches, the joints of DLR' new Hand-Arm system are are designed as biologically inspired saddle

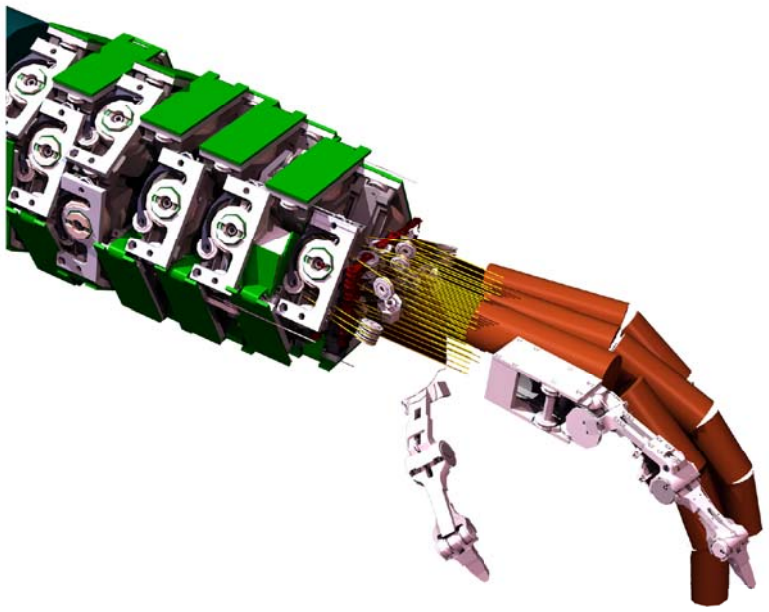

Figure 13: DLR's Hand-Arm system, source: DLR

base-joints and cylindrical ip joints. Similar to the anatomy of the human hand, there will be no mechanical coupling between the phalanges, except through the tendons. Therefore the joints can be dislocated if the tendons are slack, which makes the system overload-proof.

The whole Hand-Arm system will be actuated by an antagonistic drive system. For the tendon-driven actuation of the fingers, 38 of DLR's ILM-25 motors will be integrated to the forearm. Each motor is equipped with a spindle gear box, a position sensor and an elastic element, which enables passive compliance of the fingers. The planned maximum fingertip force is 30N at a weight of the hand of about 350g. The size will be the same as of an average European human male. The hand will be coupled to the forearm via a two-DoF wrist. The arm will have a total of seven DoF (2 wrist, 2 elbow, 3 shoulder). The Hand-Arm system is designed to a maximum weight of less than nine kilograms.

2.8 Special requirements resulting from the design of DLR's new Hand-Arm system

The design of DLR's new tendon-driven hand arm system comes along with many new challenges for the sensing system. Due to the highly integrated endoskeleton and the restricted designed space there is no possibility to include any of the existing fingertip force torque sensors into the new fingers. Therefore the measurement of forces applied during grasp has to be taken over by a new tactile sensor which must completely fit into the artificial tissue surrounding the endoskeleton. The joint angle sensors will be replaced by sensors in the tendons actuating the fingers. To enable the proprioception of the new Hand-Arm system a new combined sensing device for force measurement and tactile perception has to be developed. As no joint angle sensors are applicable in the tendon-fixed ip joints, the new artificial skin not only has to provide tactile and force information but also data that can help to determine the joint angles from stress in the skin at the ip joints.

For the application in DLR's Hand-Arm system the tactile sensor should be attachable to the highly compliant 3D surfaces of the anthropomorphic fingertips and therefore should be flexible or even stretchable. For off-the-lab application in the Hand-Arm system or in a prosthesis the sensor must be able to stand longtime wear and tear. Especially for the application in prosthesis reliability regarding function and data-validity of the sensor is crucial, and it would be desirable that the sensor is equipped with self testing routines that enable the self-detection of malfunctions. To be able to cover the whole Hand-Arm system, simple and low-cost producibility of large sensory surfaces ($> 1m^2$) is desired. The avoidance of huge numbers of contacting wires and bulky readout hardware is important to enable the successful introduction to new fields of application, see [67]. But the application in new areas, e.g. medicine comes along with additional criteria for the design of an artificial skin sensor. For the application of the sensor in MAS-instruments, the sensor should be sterilizable or low-cost and therefore disposable, furthermore bio-compatibility [112] is crucial.

2.9 Conclusion

As none of the "classical" sensor approaches (e.g. a combination of force-torque sensors and a tactile sensor) will be applicable to DLR's new Hand-Arm system, a new artificial skin sensor has to be developed. This sensor will break with the common taxonomy of intrinsic and extrinsic sensors and has to be able to replace the sensibility of the "classical" sensing approaches. Within this study a new sensor setup suitable for the anthropomorphic fingertip of DLR's new Hand-Arm system will be developed. Therefore potential pressure-sensitive materials are investigated.

3 Pressure-sensitive materials

As recommended in [87] and examined in former studies [89] piezo-resistivity is likely to be the most promising transduction principle and might be capable to meet the aforementioned requirements. Therefore at DLR different piezoresistive materials, their combination and processing technologies have been preexamined. This chapter will give a short overview of the theoretical background and the preliminary work.

3.1 Piezo-resistivity

Piezo-resistive transduction can be realized in different setups. The most common is the application of an elastic, nonconductive matrix material, that is loaded with conductive particles. In piezoresistive materials the resistivity depends on the concentration of conductive filler particles, geometric form, and distribution. A piezoresistive behavior can be observed if a non-conducting material is endowed with conductive particles. There are different approaches and models trying to describe the effects in semi-conductive, piezoresistive materials. The formation of conductive pathways within insulating elastic matrices loaded with particles of a conductive filler can be described by the percolation theory.

According to [19] many phenomena, depending on the formation of clusters, in different fields of research can be approximated with percolation theory. Even the spreading of forest fires, the process within an egg during boiling and the distribution of crude oil or natural gas in porous stone can be described with idealized and simplified models of percolation. And, important for this study, the effects of the formation of conductive pathways in materials loaded with conductive particles can be regarded as the formation of clusters and thus can be approximated with percolation phenomena. Percolation theory first has been developed in the 1940ties as an attempt to describe the phenomena of polymerization. Here a short introduction to basic percolation theory is given according to [19]. To be able to describe percolation phenomena the interesting area is divided into a quadrate grid, see figure 14. At the beginning all fields are empty.

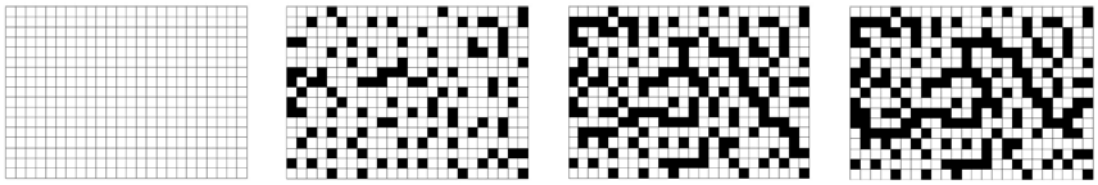

Figure 14: Percolation, adapted from [19]

Step by step the fields are filled with dots. As a simplification the dots do neither attract nor repel each other, i.e., an occupied field has no influence on the probability of the occupation of the neighboring fields. This is called random percolation. The grid consists of N fields, where N is assumed a high number. The probability that a field is occupied with a dot is denoted by p. Thus every field of the grid is randomly occupied with the probability p. If $p \cdot N$ fields are occupied with dots, there remain $(1-p)N$ empty fields. By definition only occupied fields with a shared horizontal or vertical side are considered as neighboring. Neighboring occupied fields do form clusters, and with an increasing amount of occupied fields the number and size of the formed clusters increases.

The elements of a cluster (neighboring occupied fields) can be connected with lines, forming pathways. At low concentrations only small clusters with pathways with many open ends exist. Starting from one of the borders all the pathways lead to dead ends at the edge of a cluster. At a certain concentration a first pathway connects two opposing borders of the grid $\Rightarrow$ the cluster percolates. This concentration is referred to as the percolation threshold p_c. If the concentration of dots increases further, additional pathways, connecting the borders are formed. When all the fields are occupied with dots, only one cluster without any imperfection remains, the probability p becomes equal to one. To adapt this simple model to real world challenges it can easily be adjusted and expanded. In 2D not only quadratic grids, but also triangle and hexagonal grids are possible. In 3D, amongst others, simple cubic, body-centered cubic, face-centered cubic and diamond-shape grids are possible. For theoretical considerations this model can be expanded to n dimensions. This theoretical model can be applied

for the static formation of conductive pathways in piezoresistive materials. One way of approaching the effects within an insulating material filled with conductive particles with a percolation model is to consider occupied fields of the grid as metal-filled, empty fields as insulating material. The grid is spread between two conductors with very low resistance, figure 15. If a voltage is applied over the grid between the conductors, a

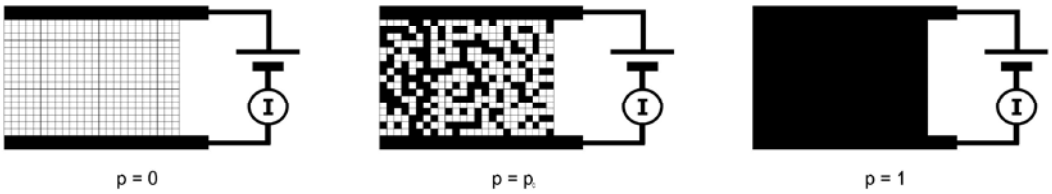

Figure 15: Percolating semiconductor, adapted from [19]

current will be measurable depending on the concentration of metal in the insulating matrix. The resistivity will range between $\sim 0\ \Omega$ at $p = 1$ (resistivity of a solid metal block) to ∞, at $p = 0$ (resistivity of the insulating matrix material). At the percolation threshold, $p = p_c$ the first conductive chain from one to the other side of the grid is formed. And a current I becomes measurable. If the concentration of the metal is further increased the resistance between the two sides of the grid decreases. Close to the percolation threshold little changes in concentration greatly affect the measurable resistance. To approach the effects of real piezoresistive materials, the ideal metal is replaced by ohmic resistances and percolation theory is supplemented with models of the conductive properties of the filler particles.

[88] derive a mathematical model that involves inter and intra particle effects in an insulating elastic matrix. The percolation model is expanded to obtain a better representation of the effects responsible for the change in resistivity in particle-filled composites. If the priezo-resistive matrix is deformed by external loads not only the static geometric properties of the filler particles but also their deformation properties become important. The mathematical model of the effect occurring in a semi-conducting compliant matrix is presented in abbreviated form in the appendix 10. This model is

only able to represent effects of conduction in ideal materials with cubic packing of the particles. Furthermore only composites without non-percolated chains can be mapped. Although this advanced model takes into account effects of changing resistances at deforming filler particles, many simplifications and estimates have to be made to derive a mathematical model, compare [88]. Especially the matrix material is idealized, assuming that the contacting particles are positioned one on the top of the other and the external force is only spread from the top particle to the subjacent. Those estimates would only be fulfilled in simple cubic packaging. Therefore not all the effects of the formation of conductive pathways in real conductive composites can be described. More recent studies on conductive polymers have shown that the conductivity might not be influenced by the size of a single particle but radically by the size of the agglomerates [39].

The static formation of conductive pathways during the polymerization process depending on the concentration of conductive filler particles is described in [110]. The authors do propose effects of phase transition prior to polymerization. Near the percolation concentration the compound of filler particles and matrix material runs through a phase transition. From a dispersed phase, with single particles encapsulated in the insulating matrix material the particles start to agglomerate. Groups of directly connected particles are formed in the so-called flocculated phase. As those effects can only go on within the uncured matrix this model does only describe the static formation of conductive pathways before the processing of the polymer. Effects within a ready cured polymer with conductive particles at the percolation threshold under external force are not describable with this model.

3.2 Sensor materials

Recently many experimental studies have been conducted aiming towards the theoretical description of the effects observable in different polymers filled with conductive particles, [52, 61, 68, 91, 99, 120] and many others. An overview of the work is given

in [39]. A short insight to the application of conductive polymers as pressure sensors is presented in [40]. As a conclusion it can be stated, that many parameters do have an impact to the resulting pressure depending resistivity. The most important parameter which is mainly responsible for the resulting conductivity is the filler ratio. The filler ratio affects the mechanical properties and the processability of the polymer filled with conductive particles [39]. If spherical carbon particles are used a high concentration (40-60wt%) of filler particles is required to reach the required low resistance. There are different approaches to avoid those effects. The utilization of carbon particles tending to the formation of structures, or the application of phase separating polymer blends, tend to be the most promising.

In multi-phase blends different immiscible polymers can be used and the carbon particles can be selectively distributed into one of the uncured blended polymers. During polymerization the different polymers are separated and the conductive particles are concentrated at the phase interfaces [39]. These approaches lead to highly conductive polymer materials with a relatively low ratio of carbon particles. Thus these materials can meet both, the required high conductivity and good processability and post-cure mechanical properties. As a result of the conducted literature research and stated in [99] there is no general theoretical model available that properly describes all the effects measurable at a conductive composite under dynamic mechanical load. In all probability the effects in real polymers filled with conductive particles are far more complex. For the application of a piezoresistive material as pressure sensor the desired material properties can only be achieved by the optimal selection of the basis material and the adjustment of the tunable properties with a focus to the desired mechanical and electrical properties.

3.3 Previous work

At DLR different transduction principles based on piezo-resistivity have been preexamined. Various pressure sensitive materials, their combination and processing technologies have been evaluated. This section will give a short overview of the work conducted prior to this study, compare [89].

3.3.1 Sensor setups

With a focus on easy and low cost producibility mechanically simple designs for the test patches were preferred. Therefore [89] focused on "classical" array setups. The first approach is based on injection-molded pads with cast in wires. As shown in

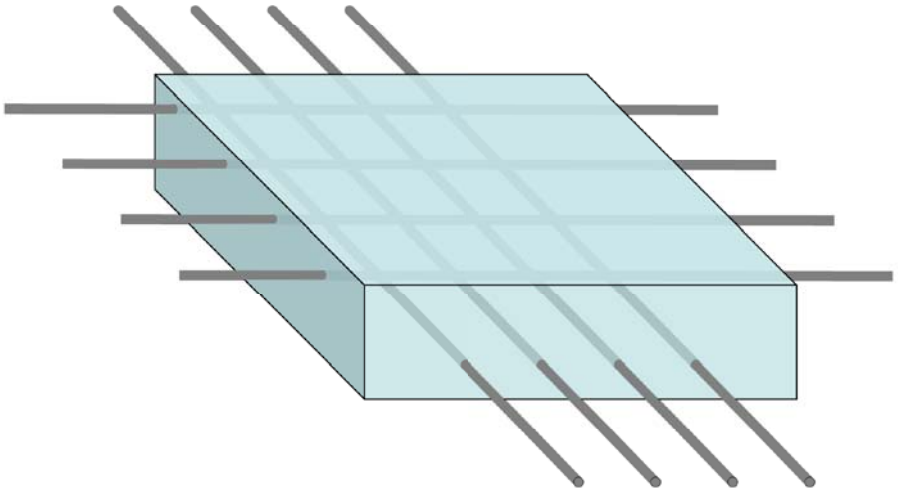

Figure 16: Layer setup, adapted from [89]

figure 16 the wires are arranged in two different layers. Those layers are separated by the piezoresistive matrix which forms sensitive areas at each crossing point of two wires. The second approach is based on a woven fabric design, see figure 17. To form the sensor array, silver plated wires are coated with a piezoresistive cover and woven to form a sensitive tissue. Thus the sensitive area is formed by two coated wires crossing each other. One of the main advantages of this approach is the possibility to produce literally tailored sensors.

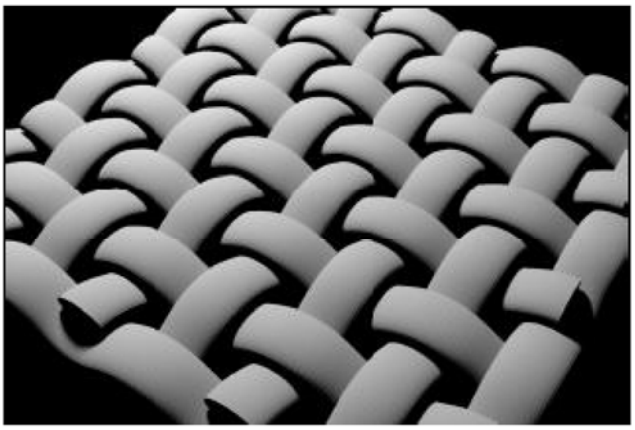

Figure 17: Woven setup, taken from [89]

3.3.2 Materials

Trying to mimic the mechanical properties of human skin, different elastic and viscoelastic soft materials have been examined. With regard to low cost producibility injection molding has been chosen as production technology. Therefore the soft material forming the sensor matrix has to meet the following demands: Miscibility with conductive fillers, tuneable mechanical properties and processability in injection molding machines. As they fit all those demands, different ultra-soft polymers were used: The only available pre-filled, injection moldable polymer was a SEBS (styrene-ethylene/butylene-styrene) carbon black pre-filled composite, (PTS-Thermoflex-EC80.1 20 * 9900N schwarz) with a filler ratio of 20% and a hardness of 76 Shore A. The material shows no piezoresistivity for the conductivity being too high. As the hardness is also significantly to high, blending with non-conductive, soft materials enables both, a lower, pressure dependent conductivity and an increased softness. The pre-filled polymer was blended with different nonconducting soft and ultra-soft polymers:

- PTS-Thermoflex-30 * 731 translucent, (34 Shore A)
- PTS-Thermoflex-21J * 700 translucent, (0 Shore A, 21 Shore 00)
- Kraiburg Thermolast TF0STL, (0 Shore A, 60 IRHD SS)
- GLS CL2003X

For self-blending experiments the following conductive fillers were used:

- SGL Conductograph 5, (graphite)
- SGL Conductograph 50, (graphite)
- Cabot Vulcan XC72 (carbon black)

3.3.3 Machinery

For the injection molding a Battenfeld MicroSystem 50 injection molding machine was used, see figure 58. This machine is designed for the processing of small volumes and molds in mm scale. For the blending and compounding experiments a Collin twin-screw extruder, shown in figure 57. was used. For granulation of the compounded material the extruder is equipped with an inline shredder.

3.3.4 Processing

The first attempt to tune the material to the desired properties was the dry mixing of the highly conductive pre-filled polymer, with softer non-conductive polymers. This mixture was filled directly to the feed hopper of the injection molding machine. It turned out that dry mixing of the basis polymers and the blending within the injection molding machine did not achieve satisfactory results. Therefore the basic polymers were blended with a twin-screw extruder. The result of the mixing was quite promising. As the available extruder does not offer a weighting apparatus the ratio of the two components has to be adjusted by varying the screw velocities. This only allows for an estimated mixing ratio.

Using a Fluke 179 multimeter no piezoresistive effect could be observed. Therefore blending highly conductive pre-filled polymers with non-conductive polymers was suspended. As alternative processing self-compounding of ultrasoft polymers with conductive filler materials was chosen. The self-compounded ultrasoft polymers could not

be granulated with the shredder of the extruder. Only if the material was cooled by liquid nitrogen the polymer could be granulated. Thus all the material had to be treated in this way. The resulting granulated material was then processed with the injection molding machine. Although a large variety of different materials and combinations has been produced, only one material combination could be identified that showed a sufficient piezoresistive effect at the desired softness: Kraiburg Thermolast TF0STL compounded with Cabot XC72. With this combination various test patches with different filler ratios were produced on the injection molding machine, see 18.

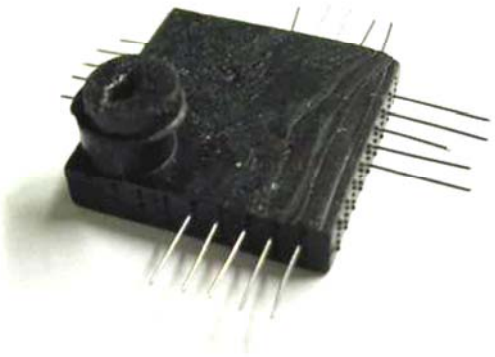

Figure 18: SEBS testpatch, taken from [89]

3.3.5 Evaluation

To ensure that the proposed materials do show a piezoresistive effect the patches have been tested with Fluke 179 multimeter. An estimated filler ratio of about $30w/w$ filler showed the best piezoresistive effect. Pressing the patches by hand resulted in measurable changes in resistance ranging from $3M\Omega$ to $100k\Omega$. Pressing the patches by hand and measuring the resistivity with a simple multimeter only allows for qualitative statements regarding piezo-resistivity. Besides only low repeatability could be obtained and unexpected effects were observed. If pressures was applied to the patches at the beginning an sharp increase of resistivity could be measured. If pressure was applied constantly the expected decrease in resistivity could be observed.

3.4 Discussion

The conducted qualitative test of the SEBS patches have shown promising results. The transduction principle realized in these test patches might be applicable in the anthropomorphic fingertip. Therefore the processed patches have to be evaluated regarding the suitability of the materials and their combination for the application in a fingertip sensor setup. To enable for quantitative statements the existing SEBS patches have to be evaluated under repeatable testing conditions. Those tests will be conducted with focus to the quality of piezoresistive effect. For this purpose and for the support of the further development of the artificial skin a special testbed is required.

Starting from the promising results of the preexamination of the piezoresistive transduction principle and the need for an alternative sensor setup for DLR's Hand-Arm system a new sensor setup for the anthropomorphic fingertip will be developed within the next chapter.

4 Bio-inspired sensor setup for DLR's Hand-Arm system

Recent advances in mechatronics enable the design of an anthropomorphic Hand-Arm system which will serve as human-like testbed. DLR's Hand-Arm system is an attempt to emulate the mechanic properties of the human arm with a robotic equivalent. Therefore the Hand-Arm system will look like a human arm and provide human-like limb dynamics. One of the main research goals is to understand how humans achieve stable, robust control in unstructured and time-varying environments. The human Hand-Arm system intrinsically solves part of these challenges by its mechanical design, e.g., by elastic muscles which are fixed in various locations and therefore offer a multi-joint behavior.

In contrast to the "classical" robotic approach, realized in DLR Hand II, the Hand-Arm system is actuated by an antagonistic drive principle. This helps to emulate human arm behavior. Features as adjustable joint stiffness, enabled by non-linear elastic elements within the actuator system, make the system adaptable to the task at hand. A major drawback of "classical" robotic approaches towards human-robot interaction are safety concerns. Not only in terms of user-safety but also in terms of robot-safety. The Hand-Arm system, as the human arm tackles this challenge by passively yielding joints. Thus the system is capable of handling unexpected impacts which are too fast to be handled by an active controller. With the development of the anthropomorphic Hand-Arm system a step towards the integration of robotic systems to the human environment is taken, [29].

When humans and robotic systems will physically interact in the future, safe human-robot interaction enabled by collision detection systems becomes very important [31]. To enable the robotic system to discriminate between intended interaction and unintended collisions an intelligent tactile sensing system is required. Another goal of the anthropomorphic design approach is to create a robotic arm applicable as a prosthesis or as an additional arm. To support acceptance of the robotic body-extension, a "nat-

ural" extro- and proprio-receptive feedback from the prosthesis is required. Especially tactile information, presented to the user in a "natural" form, comparable to the firing patterns in human afferent nerves, is important for usability and acceptance of the user. To enable autonomous human-like grasping control with a prosthesis tactile information, provided by an artificial skin sensor on the fingertips, is crucial for low-level control.

Enabling for anthropomorphic grasp control of, e.g., a prosthetic hand, information regarding the contact between the robotic hand and the gripped object has to be provided. This information is to be used by the robotic device and by the human user. For the human user the information has to be conditioned to ease the integration to the human's perceptive system. For a long term view researchers are interested to which extend a human user is able to assimilate the robotic arm to the user's own body scheme. Due to the special requirements, resulting from the design of DLR's new Hand-Arm system, "classical" technical sensing approaches that follow the common approach of proprioception of the robotic device are no longer applicable. A new anthropomorphic sensor setup, that aims towards a multi-functional tactile sensing system able to provide user-fit information, is required.

4.1 Human mechano-perception as a source of inspiration?

This study aims towards a tactile sensor which will be used in human's everyday environment and provides information which is to be used by both, the Hand-Arm system itself and the human user. Thus it is self-evident to examine how nature solves the given challenges with the human mechano-perceptive system. As the human mechano-perceptive system is very complex and still is not completely understood, it is not appropriate to try to emulate the human mechano-perceptive system. But in some aspects the human mechano-perception might serve as source of inspiration. Copying nature's solutions with technical systems is often neither possible nor promising. Nevertheless observing nature's strategies to solve problems and how to deal with con-

flictive requirements can be very useful if applied in the right way. A whole field of research deals with, how to generate benefit for humans from nature's experience and unequaled ingenuity. Bionics.

4.2 Bionics - an approach towards bio-inspired technical solutions

Today, more and more bionic solutions to human everyday tasks find their way to innovative industrial products (lotus-effect, velcro, and shark skin) [74]. From a scientific point of view bionics is defined as the "systematic technical conversion and application of constructions, procedures and development principles of biologic systems" [75]. In literature the focus of bionics research is set to the support of technical design and product development. But bionics is also used in fundamental research, especially in material sciences. [64] and [98] propose bionics as a method of product development. Bionic approaches to product development are used to find solutions for technical challenges that can not be directly solved with standard technical approaches. [36] proposes a black box method based on a catalogue of biologic solutions. [117] uses a collection of biologic principles combined with an algorithmic search strategy that uses similarities in function, boundary conditions and quality factors.

Both approaches lack efficiency due to incomplete catalogues of biologic solutions. The aforementioned authors propose different approaches how benefit for technical products can be derived from biologic solutions. Most of the authors agree, that bionic development does not aim to copy biological systems but tries to identify the principle nature uses to solve the given challenge and to derive a technical strategy or principle which is capable to solve a comparable challenge. Within this study bionics is not used as a method of product development but to derive a bio-inspired sensing principle for DLR's new Hand-Arm system. Therefore the proposed bionic strategies have to be adapted to be applicable in research. The general procedure is drawn on [36].

Bionic method to tackle technical challenges:

- Analysis of the technical challenge
- Abstraction of the technical challenge
- Search for a biologic system that is capable to solve a comparable challenge
- Analysis: Derivation of the solution principle
- Synthesis: Derivation of a technical solution
- Realization of the technical solution

4.3 A bio-inspired sensor setup for DLR's Hand-Arm system

Within this chapter bionics is applied to derive a bio-inspired technical sensor setup for DLR's Hand-Arm system. The requirements presented in chapter 2 are essential for a valuable technical tactile sensor. While "classical" technical approaches are capable to meet at least most of the general requirements, conflicts of goals emerge if both, general and special requirements, resulting from the design of DLR's new Hand-Arm system, are to be met. Therefore the sensor setup aims towards a bio-inspired tactile sensor that intrinsically solves the conflicts between the different requirements; And thus can be designed to fulfill both, the general requirements and the special requirements. The following procedure is used to identify new research approaches and to derive a bio-inspired sensor setup:

A consistency-matrix is used to classify the requirements, to analyze their interaction and thus identify critical conflicts of goals. Therefore the requirements are evaluated and the interaction between the elements is pairwise analyzed and weighted according to its relevance. Possible conflicts between the requirements are identified and evaluated. The conflicts are analyzed and classified whether the conflict is solvable with

"classical" technical approaches or not. For the remaining, non-solvable conflicts, solutions are developed using bionics. For each non-solvable conflict the solution realized in human mechano-perception is analyzed and if applicable the underlying strategy is formulated. Therefore the general bionic method is adapted for this study:

- Abstraction of the technical challenge
- Analysis of the functionality in human tactile perception
- Abstraction of the functional principle; Nature's strategy?
- Propagation of the functional principles to a technical system
- Possible technical approaches

The derived partial solutions are combined to a bio-inspired sensor setup for DLR's Hand-Arm system.

4.3.1 Classification and evaluation of the requirements

The general requirements for valuable tactile sensors and the special requirements resulting form the design of DLR's Hand-Arm system are classified and analyzed using a consistency matrix according to [64]. The following requirements and the connecting relationships are evaluated:

- General Requirements
  - compliant sensing surface
  - durable sensing surface
  - $1mm$ *to* $2mm$ spatial resolution
  - $1g$ minimum pressure sensitivity
  - about $1000 : 1$ dynamic range

  - monotonic output response
  - at least $100Hz$ frequency response
  - good stability and repeatability
  - low hysteresis

- Special Requirements
  - detailed contact information
  - minimization
  - attachable to 3D surfaces (fingertip)
  - applicable to a viscoelastic basis material
  - flexibility
  - few readout wires
  - low computational effort
  - biocompatible
  - sterilizable
  - low cost producibility
  - large surface

To identify conflicts of goals between the requirements the relationships are analyzed and classified according to:

- no relationship (0)
- existing relationship without conflict (1)
- possible conflict of goals (3)
- conflict of goals → technical approach possible (9)
- unsolvable conflict of goals → bionic approach (99)

The procedure of the analysis is exemplarily shown at the instance of the claimed compliant sensor surface. One by one the other requirements are analyzed whether there is a relationship to the demanded compliant sensor surface or not, e.g., there is a relationship to the required durable surface. If a relationship exists, it is analyzed whether there is a conflict of goals or not, e.g., there are compliant and durable materials available that can be used to cover the sensor. As there exists no obvious conflict of goals the analysis can be stopped at this point. The above mentioned example would be classified with (1), as there is a relationship between the requirements but a possible solution exists, that is capable to fulfill both requirements.

For an other requirement under certain circumstance a conflict of goals might emerge, e.g., a solution is possible that is cost-intensive or time-consuming, if an additional requirement as low overall cost is formulated, a conflict of goals is possible. This example is classified as (3). If a conflict of goals is obvious but a technical approach is possible, e.g., the application of a different material, the relationship is classified as (9). For certain pairs of requirements obvious conflicts of goals exist and no technical solution is proximate, e.g., $1mm$ *to* $2mm$ spatial resolution and only few readout wires (99). As a high resolution necessitated many sensory cells, many readout wires are required. Due to the the sheer enormity of the number of readout channels "classical" technical approaches as array setups and multiplexers would not lead to the required minimization of the number of readout wires. Therefore a reduction of readout wires would result in a lower resolution.

The conflict is not solvable with a "classical" technical approach. For those conflicts of goals an approach for an intrinsic solution is investigated using bionics. Applying this procedure to all requirements, step by step all the possible combination of requirements are evaluated and possible relationships are classified, see figure 19. For the lack of space the complete consistency matrix is presented in the appendix 59.

Consistency Matrix

General Requirements	compliant sensing surface	durable sensing surface	1 to 2mm spatial resolution	piezoelectric and pyroelectric	1g minimum pressure sensitivity	about 1000:1 dynamic range	monotonic output response	at least 100Hz frequency response	good stability and repeatability	low hysteresis	Special Requirements	detailed contact information	minimization	Attachable to 3D surfaces (Fingertip)	Applicable to a viscoelastic basis material
compliant sensing surface		1	0	0	0	0	1	0	9	9		1	9	1	1
durable sensing surface			3	0	99	0	0	3	0	3		3	9	3	3
1 to 2mm spatial resolution				1	1	0	0	0	0	0		1	9	9	3
piezoelectric and pyroelectric					3	3	3	3	9	9		3	9	3	3
1g minimum pressure sensitivity						1	0	1	1	1		1	1	3	3
about 1000:1 dynamic range							0	1	0	1		1	0	1	1
monotonic output response								1	1	1		1	0	0	0
at least 100Hz frequency response									1	0		1	0	1	1
good stability and repeatability										0		1	9	3	9

Figure 19: Consistency matrix

As the result of the conducted analysis the following, technically unsolvable, conflicts of goals have been identified:

- Durable sensor surface - 1g minimum sensitivity
- Low hysteresis - application in a viscoelastic artificial tissue
- Detailed contact information - few readout wires / low computation effort
- High resolution - few readout wires / low computational effort

In the following chapter bionics is applied to those conflicting requirements to derive possible bio-inspired intrinsic solutions.

4.3.2 Conflicting requirements within the general requirements

Durable sensor surface - 1g minimum sensitivity

If piezo-resistivity is used as transduction principle the sensor material has to be deformed to generate a measurable signal. Even if the specified minimum sensitivity of one gram is correlated to a small indentation probe of only $1mm^2$, the resulting pressure is still very low $\left(0.01\ \frac{N}{mm^2}\right)$. Therefore the sensor material has to allow for an significant deformation at small pressures. At the same time a high durability is stipulated. To create a sensor surface that is capable to withstand long term wear and tear an abrasion-resistant material has to be used which is able to withstand highly dynamic mechanical load. Therefore the material must be ductile. The required ductility is conflicting with the claim for easy deformability. As this conflict is not directly solvable with a technical approach an intrinsic solution might be derivable using bionics.

Abstraction of the technical challenge

For the transduction principle mechanical deformation of the sensor is necessary. At the same time a ductile material is required for a durable protective layer. The following conflict has to be solved: The durable protective layer prevents indentations at small pressures.

Analysis of the functionality in human tactile perception

Human skin acts as a durable protective layer and at the same time allows for significant indentations at small pressures. Therefore the mechanical construction and the functionality of human skin is presented in the next paragraph. The inner human body is protected by the skin, which forms a mechanically durable, waterproof barrier, [1] against environmental influences and infections [81]. And plays an important role in the thermoregulation of the human body [95]. The following paragraph gives a brief overview of the anatomy of human skin according to [35]. As the thickness of the different skin layers is highly variant, depending on the body site, the values of the

human forearm are exemplarily presented according to [35]. The given numbers are intended as an orientation. There are different types of skin that can be divided into glabrous (smooth) and hairy skin. The human body is in large part covered by hairy skin. Glabrous skin can be found on the lips, the palm, the fingers, and on the sole of foot. Human skin consists of three main layers: epidermis, dermis and hypodermis. Figure 20 shows the detailed composition of the layers of the skin. The living epider-

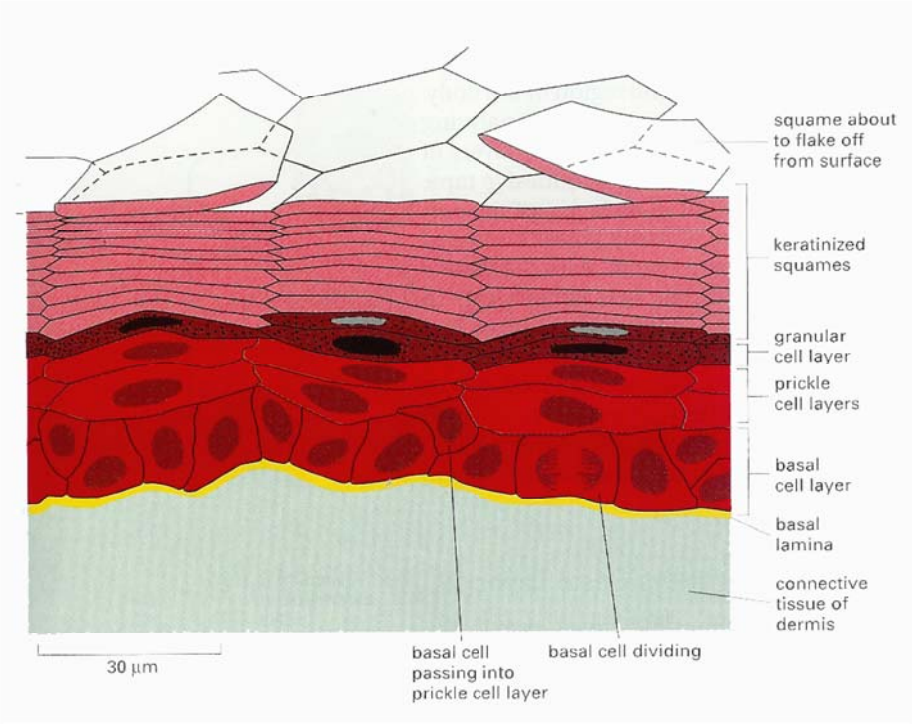

Figure 20: Microstructure of the dermal layers, taken from [1]

mis is approximately $0.03mm$ *to* $0.13mm$ thick. It shows the characteristic pattern of the epidermal ridges, which are hereditarily determined. The epidermis consists of five layers which are subjected to a continuous process of regeneration. While cells are lost on the surface by mechanic abrasion, new cells are produced in the innermost layer of the epidermis, the stratum basale (also stratum germanitivum or basal layer). Those cells, the so-called basal cells are regenerated by mitotic cell division. Within the stratum basale the keratinocytes have a columnar shape. While they transform in the process of cell maturation, they move outward into the next layer, the stratum spinosum. In this phase the keratinocytes have a cuboidal shape and contain a large

nucleus and cytoplasm. In the stratum spinosum the cells form intracellular filaments, which form part of the cytoskeleton. Those intracellular structures are connected to the desmosomes which enable cell to cell adhesion. The cytoskeleton and the adhesions between adjacent cells helps the skin to absorb shear forces and to withstand abrasion. As the epidermis is avascular, i.e., there are no blood vessels, the cells of the epidermis are supplied with nutrients that diffuse from the blood vessels within the dermis.

When the epidermal cells continue to migrate outward, the supply with nutrients decreases as the distance to the blood vessels, and thus the diffusion distance increases. Due to this undersupply the mitochondria and the nuclei start to degenerate. At the same time, the cells accumulate keratin and lipid containing granules. The size of the cells decreases as they develop a flatted shape. All those processes support the generation of the next skin layer, the stratum granulosum.

As the cells continue to migrate they die due to the lack of nutrients. Processes of self-digestion of the cell organelles start. The dead cells form the next layer, the stratum lucidum which is a waterproof barrier, that helps to protect the human body. The outermost layer of the epidermis, the stratum corneum (thickness 0.01mm-0.02mm) is formed by dead, anucleate cells. As the cells have reached the final stage of the differentiation, they are called corneocytes.

Abstraction of the functional principle; Nature's strategy

The mechanical composition of human skin enables for significant indentation at small pressures. Although the topmost layer of the skin is durable it is not designed to withstand wear and tear for a long period of time. As the protective layer (stratum corneum) is very thin it is abraded by the mechanical load. Human skin is able to self-regenerate, i.e., the protective layer is continuously replaced from within. Step by step the protective layer is exchanged. Therefore the protective layer can be designed very thin and thus allows for significant indentation at small pressures.

Propagation of the functional principle to a technical system

As a self-regeneration in the form of a regrowth is not possible for technical materials the protective layer has to be easily exchangeable. If the technical protective layer has to be disposable it must be low cost to keep running expenses for the sensor system down.

Possible technical approaches

Thin technical protecting layers are well established in form of latex gloves for various applications.

4.3.3 Conflictive requirements resulting from the design of DLR's new Hand-Arm system

Low hysteresis - application in a viscoelastic artificial tissue

As claimed in the general requirements a low hysteresis of the tactile sensor is desirable. A low hysteresis allows for the quantitative evaluation of the contact forces independent form the loads prior to the measurement. The tactile sensor is to be used with the artificial tissue of DLR's new Hand-Arm system which shows a viscoelastic behavior, see figure 21. If the piezo-resistive sensor is based on a viscoelastic material the relaxation

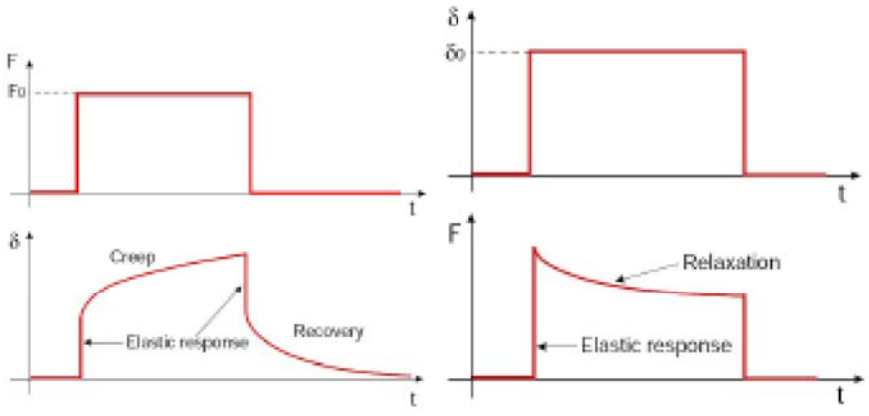

Figure 21: Viscoelastic behavior, taken from [89]

time delay is transferred form the viscoelastic material to the piezo-resistive material. The relaxation effects result in an offset signal of the sensor depending on the applied load prior to the current measurement. The application of a viscoelastic basis material and a low hysteresis are conflicting requirements which are to be met. As no technical solution is apparent the bionic method may lead to an approach that is capable to solve this conflict.

Abstraction of the technical challenge

The desired viscoelastic basis material shows a hysteresis if the material is loaded and released. For the sensor a low hysteresis is claimed, but both systems are mechanically coupled. The basis material transfers its characteristic hysteresis curve to the tactile sensor.

Analysis of the functionality in human tactile perception

Within human skin the protective layer formed by the epidermis is supported by the dermis. According to [35] the dermis of the human forearm exhibits a thickness of $1.1mm$. It makes up $15 - 20\%$ of the total body weight and contains many physiologically important structures such as blood and lymph vessels, sweat glands, hair follicles, nerves and many sensory elements. It mainly consists of connective tissue which is formed by fibroblasts that aid to produce the intercellular substance of the connective tissue. The intercellular substance mainly is formed by the fibrin proteins, collagen, elastin, reticulin and a ground substance. As the connective tissue of the skin is mechanically loaded in all directions the collagenous fibrils are orientated in all directions and form meshwork structures that are responsible for the mechanical durability and elasticity of the skin. The dermis itself cuts into two layers, the papillary dermis and the reticular dermis. The topmost ten percent of the thickness of the dermis are referred to as the papillary dermis. The papillary dermis is formed by a greater fraction of ground substance and less densely arranged fibrils. It forms the interconnection between dermis and epidermis, the dermo-epidermal junction. The reticular dermis

consists of dense connective tissue with a higher fraction of collagenous fibrils and less cells. The innermost layer of human skin is referred to as the hypodermis or subcutis. It mainly consists of adipose, i.e., fatty, tissue. It is responsible for the relocateability of the skin. The thickness of the subcutaneous fat layer varies individually according to site, sex and age. Within those pads energy is stored in the form of fat. In addition the subcutis functions as insulation, which helps to maintain and control the temperature of the body.

Following the mechanical properties of human skin are presented. The mechanical properties of human skin significantly change from living to dead tissue. In addition the properties are highly variable regarding to the investigated body site. As an in vivo dissection of the human skin layers is not possible, researchers try to examine the properties of the composite in different measurement techniques (indentation [18], extensometry [21], suction [35] or torsion [30]). Thus only indirect in vivo measurements of the single layers are possible. The values of the mechanical properties presented in this chapter are taken from [35]. Due to the aforementioned indirect measurement techniques the given numbers are intended as orientation. The mechanical properties of human skin are highly anisotropic, i.e., depend on the direction of the load. Furthermore the deformation behavior is time-dependent.

Human skin shows a viscoelastic deformation behavior. Thus the deformation consists of non-linear elastic and viscose deformation. If a non-linear elastic material is cyclicly loaded the deformation shows a hysteresis loop. Viscose deformation is characterized by creep and relaxation processes. The ratio of elastic and viscose deformation is time-dependent. If a viscoelastic material is loaded very fast, it predominantly shows an elastic deformation. If the material is slowly or permanently loaded the material shows predominantly viscose behavior as do highly viscose fluids. This behavior depends also on the temperature of the material. The deformability of human skin is influenced by the fraction of the fibrin proteins, collagen and elastin, while the remaining constituents reticulin and the ground substance play a minor role. According to [35] 75% of the fat free dry weight and 18% *to* 30% of the volume of the dermis consist

of collagen. Collagen shows a time-depended behavior, which can be simulated with a combination of a spring with a damper. The Young's modulus of collagen varies between $0.1GPa$ *and* $1GPa$, it shows a low extensibility of about 5% *to* 6%. While elastin fibres only contribute 4% of the fat free dry weight and 1% of the volume of the dermis. Those elastin fibres show a linear elastic behavior. Therefore they can be simulated with a spring. Elastin shows a lower stiffness than collagen but exhibits reversible strains of about 100%.

The gel-like behavior of the dermis is created by the water that is incorporated into the chains of polysaccarides of which the ground substance consists. Even under high physical pressure the gel/water does not leak out of the skin. The performed literature research showed, that despite of intensive investigation the mechanical properties of the different layers of human skin can be measured only indirectly. Many parameters, e.g., body site, relative humidity and test setup lead to a very high variance of the calculated mechanical properties. Nevertheless quantitative conclusions might be applicable.

Abstraction of the functional principle; Nature's strategy

Human skin is equipped with layers that greatly differ regarding thickness and mechanical properties. Simplified the layer composition is based on the combination of a predominantly viscoelastic basis material for the tissue that surrounds the bone, with a predominantly elastic superficial layer and a ultra-thin protective top-layer. Resulting from this setup a fast restoration of the evenness of the skin can be observed for small indentations. To a certain extend the restoring force of the epidermis contributes to a fast restoration of the evenness of the skin. For large scale deformation very long (viscoelastic deformation) or infinite (plastic deformation) time constants are observable. Especially after high applied pressures, the restoring force of the outer skin layers is not sufficient to fully restore the initial shape. The material shows a hysteresis curve. Future indentations increase the internal pressure and therefore enable a complete restoration.

Propagation of the functional principle to a technical system

A setup of different materials that show different thickness and mechanical properties might help to minimize hysteresis of the attached sensor.

Possible technical approaches

There are various elastic and viscoelastic materials available that can be applied for an anthropomorphic setup of the different layers of the fingertip. Considering the results of the aforementioned approach for the exchangeable protective layer a mechanically stable connection between protective layer and subjacent layers is crucial to be able to utilize the restoring forces of the protecting layer. This can be realized via elastic adhesive agents or negative pressure.

Detailed contact information - few readout wires / low computation effort

As presented in chapter 2, DLR's Hand-Arm system does not offer enough designed space to include "classical" 6 DoF force torque sensors. Therefore one of the major requirements for the tactile sensor is the claim for detailed contact information. The most interesting modalities are the orientation and value of the force vector and the exact contact location. In addition, the sensor should be capable to detect shear forces and slippage as well as strain. At the same time the development of the sensor is confronted with the claim for a small number of readout wires and a minimum computational effort. Although not all the transduction processes within human mechano-perception are fully understood, the bionic method might lead to some inspiration for a sensor setup that is able to solve the conflict of goals.

Abstraction of the technical challenge

Although detailed contact information is required only few readout wires and restricted computational power are available. Therefore the sensor setup has to provide detailed contact information in an easy to handle form.

Analysis of the functionality in human tactile perception

The human mechano-perceptive system is a very powerful sensory organ. To this day only a fraction of the functionalities is fully understood. Therefore the following chapter outlines the basic anatomy and the functionalities according to [50] as far as they are understood. Regarding its size human skin is the most prominent sensory organ. The sensory capabilities are:

- mechanoperception (pressure, touch, vibration and titillation)
- proprioception (joint angle, static position of the limbs)
- thermal-reception(warmth, coldness, thermal conductivity)
- and nociception (pain, itching)

As this study is focused on gathering of tactile information, only the mechano-perception with the following quantities is considered: touch, vibration, pressure and stretch. Specialized sensory structures within the human skin, the mechano-receptors, allow the transduction of the information of environmental stimuli into firing patterns, which are relayed via nerve fibers to the central nervous system. Every type of mechanoreceptor is specialized to a specific mechanical stimulus, the adequate stimulus, i.e., every mechanoreceptor is eminently sensitive to a different kind of mechanical stimulation like pressure or vibration.

Although there are mechano-receptors which occur in both, glabrous and hairy skin, every type of skin features its own specific mechano-receptors. The mechano-receptors are inhomogeneously distributed, according to their location within the skin layers and according to their concentration in the different sites of the body. The so-called two point threshold, i.e., the minimum distance to distinguish between a single point-contact and a pair of point-contacts varies depending on the site of the body, see figure 22. The inhomogeneous distribution of the mechanoreceptors over the body originates in the varying required resolution. Parts of the body that are involved in haptic exploration and fine manipulation (esp. fingertips and lips) show a high density

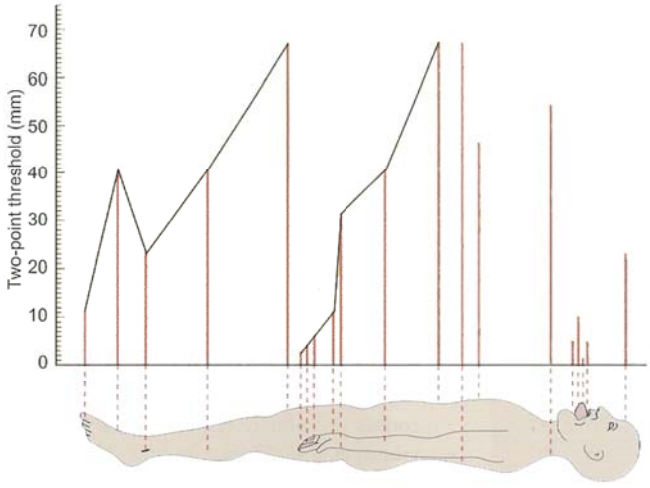

Figure 22: Two-point threshold, taken from [81]

of sensory cells. The sensory cells in human skin are innervated via primary sensory neurons (or dorsal root ganglia), see figure 23. The area which is innervated by a primary sensory neuron is called a receptive field. The size of the receptive field depends on the location of the mechanoreceptor within the skin layers. Receptors which are located near the surface do have a small and sharply circumscribed receptive field with a diameter of about $2mm$ *to* $3mm$ at the fingertip and about $10mm$ at the palm. Whereas receptors which are located within the deeper skin layers have lager, jet less sharply circumscribed receptive fields. The superficial sensory cells form clusters that are innervated by one dorsal root ganglion. Hence many signals of different sensory cells are queried by one dorsal root ganglion. Neighboring clusters have overlapping receptive fields. Thus a single mechanical stimulus can excite more than one receptive field and therefore generate a signal in multiple dorsal root ganglia. As the number of the dermal sensory cells is minor and the distance between two neighboring cells is greater each cell is innervated by one primary sensory neuron.

As mentioned before till this day it is not fully known in which way the different mechanoreceptors contribute to the resulting complex sensation of touch. The following paragraph gives a short overview according to [50] of the assumed functionalities

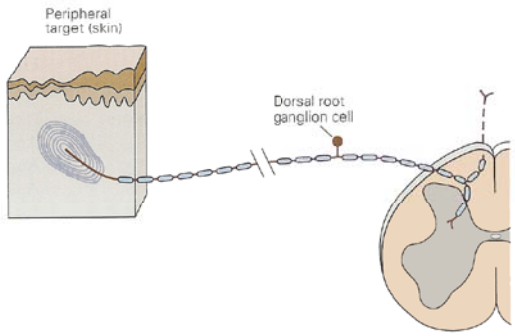

Figure 23: Dorsal root ganglion, taken from [50]

and transduction principles as far as they are understood. The mechanoreceptors can be subdivided according to their reaction to mechanical stimuli and according to the size of their receptive fields (location within the layers of the skin). The different mechano-receptors react in different ways if skin is indented. If the indentation is sustained the mechano-receptors change their firing behavior, they adapt. Simplified the following transduction modalities can be allocated to the different types of mechanoreceptors [92]:

- Slowly adapting type two (SA II) code for the depth of the indentation (x)
- Slowly adapting type one (SA I) code for depth and speed $\left(x, \frac{dx}{dt}\right)$
- Rapid adapting (RA) code for the speed of the indentation $\left(\frac{dx}{dt}\right)$
- Pacinian corpuscles (PC) code for the acceleration of the indentation $\left(\frac{d^2x}{dt^2}\right)$

The taxonomy of the mechanoreceptors is presented according to [50]. Within glabrous skin there are several different structures that are considered to participate in mechanoperception, see figure 24. The four better known structures are the so-called Meissner's corpuscles, the Pacinian corpuscles, the Merkel cells, or disc receptors and the Ruffini's corpuscles. Meissner's corpuscles are located in the dermo-epidermal junction. They are mechanically coupled to the edges of the papillary ridges. As the dermo-epidermal junction is located near the surface of the skin the Meissner's corpuscles possess small,

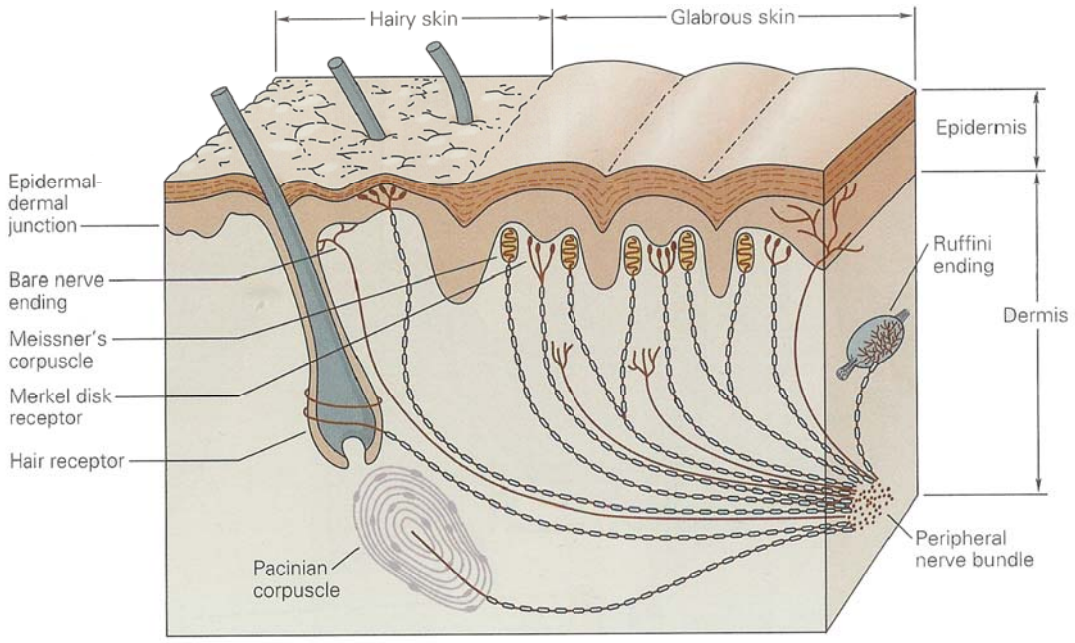

Figure 24: Location of the mechano-receptors in human skin, taken from [50]

sharply bordered receptive fields. Meissner's corpuscles are fast adapting, thus this sensing structure is optimized to sense the velocity of the skin indentation. Pacinian corpuscles are located within the deep layers of the dermis, therefore they have large, less sharply bordered receptive fields. Pacinian corpuscles are very fast adapting sensory structures, thus they are capable to sense the acceleration of the skin indentation. The adequate stimulus for the pacinian corpuscles is vibration. Merkel cells, or disc receptors (SA I) show small receptive fields as they are located at the center of the papillary ridges within the dermo-epidermal junction. They adapt slowly to stimuli and therefore are capable to code for the depth and the speed of the indentation. Ruffini's corpuscles (SA II) are found in the dermis, therefore they exhibit large receptive fields. Ruffini's corpuscles are coupled to structures within the subcutaneous tissue that are connected to folds of the skin, e.g. at the phalangeal joints. Therefore they are especially sensitive to skin stretch. They code for the depth of the indentation. Within hairy skin different mechano-receptors can be found, but they fulfil similar tasks. As the parts of the skin, that are involved in fine manipulation (finger-

tips, palm and lips) are covered with glabrous skin, the mechano-receptors of the hairy skin are not considered within this study. It is generally assumed that the functionality of the mechano-receptors is enabled by the mechanical coupling of the skin tissue to the specialized terminals of the dorsal root ganglia. If pressure is applied to the skin the mechanical structure of the nerve terminal converts the applied pressure to a stretch of the cell membrane. The cell membrane of the nerve terminal is endowed with mechanically activated transmembrane ion channels, see figure 25. If the cell

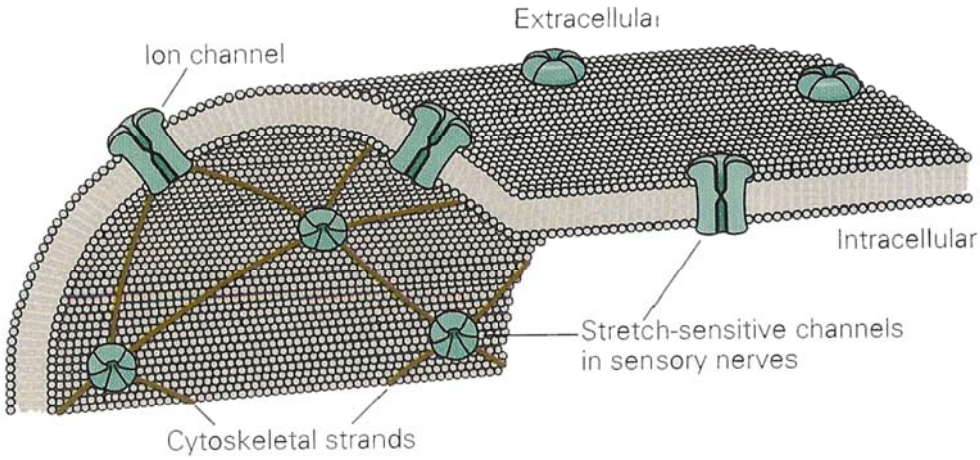

Figure 25: Transmembrane ion-channels, taken from [50]

membrane is stretched the ion channels are opened. Through the open channel cations (assumedly Na^+ and Ca^+) flow into the nerve fiber and create a receptor potential. If the receptor potential exceeds a certain level an action potential in the dorsal root ganglion is triggered. The frequency of the action potentials codes the depth, speed, acceleration and direction of the indentation. This information is propagated to the sensomotor cortex [50]. Although the effects are not jet fully understood, recent studies [7] have shown that the sensory cells are capable to encode the direction of the mechanical stimulus. There seems to exist a correlation between the microanatomy of the terminal structures, the orientation of the terminal structure within the skin and the preference of the sensory cell to mechanical stimuli in a certain direction.

Abstraction of the functional principle; Nature's strategy

For each of the modalities of a mechanical stimulus the human perception system is equipped with a specialized type of sensor. The concentration of sensory cells and therefore the resolution of the receptive fields varies according the body site. The amount of sensory cells is optimized to the minimum required resolution. The distribution of the different types of mechano-receptors within the different layers of the skin is eminently important for the transduction of the mechanical stimulus. The different receptors in the superficial layer are positioned at the contrary ends of the papillae. This might be a strategy to transform the applied pressure to local strain in the dermo-epidermal junction.

Superficial receptors exhibit small receptive fields, dermal receptors show large receptive fields. Overlapping receptive fields enable for redundant data regarding a mechanical stimulus. Clusters of sensory cells are innervated via one dorsal root ganglion. Thus many sensory cells contribute to a signal in the dorsal root ganglion. Anisotropic transduction properties of the nerve terminals enable for the intrinsic decoding of the direction of the mechanical stimuli. The mechanical stimulus is filtered and conditioned by the mechanical composition of the skin and the specialized structures of the nerve endings. The amplitude of the mechanical stimulus is transduced to an electric potential. This receptor potential is coded in a frequency signal, the so-called action potential in the dorsal root ganglion. This action potentials are propagated to the central nervous system.

Propagation of the functional principle to a technical system

The strategy to utilize different sensor types for the different modalities of the stimulus may be applicable in a technical sensor. If these cells show anisotropic sensing properties the direction of the stimulus is intrinsically encoded. Moreover the arrangement of sensors in different depth creates receptive fields of varying dimensions. This strategy can be adapted for the setup of the technical sensor by arranging the different sensor types in different layers of the artificial fingertip. To provide detailed contact infor-

mation both, the applied pressure and the resulting strain in the artificial skin layers should be measured. For the design of the sensor, it is important to enable a resulting output signal proportional to the mechanical stimulus. A further strategy that might be applicable in a technical sensor is the decoding of the resulting electrical signal into a frequency signal. This could be helpful to ensure reliable and fast signal propagation from the sensor to the readout facility.

Possible technical approaches

For the technical realization of the proposed strategies different sensor types are available. Beneath the proposed pressure sensitive materials, strain sensors like strain gauges could be realized in the bio-inspired sensor setup. The proposed strain gauges inherently show the desired anisotropic transduction properties. Another possible technical approach for the transduction of the applied pressure to strain is the design of an artificial papillary structure. The mechanical functionality of the papillae has been researched in [27]. The author proposes a possible effect of contrast enhancement by the mechanical composition of the dermo-epidermal junction. A further possible approach would be the application of structures that show a mechanically defined resonant frequency that could be used to condition the stimulus for the applied sensors.

High resolution - few readout wires / low computational effort

An obvious conflict of goals is posed by the required resolution of $1mm$ *to* $2mm$ and the demanded minimization of the number of readout wires. This conflict typically is tackled with array approaches. In combination with the special requirement of sensor surfaces of $1m^2$ an array sensor offering the required solution would come along with 1000 *to* 2000 readout wires. But not only the claim for few readout wires conflicts with the high resolution but also the demand for a low computational effort forms a conflict of goals. The high resolution results in a high number of channels that have to be analyzed by the readout electronics. The "classical" approach is the application of multiplexers. Today there are mm-scale multiplexers available, that offer 8 to 16 input

channels. But the sheer enormity of the number of readout channels still would lead to bulky and energy consuming evaluation electronics. Therefore the human tactile perception will be analyzed using bionics.

Abstraction of the technical challenge

Many sensory cells are required that have to be connected with the readout electronics via few connecting wires.

Analysis of the functionality in human tactile perception

To draw on human mechano-perception the signal propagation and preconditioning is briefly reviewed in this paragraph. The signal propagation from skin to cortex is presented according to [81] and [50] in figure 26. A larger print of this figure is added in the appendix, 61. The signals from the overlapping receptive fields are not directly propagated to the central nervous system (CNS), see figure 27. The information is relayed in different relay points. Where a process of divergence and convergence is applied to enable for reliable and meaningful propagation of the information from the mechano-receptors to the CNS, see figure 28. The first step of convergence is the innervation of a cluster of receptor cells by a single dorsal root ganglion.

Thus the receptive field represented by a dorsal root ganglion is larger than the receptive field of a single receptor cell. The information is further relayed in the medulla and in the thalamus. In each relay point the information converges further. A single nerve cell in the CNS may receive action potentials form multiple receptive fields. The virtual receptive field of this CNS neuron is lager than the actual receptive field. On the other hand dorsal root ganglia make contact with various second order sensory neurons, thus the information of a single receptive field is spread to multiple second order sensory neurons, this effect is called divergence. To avoid that the information is spread too far, limiting lateral inhibition processes are realized by so-called interneurons. These small neurons connect the second and higher order neurons. There are different inhibition

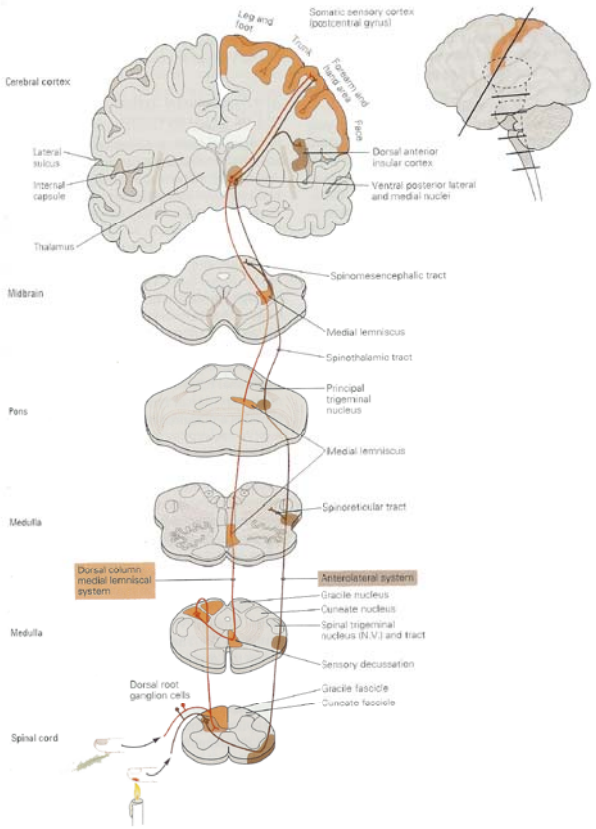

Figure 26: Signal propagation from skin to cortex, taken from [50]

processes that enable for a "the winner takes all" - strategy [50]. Simplified the process can be described as a comparison of the action potentials of neighboring neurons, see figure 29. According to the strategy only the signal from the most excited neuron is propagated further.

Abstraction of the functional principle; Nature's strategy

The information of the overlapping receptive fields is utilized to ensure reliable signal propagation to the CNS. Therefore strategies of convergence and divergence of the transmitted information are applied. As the firing patterns are propagated via connected nerve fibers the signal is transduced several times from one means of propagation to another (electrical to chemical to electrical and so on). Those relay points offer the possibility to route, amplify or inhibit electrically propagated signals. While they are

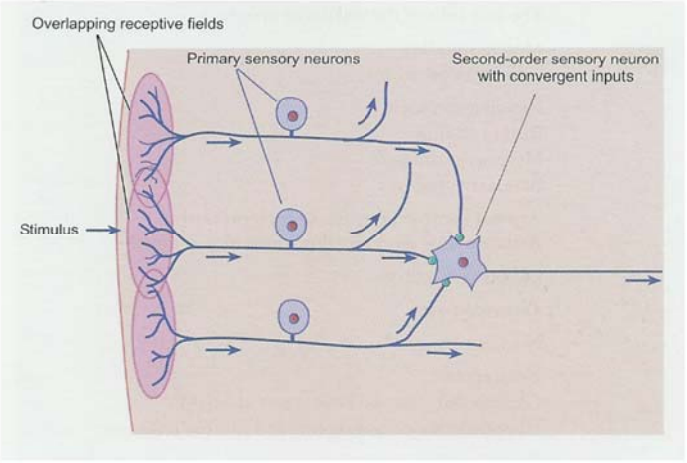

Figure 27: Overlapping receptive fields, taken from [81]

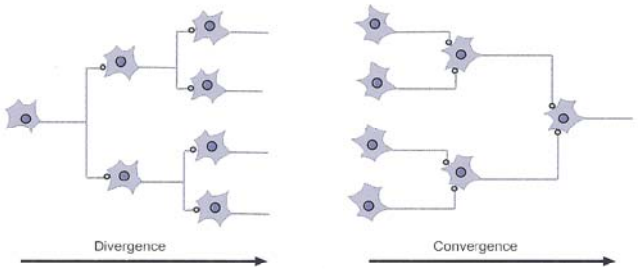

Figure 28: Divergence and convergence, taken from [81]

transmitted over the synaptic gap as chemical information, inhibiting chemicals can easily suppress the propagation of the signal. Hence a strategy of: the winner takes it all is realized. The redundant data is used in contrast enhancing mechanisms.

Propagation of the functional principle to a technical system

The realization of mechanisms of convergence of the gathered information is very useful if the resolution of the sensor is higher then required. But in combination with overlapping sensible fields and the resulting redundant data convergence becomes interesting. The spare information can be utilized in contrast increasing mechanisms. Sensors applied within an elastic material are likely to provide redundant data as the mechanical stimulus is transferred from one sensory cell to the neighboring through the

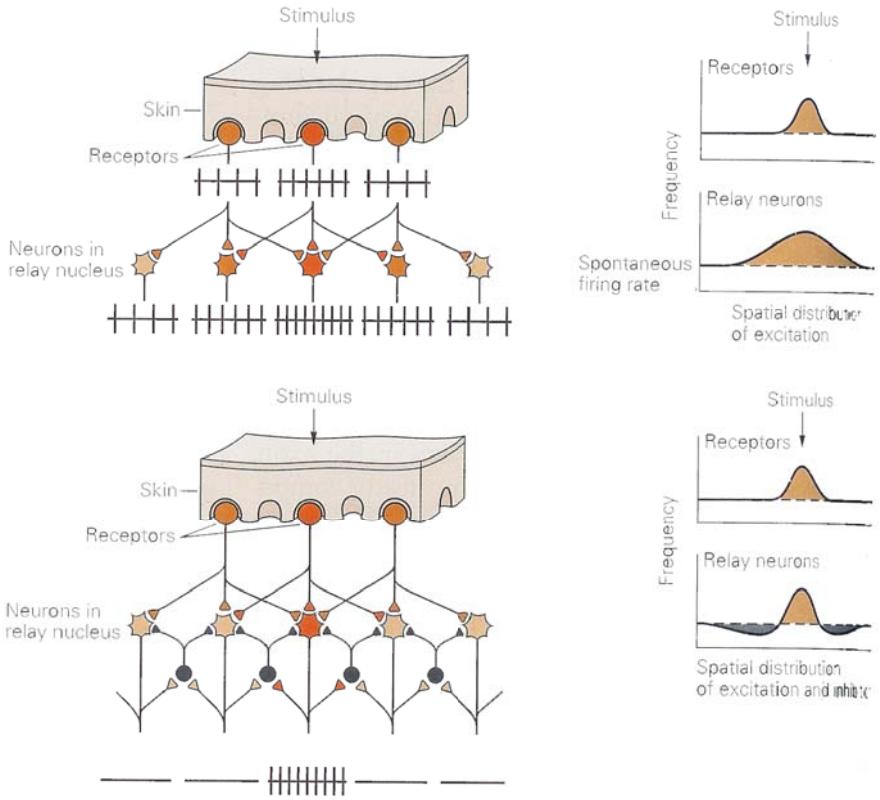

Figure 29: Lateral inhibition, taken from [50]

elastic sensor material. Furthermore lots of redundant data will be provided if the indentation probe is larger than the resolution of the sensor therefore a convergent signal transmission would be paying. Hence the necessary number of readout wires could be minimized. Furthermore the encoding of the contact location via the identification of the excited "nerve fiber" could be realized in a technical system. Therefore the signal of the single sensory cells could be labeled and propagated via a single wire.

Possible technical approaches

A sensor setup of distributed wires within a piezoresistive fingertip matrix would allow for a measurement of resistances between every combination of wires. If a group of wires is connected the resistivity between the group and a single reference wire would

be enabled. Thus virtual clusters of sensory cells with partly overlapping sensory fields are created that are "innervated" by few artificial "nerve fibers". Even if only pairs of wires are evaluated 2^n readout combinations would be possible. Thus the number of readout wires could be decreased without decreasing the resolution. In addition there are operational amplifiers available that enable a comparison of analog signals, e.g. from a piezoresistive sensor, and thus enable a system of converging signals in a technical system.

4.3.4 Discussion

The derived approaches are highly variant regarding their sophistication and the efforts necessary for their realization. Hence not all the approaches are suitable for the application in DLR's Hand-Arm system. The proposed approaches have to be evaluated according to technical feasibility, short term - long term chances, effort, benefit etc. Therefore in the following chapter a rating matrix is applied.

4.4 Derivation of a bio-inspired sensor setup

The proposed bio-inspired approaches towards intrinsic solutions for the conflicts of goals are assessed according to their technical feasibility, effort and benefit for DLR's new Hand-Arm system. The most convenient approaches are combined to a bio-inspired sensor setup for DLR's Hand-Arm system. To realize the assessment of the derived approaches a rating matrix is applied. Therefore every approach is analyzed according to the technical feasibility, the resulting benefit and the required effort as well as the estimated time frame. The criteria are weighted and performance figures are calculated. According to the performance figures the realization of the proposed approaches is classified. If there is no technical feasibility the approach is rated as "none;(0)", if there is basic research necessary for the approach is rated as "realization at long-term, 5 years;(1)" or "medium-term, 2 years;(3)". Approaches that are likely to be realizable at short term are rated with "within this study;(9)", see figure 30. Exemplarily the

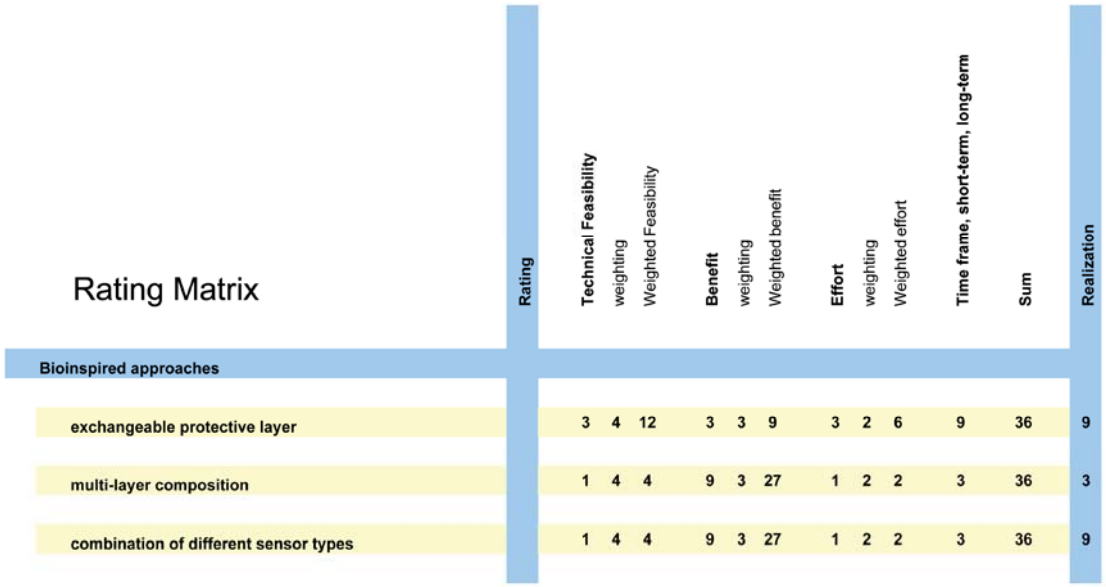

Rating Matrix	Rating	Technical Feasibility	weighting	Weighted Feasibility	Benefit	weighting	Weighted benefit	Effort	weighting	Weighted effort	Time frame, short-term, long-term	Sum	Realization
Bioinspired approaches													
exchangeable protective layer		3	4	12	3	3	9	3	2	6	9	36	9
multi-layer composition		1	4	4	9	3	27	1	2	2	3	36	3
combination of different sensor types		1	4	4	9	3	27	1	2	2	3	36	9

Figure 30: Rating matrix

evaluation of the exchangeable protective layer is presented. The approach is classified according to: The technical feasibility is state-of-the-art(3), weighted(4). The achievable benefit is considerable(3), weighted(3); and the necessary effort for the realization is low(3), weighted(2). Resulting from the low effort the time frame for the realization is rated with "short-term;(9)". Thus the performance figure is calculated with 36, resulting in a rating of the realizability of "within this study;(9)". According to this procedure all proposed approaches are analyzed and classified. The entire rating matrix is shown in the appendix, 60. Approaches that can be realized within this study:

- exchangeable protective layer
- combination of different sensor types
- arrangement of sensors in different depth
- measurement of pressure and strain
- overlapping receptive fields
- virtual clusters of sensory cells

- distributed artificial nerve fibers
- superficial sensor
- "dermal" sensor

Approaches that are promising at medium-term:

- multi-layer composition
- generation of an proportional electrical signal
- encoding of the signal to a frequency signal
- convergence
- divergence

Approaches that are promising at long-term:

- artificial papillary structure
- labeling of the sensory channel
- anisotropic sensing properties

The derived technical approaches that are likely to be realizable within this study are combined to a bio-inspired sensor setup. As proposed, different sensor types will be arranged in different depth, to create a fingertip sensor that is capable to measure pressure and superficial strain. A "dermal" sensor enabling for pressure measurement and the analysis of the force vector will be designed. Starting form the promising results of the preexamination of different piezoresistive materials the possible application of those materials in a compliant fingertip sensor is evaluated. The setup of the pressure-sensitive "dermal" sensor will be based on the formation of sensory cells between multiple metal wires cast into a piezoresistive matrix material forming a compliant fingertip. If the matrix is compressed the piezoresistive material separating the

metal wires shows a decreasing resistance. If a voltage is applied to the interesting wires a current through the piezoresistive matrix material is measurable. To realize the "dermal" sensor metal wires will be cast into the piezoresistive matrix forming the artificial tissue surrounding the bone. The piezoresistive matrix material between the endings of the wires forms pressure-sensitive sensory cells. If the wires are combined for the measurement, virtual clusters of sensory cells are created.

Since the sensory cells of the artificial "dermal" sensor are located relatively deep in the sensor matrix the receptive fields of the sensory cells are expected to be relatively large and show diffuse borders. To enable superficial strain detection a strain-sensitive layer will be designed for the fingertip. The superficial sensor layer will be based on a highly elastic material. Therefore the possible application of piezoresistive materials as strain sensors will be investigated. The whole setup will be covered with a thin exchangeable protective layer, see figure 31. The setup is designed to surmount the

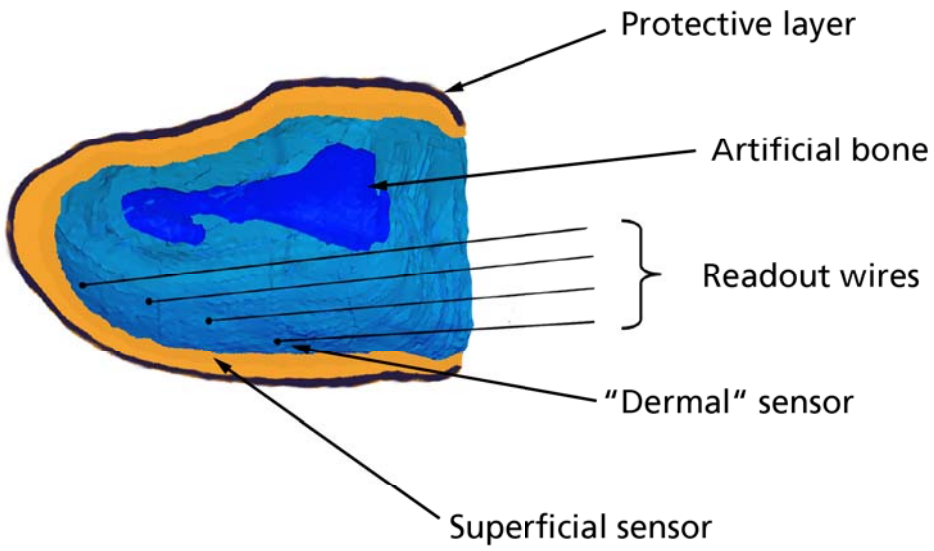

Figure 31: Bio-inspired sensor setup, based on NMR data of a human fingertip, [82]

conflicts of goals between the different requirements. The conflict between the claim for a durable sensor surface and the required $1g$ minimum sensitivity is intrinsically

solved by the layer composition and the arrangement of the different sensors within the fingertip. The superficial sensor layer allows for the detection of very small forces. As this sensor will consist of a highly elastic material that will be literally thin-skinned. Therefore it will be covered by a ultra-thin protective layer. The protective layer will also contribute to the solution of the conflict between the demanded low hysteresis of the fingertip sensor and the required applicability on a viscoelastic artificial tissue. The elastic layer of the superficial sensor in combination with the protective layer will enable for fast restoration after small indentations.

But even if the underlying artificial tissue is plastically deformed the combination of different sensor types offers means to compensate these effects. For example the information "no contact" form the superficial sensor can be used to reset the dermal sensor. Although not all the derived approaches will be realized within the proposed sensor setup, it is a first attempt towards intrinsic solutions for the most important conflicts:

The required detailed contact information, a high resolution and the available few readout wires. The proposed sensor setup offers the possibility to vary the resolution of the superficial sensor according to the minimum required discriminatory power at the interesting site of the fingertip or hand/arm. This very simple strategy enables for a significant reduction of the readout wires without a derogation of the desired dexterity of the robotic hand.

The arrangement of specialized sensors for different modalities of the stimulus within different depth of the fingertip sensor enables for detailed contact information. Thus the sensor setup will be able to discriminate the exact contact location, to measure the applied force, analyze the force vector and to detect shear forces as well as object slippage. In combination with overlapping receptive fields of the superficial sensor, the possible formation of virtual clusters of sensory cells might be an attempt to provide detailed contact information without the need of huge numbers of readout wires.

4.5 Discussion

Starting from the analysis of the general and special requirements conflicts of gaols between the requirements have been identified. The conflicts of goals have been assessed and unsolvable conflicts of goals have been outlined. For these conflicts of goals bionics has been applied to derive possible technical approaches towards intrinsic solutions. The derived technical approaches have been assessed and classified. Approaches that are likely to be realizable within this study have been selected and combined to a bio-inspired sensor setup for DLR's Hand-Arm system.

Within this study possible pressure and strain-sensitive materials and their combinations will be investigated. For the proposed sensor setup a proof of concept has to be performed. If possible, a prototype fingertip sensor featuring the bio-inspired sensor setup will be realized. Although the remaining approaches are promising they are not treated within this study for reasons of time. The relevance of the dermo-epidermal junction in the filtering and preprocessing of the mechanical stimulus has been hypothesized and might be interesting for future investigation.

To be able to proof the concept of the proposed sensor setup and to facilitate the realization of a sensor prototype a special testbed is required. Its development and realization is described in the next chapter.

5 Development of a testbed for artificial skin

The testbed is basically designed to conduct indentation tests to be able to determine whether a sensor prototype meets the requirements presented in chapter 2. But the testbed will also be used to support the evaluation and optimization of different pressure-sensitive materials and sensor setups. A long-term application is the utilization of the testbed as calibration unit for tactile sensors mounted to robotic hands and arms. The following chapter describes the development and the applied components of the testbed.

5.1 Assessment criteria for a tactile sensor

As this thesis aims towards the development and optimization of the hardware of a tactile sensor and for reasons of economy only criteria related to the mechanical setup of the sensor will be considered in the development of the testbed. To enable for the hardware optimization the following selection of the general requirements has to be testable with the testbed:

- $1mm$ *to* $2mm$ spatial resolution
- $1g$ minimum pressure sensitivity
- about $1000 : 1$ dynamic range
- monotonic output response
- at least $100Hz$ frequency response
- good stability and repeatability
- low hysteresis

An other goal of the development of the testbed is a maximum flexibility and accuracy at rational cost. Therefore the elements of the testbed are selected according their

cost-benefit ratio. If applicable elements that are available within the institute are to be applied.

5.2 Development of the testbed

As the developed artificial skin is still in the phase of a prototype, only the most important requirements can be met. Therefore the testbed at present only has to be able to evaluate those requirements. To be able to evaluate the other requirements in the future the testbed is to be designed in a modular concept. For the integration of additional features in the future, and to schedule future extension of the testbed towards a calibration facility, sufficient designed space has to be provided. Hence a testbed has to be designed that is capable to test, analyze and calibrate future tactile sensing devices mounted on a robotic finger, hand or even a complete forearm. To allow for indentation tests an indentation probe and an opposing support for the sample fixed in a framework have to be provided, see figure 32. The construction of the framework is presented in the next paragraph.

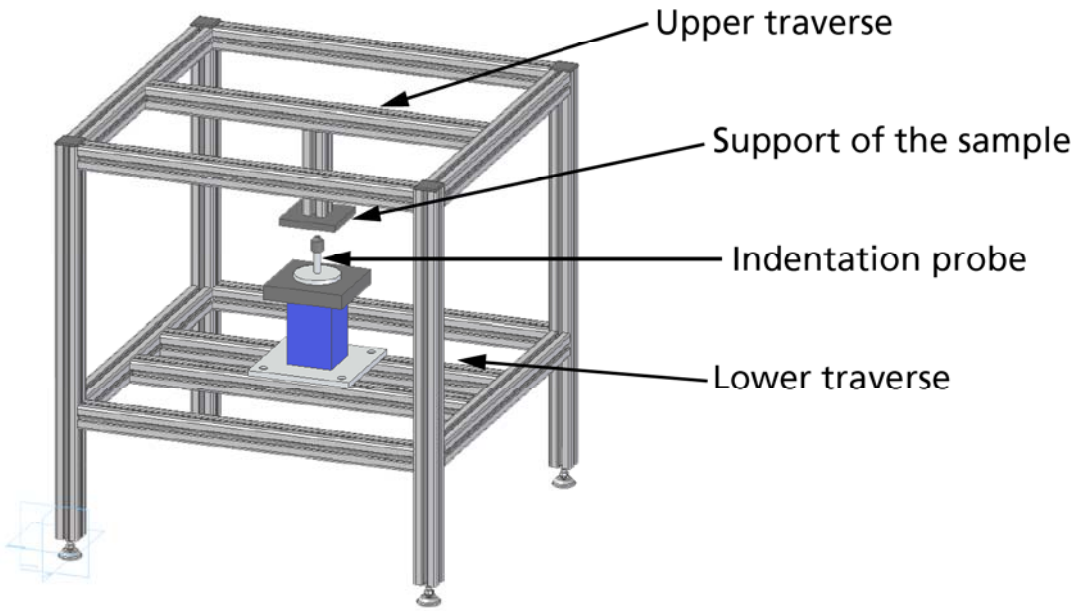

Figure 32: Framework of the proposed testbed

5.3 Components of the testbed

5.3.1 Framework

For the testbed a framework that facilitates future modification and fixation of additional components is required. In addition the framework has to provide sufficient mechanical support to ensure, that the motion between the indentation probe and the tested skin sensor is not affected by the deformation of the framework. Therefore standard aluminium profiles have been chosen for the framework. The testbed has to be capable to exert loads equal or higher than the sensor has to face in the future application.

To simulate indentations that are common in human environment forces ranging from mN-scale to $500N$ are required. To determine the maximum deflection of the framework the bending of the least stable element, the single aluminium profile of the upper traverse, is calculated. The profile of the upper traverse is fixed to the frame profiles. If the profile of the upper traverse is bent, the profiles of the frame are loaded with a torsional moment. As the applied profiles show a low torsional stiffness the bearings between the upper traverse and the frame profiles are regarded as pivotable. Therefore the aluminium profile is treated as a beam in bending, fixed at both ends in pivotable bearings, loaded at the center. Thus the following equation has to be applied for the calculation of the deflection:

$$\Delta z = \frac{F \cdot l^3}{48 \cdot E \cdot I} \tag{2}$$

Where Δz is the deflection at the center of the profile, F the force applied at the center, l the length of the profile, E the Young's Modulus of the material of the profile and I the Moment of Inertia of the profile. For the calculation of the applied aluminium profile the following values are used: $E = 70000\ \frac{N}{mm^2}; l = 600mm; I = 9cm^4$. For an applied force of $500N$ the expected deflection at the center of the profile is calculated with $0.357mm$. Maximum forces for today's robotic hands are about $50N$, thus the deflection at the center of the profile is expected to be less or equal to $0.0357mm$. For test of the desired highly compliant tactile sensors and the applied very small forces

the deflection of the framework is negligible. But for tests of thin and rigid sample at high forces, e.g., for the determination of the maximum applicable force of the sample, the deflection has to be considered in the calculation. The assembled framework of the testbed is shown in 62.

5.3.2 The support for the sample

The support for the sample has to be designed for a variety of tasks, the fixation, the locomotion in two axes and the electrical connection of the sample. To avoid outside influences on the sample, resulting from deformation through clamps or vacuum, self adhesion, or if this is not sufficient, adhesive foil is used to ensure a reliable mechanical connection between sample and support. For the tests of fingertip-shaped sensors the support is retrofit with a receptacle for future artificial bones. To enable the testing of the spacial resolution the support of the sample is equipped with two μm-positioning boards for the locomotion in x- and y-axis, which in the first version are non-actuated and have to be moved manually, see 63.

To be able to test sensor prototypes without an insulating coating the support as well as the indentation probe have to be electrically insulating. As not only sensor prototypes with cast in wires have to be tested, but also sample of piezoresistive materials without wires, the testbed has to offer the possibility to acquire the resistance between the surfaces of a test sample. Therefore contact plates have to be attached to the support and the indentation probe.

5.3.3 Actuator

In the first version the testbed will be equipped with a single actuated axis. For reasons of accuracy and economy one of DLR's homegrown linear motors will be used as actuator for the z-axis, see 64. The incorporated mechanics are based on DLR's patented planetary roller spindle drive. The linear axis is actuated by a dead spindle forming a self-blocking gear. This setup enables for repeatable indentation as the self-

blocking gear shows very little play. For further minimization of the play the motor is sheeted upside down in the testbed. The maximum force is approximately 450N at a top speed of $200\frac{mm}{s}$. The motor is supplied with $24VDC$ and offers a traverse path of $52.4mm$. Moreover the motor is equipped with an internal 14-bit position sensor with a resolution of $3.2\mu m$ and a force sensor enabling for position, force and impedance control. As the resolution of the internal force sensors (about $1N$) is not sufficient for the utilization as measuring instrument an additional external force sensor is required.

As mentioned before, the testbed will be expanded in future stages of extension. Regarding actuators, the installation of an actuated xyz-moving unit and a piezo-actuator for the stimulation of the skin with defined vibrations is planned.

5.3.4 Force sensor

The quality of the piezoresistive effect of the different materials and their combinations has to be measurable. Therefore the testbed has to be equipped with a force sensor offering a sufficient resolution and a broad range. As planned for future stages of extension not only forces in one axis but multidirectional load should be measurable. Therefore the testbed will be equipped with a 6DoF force torque sensor (FTS). Hence different force torque sensors have been considered, e.g. strain gauge based FTS (ATI Micro, Nano) and optical FTS (Space Control OFTS). The most important properties of the force sensor are a high resolution and a force range covering forces from mN to several hundred N, as they are common in human every day environment.

As the linear motor provides sufficient power the size and weight of the force sensor is of secondary importance. Regarding cost-performance ratio the SpaceControl OFTS offered the best opportunity, see 65. The opto-electronic transduction of the OFTS is based on DLR's Space Mouse technology. The sensor needs a deflection (maximum $\pm\ 0.1mm, \pm\ 0.3°$). The OFTS enables for the analysis of a load in 6DoF. The maximum applicable force is $\pm\ 400N$ with a minimum resolution of $0.02N$. Besides forces also torque in measurable, where the maximum torque is specified with $\pm 20Nm$ at a

minimum resolution of $0.01Nm$. While the support of the sample will be mechanically coupled to the framework via the positioning boards, the indentation probe will be mounted to the FTS. To enable the test of the spacial resolution the testbed must offer the possibility to use different indentation probes without time-consuming re-tooling. A valuable and low-priced setup for fast tool exchange are three jaw drill chucks, as commonly used in power drills. Moreover the drill chucks are available for mm-scale drills and are therefore suitable for very small indentation probes. To allow for the mechanical coupling the drill chuck is modified and an adapter plate is constructed.

5.3.5 DAQ-Card

For the acquisition of the data form the tactile sensors a data acquisition (DAQ) card is required for the testbed. Due to the fact, that at the beginning of the development of the sensor hardware only few readout channels are expected, only a DAQ-card with a small amount of input channels is required. Hence for the first version a used DAQ-card, which is available at the institute, will be integrated to the testbed. The DAQ-card (NI 6023E PCI) offers 16 analog input channels with a resolution of 12 bits and a sampling rate of 200 $\frac{kSamples}{s}$. The analog input signals can range from $\pm 0.05V \; to \; \pm 5V$. This enables a resolution of $2.44mV$.

5.3.6 Pre-amplification

Preliminary tests of the sensor patches showed resistances ranging from $10k\Omega \; to \; 50M\Omega$. As the sensor will be supplied with 5V DC from the DAQ-card the resulting current through the sensor material is expected to range from:

$$I_{10k} = \frac{5V}{10k\Omega} = 0.5mA \; to \; I_{50M} = \frac{5V}{50M\Omega} = 0.1\mu A \tag{3}$$

The current has to be transduced to a voltage that is measurable with the DAQ-card. To be able to utilize the full modulation amplitude of the DAQ-card a maximum input voltage of $5V$ is required. Thus a $10k\Omega$ precision resistor is required for the

transduction. The input voltage ranges from $5V$ *to* $1mV$. As the DAQ-card requires a minimum input voltage of $50\mu V$ not the whole range of resistivity of the tactile sensors would be measurable. For this reason and to ease the electrical connection of the sensor patches a pre-amplification board is desirable. Therefore an operational amplifier circuit with an hyperbolic characteristic curve is designed and realized.

5.3.7 Computer system and software

The presented components of the testbed are connected to a realtime computer utilizing QNX as operating system. The DAQ-card is directly connected to the PCI bus, while the FTS and the linear motor are connected via the serial ports of the PC. The components are addressed using a Matlab/Simulink model which is running on an additional windows PC. The communication between the two computers, that are interfaced via TCP/IP, is scheduled by RT Lab. To allow for a direct control of the components of the testbed from the Matlab/Simulink model special drivers are developed in cooperation with DLR's IT specialists.

This rather complex setup enables both, the real-time compatibility of the active components and the application of a powerful readout and control software. Therefore a Matlab/Simulink user interface is developed to enlarge the flexibility and adaptability of the control and to enable an easy handling of the control parameters. This interface allows for the determination of the test parameters and enables automated test procedures with tunable parameters. In addition the model affords the display, conditioning and storage of the readout signals from the FTS and the DAQ-card. Due to the utilization of a real-time operating system the acquired data from the different devices is under conditions of chronological synchronism. Therefore no trigger signals or external timestamps are necessary what facilitates an efficient data evaluation.

5.4 Integration and assembly

The pre-trimmed aluminium profiles are assembled forming the framework of the testbed. Following linear motor, FTS, support and pre-amplification board are integrated to the framework. For further reduction of the play the support for the sample is attached to the upper traverse while the linear motor is fixed on the center traverse. Due to this arrangement gravitation prevents play in the linear motor. The sample is attached to rear side of the support and is indented from below.

The exchangeable indentation probes can be fixed in the drill chuck which is attached to the FTS via a setscrew and the constructed adapter plate. The FTS itself is fixed to the upper plate of the linear motor which is mounted to the center traverse of the testbed. With this setup the forces exerted by the linear motor to the test sample are transmitted to the framework of the testbed, see figure 33. The components are connected to a central power supply and to the computers. Figure 34 shows the indentation probe and the support of the sample as well as the contacting plates in detail.

5.5 Calibration of the testbed

5.5.1 Calibration of the linear motor

To scale the command parameters of the linear motor a high precision gauge is attached to the testbed. Thus the measurement can be conducted between the indentation probe and the support of the sample. For the calibration the traverse path of the linear motor resulting from the commands in the Matlab/Simulink model is measured. After this the increments are scaled to enable a repeatable and exact determination of the indentation in μm. As the result of the scaling the altering of one increment within the Matlab/Simulink model results in a displacement of the linear motor of $10\mu m$.

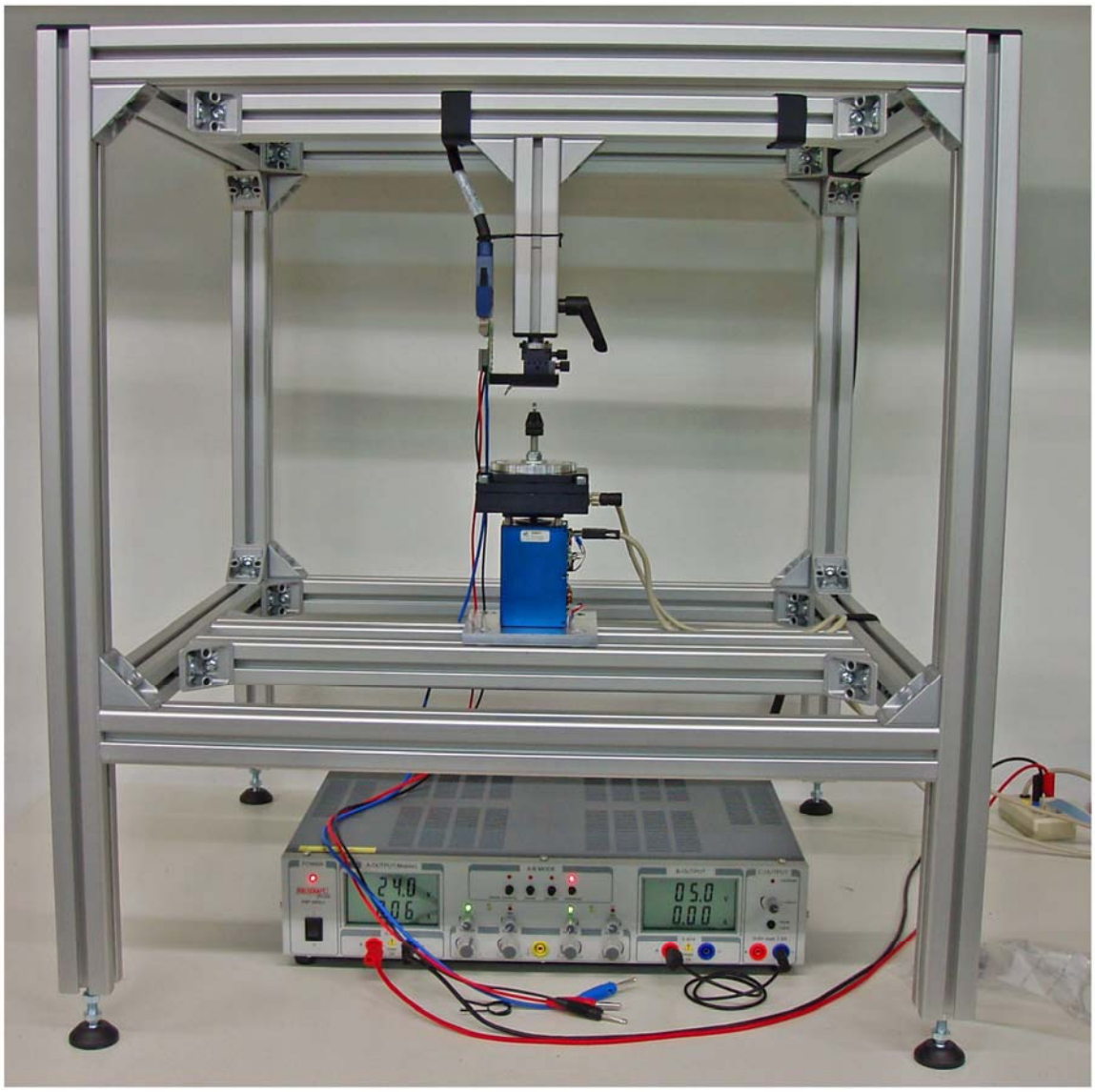

Figure 33: Assembled testbed

5.5.2 Calibration of the force sensor

To ensure, that the readout values of the FTS correlate with the actual external load, the FTS has to be calibrated. For it the FTS is loaded in its z-axis with precision weights. The readout values are scaled in the Matlab/Simulink model to ensure an exact mapping of the exerted forces. The calibration showed, that the properties, guarantied by the manufacturer are abided. The resolution of the FTS is $20mN$. To facilitate data analysis the readout values are scaled in N.

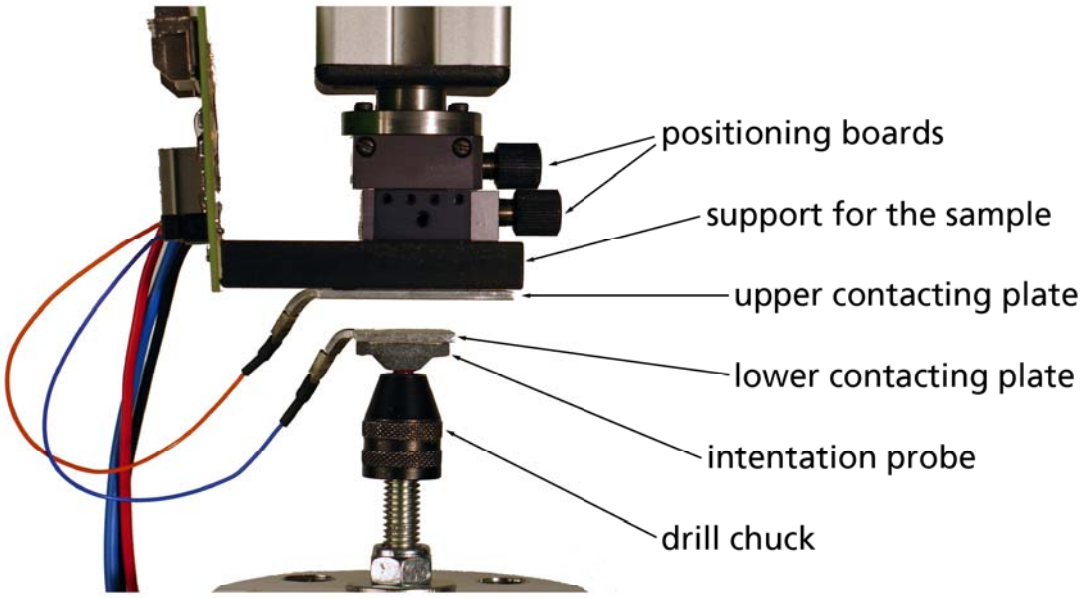

Figure 34: Detail of the testbed

5.5.3 Evaluation of the pre-amplification board

To evaluate the amplification board, different precision resistors with known resistivity are connected to the board and the hyperbolic characteristic curve of the operational amplifier circuit is recorded. The recorded data is analyzed with Matlab and the inverse transfer function is calculated and realized in an additional Simulink-block. This enables to display the measured resistivity in Ohm. Thus the correlation between the indenting force, the indentation depth and its derivatives and the resulting resistances are evaluable. At the same time this procedure allows for the verification of the properties of the hyperbolic amplification.

5.6 Discussion

Starting from the selection of the requirements that have to be evaluable a testbed was designed. Special attention was payed to the realization of a modular concept enabling for future extension of the tedbed. The testbed was constructed, assembled and the utilized components relayed to a readout and control computer setup. A

Matlab/Simulink model was developed which allows for tunable automated testing and comfortable data analysis. As a result of the conducted work a test environment that is capable to support the development of artificial skin prototypes could be realized. The current version permits the evaluation of material properties and the repeatable indentation testing of sample, realized in flat square or fingertip shape. For future, more elaborate, tactile sensors the testbed can be extended.

6 Evaluation and Optimization of skin materials

Within this section different piezoresistive materials and their applicability in the bio-inspired sensor setup are investigated. Two different types of sensors are developed for the proposed "dermal" and superficial sensors. For the "dermal" sensor the piezoresistive behavior under pressure is examined. While for the superficial sensor a possible adaptation of the researched sensor materials as strain sensor is considered.

6.1 Evaluation of the existing SEBS-patches

As presented in chapter 3, various SEBS sensor patches have been manufactured prior to this study [89]. To evaluate the quality of the piezoresistive effect and to determine whether the proposed sensor setup is applicable for the "dermal" sensor of the anthropomorphic fingertip the SEBS patches are tested on the testbed.

6.1.1 Materials and Methods

The examined SEBS patches have been manufactured prior to this study, [89]. Different mixing ratios of Kraiburg Thermolast TF0STL compounded with Cabot XC72 have been produced. The patches are equipped with cast-in steel wires, see figure 35.

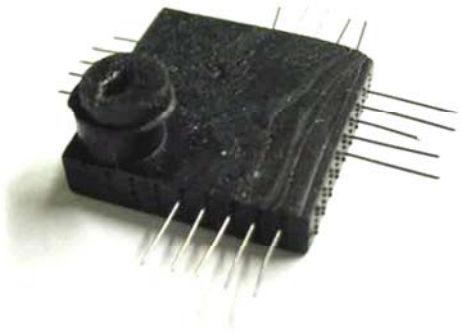

Figure 35: SEBS testpatch, taken from [89]

For the tests the patches are covered with an electrically insulating foil to ensure the sole measurement of the effects within the patch. A square aluminum plate with a surface of $400mm^2$ is used as indentation probe. Thus the probe covers the entire patch avoiding possible influences of a varying indentation location. For the readout of the resistance two crossing cast-in wires are connected to the pre-amplification board.

6.1.2 Experiments

The patches are loaded with a trapezoid indentation path, shown in figure 36. Therefore

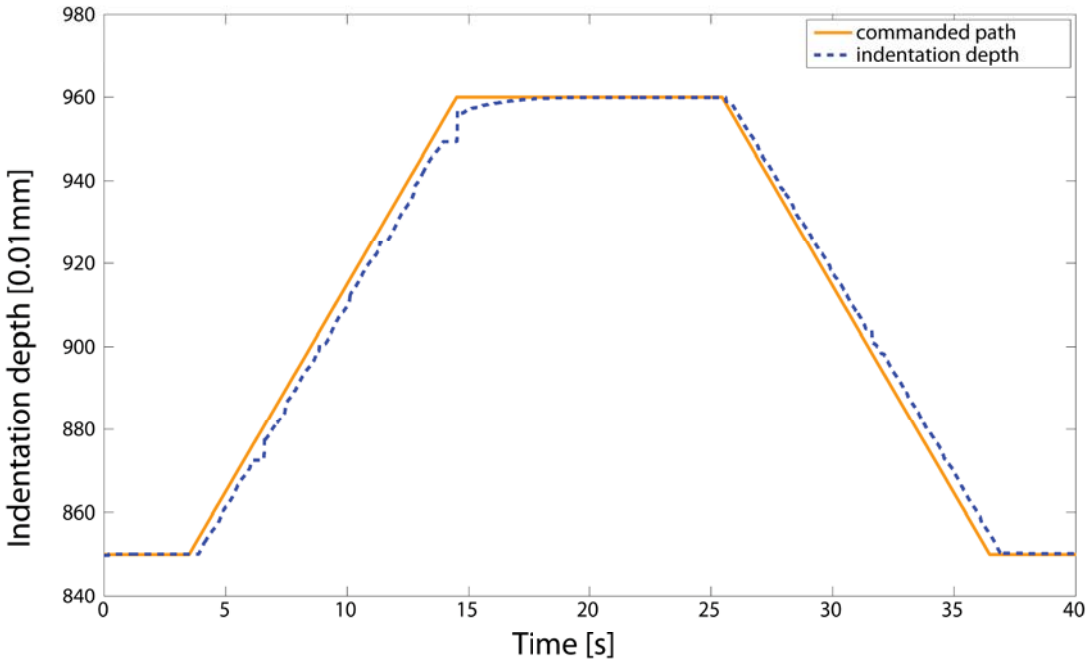

Figure 36: Indentation curve

the linear motor is operated in position control mode and commanded to indent the patch with a certain speed, stop and maintain a pre-set indentation depth for a defined period of time and then to release the patch, again with a defined velocity. The difference between the commanded position and the indentation depth results from the position control of the linear motor.

For every mixing ratio a patch is tested with the following parameters:

- indentation depth $1mm$
- indentation speed $100\frac{\mu m}{s}$ *to* $1000\frac{\mu m}{s}$
- maximum indentation force $55N$
- hold time $10s$
- release speed $100\frac{\mu m}{s}$ *to* $1000\frac{\mu m}{s}$

For the evaluation of piezoresistive effect the following data is recorded and stored:

- time
- commanded indentation depth
- actual indentation depth
- force in z-axis
- measured voltage
- calculated resistance

6.1.3 Results

The SEBS prototype patches manufactured by [89] clearly show a piezoresistive effect. But the test of the patches on the testbed also show an unexpected behavior. If the load is increased faster than $500\frac{\mu m}{s}$ the measured voltage shows an unexpected dip. Contrary to the expected behavior an initial increase of the resistance is observable, see figure 37. In region A the force increases exponentially due to the indentation, while the measured voltage shows an unexpected behavior, it decreases (i.e., the resistance increases). Within region B the patch exhibits the expected piezoresistive behavior, as the voltage increases exponentially while the force increases linearly. During the

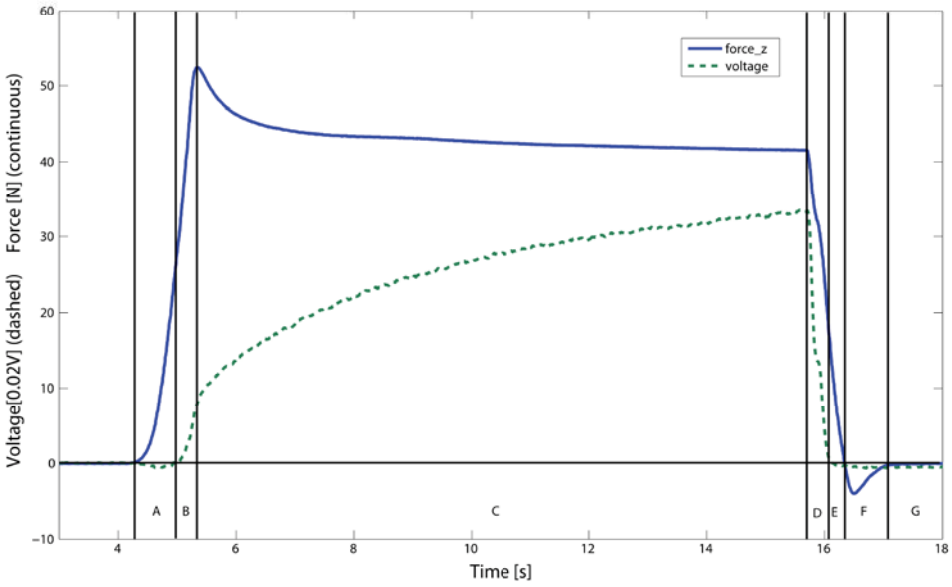

Figure 37: Piezoresistive behavior - SEBS

pre-set hold time (region C) the curve of the force shows a typical course for highly compliant materials. While the given position is maintained the material shunnes from the load and the force slowly decreases. Due to the applied force an increasing amount of conductive pathways is formed within the piezoresistive matrix material, therefore the voltage slowly increases towards a saturation. In region D the voltage decreases proportional to the decrease of the force. While the force decreases further in region E, the voltage converges to a constant value slightly below its initial value. Within region F a negative force is observable, while the measured voltage decreases only slightly. At the end of the indentation test the force reaches its initial value and the voltage maintains a value slightly below its initial value. Following possible causes of the observed behavior are discussed.

6.1.4 Possible causes

If pressure is applied to the patch, the matrix material shunnes from the load. Due to the difference in elasticity a relative movement between wires and sensor matrix is

induced. Fast indentation of the patches results in increasing resistivity. This effect might be caused by an altering transfer resistance between matrix and cast-in wires. When the matrix material is deformed fast it partly lifts off from the metal wires and the transfer resistance temporarily increases. Possibly the slow indentation allowes the material to maintain sliding contact to the wires, which has only minor influence to the transition resistivity. To show the causative effects in collaboration with DLR's simulation experts the behavior of the SEBS patches with cast-in steel wires is simulated.

Materials and Methods

To minimize computational effort, a thin slice of matrix material is calculated in $2D$. Within the matrix material a hole is defined containing a metal cylinder representing the wire. The connection between the cylinder and the surrounding matrix is defined as loose. The following parameters are applied:

For the wire the following "AL2014" is used. It exhibits an isotropic density of 0.00279355 $\frac{g}{mm^3}$, a Young's Modulus of $7.30844 \cdot 10^{10}$ $\frac{g}{mm \cdot s^2}$, and a Poisson's Ratio of 0.33). For the compliant matrix material "Silastic" is applied, with an isotropic density of 0.0002 $\frac{g}{mm^3}$; an idealized Young's Modulus of $2.05 \cdot 10^6$ $\frac{g}{mm \cdot s^2}$; and a Poisson's Ratio of 0.4)

Experiments

The top plane of the modelled slice of the compliant matrix material is laminarly loaded with a load in the y-axis. While the bottom plane is fixed. To allow the material to shun from the load the side planes are defined as freely deformable. Then the model is statically loaded with $10N$ and the resulting displacement in $2D$ is shown in different colors.

Results

Due to the applied force the matrix material bulges to the sides. In addition, the highly compliant matrix material shunnes from the load and lifts off the wire in the x-axis, 38. To proof the results of the simulation the SEBS patches are examined using

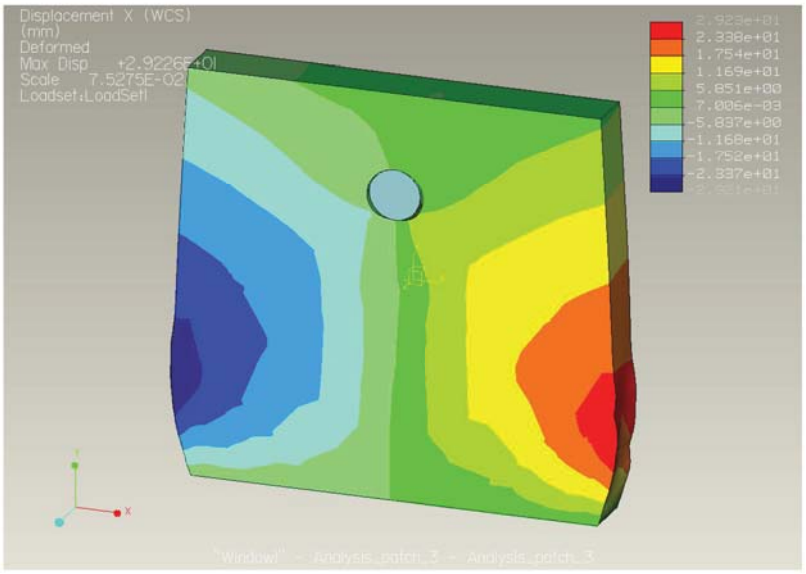

Figure 38: Simulation of the cast-in wire, courtesy of [82]

scanning electron microscopy (SEM), 39. The examination with the SEM reveals the most likely reason for the observed phenomena: The unsatisfying adhesion between the SEBS matrix and the cast-in steel wires. SEM of the cast-in and pulled out steel wires shows that no matrix material at all adhered to the metal wires.

6.1.5 Discussion

The SEBS patches have been examined on the testbed. As predicted in the preliminary tests the patches showed a piezoresistive effect. But the exact measurement of the characteristics of the correlation between indentation and and resulting resistance revealed a non-monotonic, velocity-dependent behavior. This behavior most likely results from the unsatisfactory adhesion between the matrix material and the cast-in wires. Although special pre-treatment of the wires, like grid blasting, prior to the injection

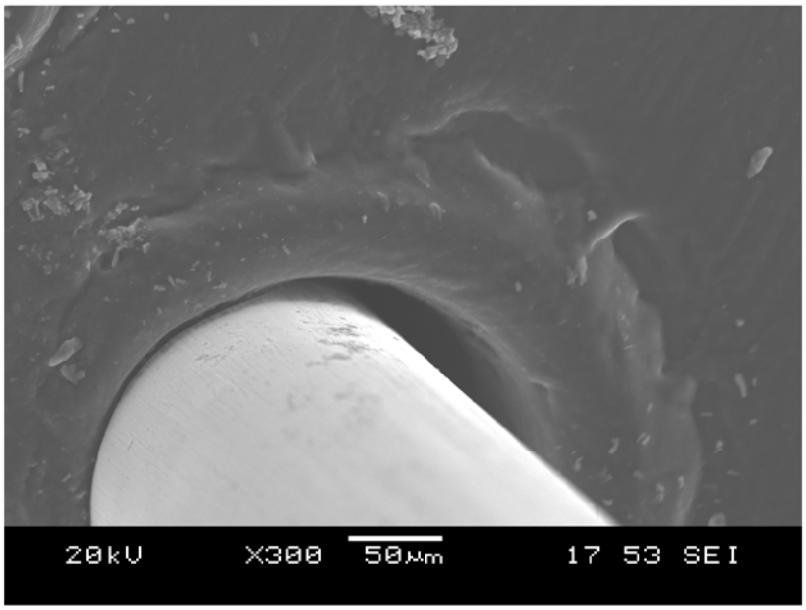

Figure 39: SEM of the wire cast into SEBS

molding process has been applied, no adhesion could be obtained. While the SEBS patches show good mechanical properties the piezoresistive behavior does not show a monotonic output claimed in the general requirements for a valuable tactile sensor. Therefore an application of SEBS in the tactile sensor system of DLR's Hand-Arm system will not be considered. Nevertheless the sensing principle might be applicable with alternative piezoresistive matrix materials.

6.2 Alternative sensor material

A possible substitution for SEBS as matrix material is polysiloxane (silicone). The mechanical properties of silicones are tunable and cover a very wide range from silicone oil to solid crystal. Due to this versatility silicone is used in a broad range of applications and has become an important mass product. Thus lots of different silicones are commercially available at low cost. Silicones offer a series of advantages that make them interesting for application as matrix material for tactile sensors. Of special interest is the low temperature dependency of the mechanical properties and the availability of conducting silicones. In addition, the processing of silicones does not

necessarily require sophisticated and costly processing machinery. This turns silicones into an interesting alternative matrix material for the “dermal” senor setup.

6.2.1 Silicone, fillers and blends

The following section gives a brief introduction to silicones and their processing. The structure of silicones results from the gradual organic modification of quartz, [103]. Silicones rank among the class of polysiloxanes, which are based on oligomer or polymer compounds consisting of altering Si-O-Si compounds. As silicone is tetravalent it is able to bind four oxygen atoms or organic substituents. Depending on the number of attached oxygen atoms the following functionalities are possible: mono-, di-, tri- and tetra-functional. Where monofunctional units form chain terminals, difunctional units form higher molecular chains or rings. While tri- and tetrafunctional units form branching points enabling the formation of spacial cross-linked molecules [103]. Most of the silicones with industrial relevance have methyl groups as organic substituents. According to the combination of the different units a vast variety of products is derivable. For injection molding mostly addition-crosslinking silicones are applied.

Wherein the crosslinking process is based on a platinum-catalyzed conversion of venyl-functional polymers with SiH-functional oligosiloxanes.As this process already starts at room temperature silicones are mostly provided as two-component system. One of the components contains the platinum-catalyst enabling the crosslinking of the two components. The uncured, liquid silicones can be mixed manually or directly in the injection molding machine. The mixed components are filled to a heated mold and cure at elevated temperature and under pressure. For different industrial applications conductive silicones are available. Both, insulating silicones with a specific volume resistance of about $10^{15}\Omega cm$ *to* $10^{17}\Omega cm$ and highly conductive silicones ranging from $2\Omega cm$ *to* $10\Omega cm$ are commercially available. One of the few industrial application where silicones with a specific volume resistance of about $1k\Omega cm$ *to* $5k\Omega cm$ are needed are non-conductive but antistatic silicones. Similar to other polymers filled with conductive particles silicones show a piezoresistive effect at certain filler concentrations.

For industrial applications the piezoresistive effect in conducting silicones is undesired because no pressure dependency is required in standard industrial applications. Therefore manufacturers forbear from the development of silicones with such properties because a little change in the concentration of the filler greatly affects the resistivity. Today many research groups are investigating the processing and behavior of conductive silicones [84, 90, 118, 119]. For the application as pressure sensor a silicone with a conductive filler content close to the percolation threshold is required.

As mentioned before the manufacturers do not offer silicones tuned to the percolation threshold. Thus the available conductive silicones have to be tuned or an insulating silicone has to be self-mixed with conductive particles. The most critical step of preparing the composites and the filler is the mixing of the dry conductive filler with the liquid silicone components. Different mixing techniques have been researched by [40]. Via dry mixing of the composites only a non-uniform distribution of the filler particles has been achieved. This leads to little reproducibility of the resistivity in the different patches. Better but still not totally satisfying results have been achieved if the dry conductive filler is pre-mixed with solvents. A more doable way to obtain a conductive silicone with the desired filler content is to mix a highly conductive silicone, pre-filled by the manufacturer, with an insulating silicone. Thus homogenous distribution of the filler particles and a reproducibility of the desired conductivity can be obtained. Following a first set of test of the piezoresistive behavior of the provided pre-filled conductive silicones is described. According to the results of those teste the most suitable basis material will be chosen for the development of the tactile sensor.

6.2.2 Materials and Methods

Different conductive silicones are evaluated for their application as matrix material for the "dermal" sensor of the bio-inspired sensor setup. Material 1 is developed to form connecting systems for high voltage cables. Both, component A and B are pre-filled with black particles that exhibit a size of tens of nm. Thus the distribution of the carbon black particles in the unblended silicone (mixed 1:1) is uniform and

does not depend on the mixing of components A and B. As structure forming carbon particles are used a low volume resistivity ranging about $45\Omega \cdot cm$ can be obtained using a relatively small (approximately $5w/w$)content of carbon black. Moreover the material is adjusted shortly over the percolation threshold. Materials 2 and 3 are laboratory prototypes, thus no detailed information or data-sheet could be obtained from the manufacturer. To keep the variable parameters at a reasonable level the processing parameters, curing time, pressure, curing temperature and tempering time as well as temperature are not changed. To achieve optimal results the parameters recommended by the manufacturers are applied. For the manufacturing of all test-patches the following procedure is applied:

As recommended by the manufacturer the liquid components A and B are weighed in the ratio $1:1$ and poured into a mixing pot. For the blending a simple kitchen mixer is used. To ensure uniform distribution all components are mixed at top speed of the mixer for 90s per 100g silicone. The mixing time has to be limited as otherwise the curing starts resulting to the applied heat that results from the internal friction in the uncured silicone. The mixed silicone is poured into a $80mm \cdot 80mm \cdot 6mm$ steel mould. To avoid air pockets the mould is overfilled by approximately $20Vol\%$. Afterwards the mould is put into a Collin $P300P$ press with heatable plates and the silicone is cured at $200°C$ and $50bar$ for $600s$. After the pressing the mold is removed and cooled to room temperature in a water quench. Then the silicone patches are removed from the mold and put into a conditioning cabined where they are post cured at $200°C$ for four hours. Applying this process, test-patches of the basis materials are manufactured. Then the resulting patches are tested on the testbed.

6.2.3 Experiments

Same as the SEBS patches, the test-patches of the silicone basis materials are loaded with a trapezoid indentation path, see 6.1.2. For every basis material a patch is tested with the following parameters:

- indentation depth $650\mu m$
- indentation speed $100\frac{\mu m}{s}$
- maximum indentation force $65N$
- hold time $10s$
- release speed $100\frac{\mu m}{s}$

6.2.4 Results

The examined material 2 patch shows a change in the measurable voltage of $200mV$ at a maximum force of $50N$. Whereas the loading with $65N$ of material 3 results in a change in voltage of $600mV$. While material 1 shows a resulting force of $40N$ it exhibits a change in measurable voltage of $750mV$, see figure 40. All tested patches show a piezoresistive effect, but the measured change of voltage is low.

6.2.5 Discussion

The interesting pressure dependent resistance of the silicone patches ranges in the same magnitude as the surface resistance of the patch as well as the transition resistance between contacting plates and the patch. Thus the measurement of the resistance can easily be affected by side effects, which results in a high variability. Although the tests allow for a qualitative evaluation of the different basis materials. As the indentation depth is constant for all indentation test the resulting maximum force allows for a qualitative assessment of the hardness of the materials.

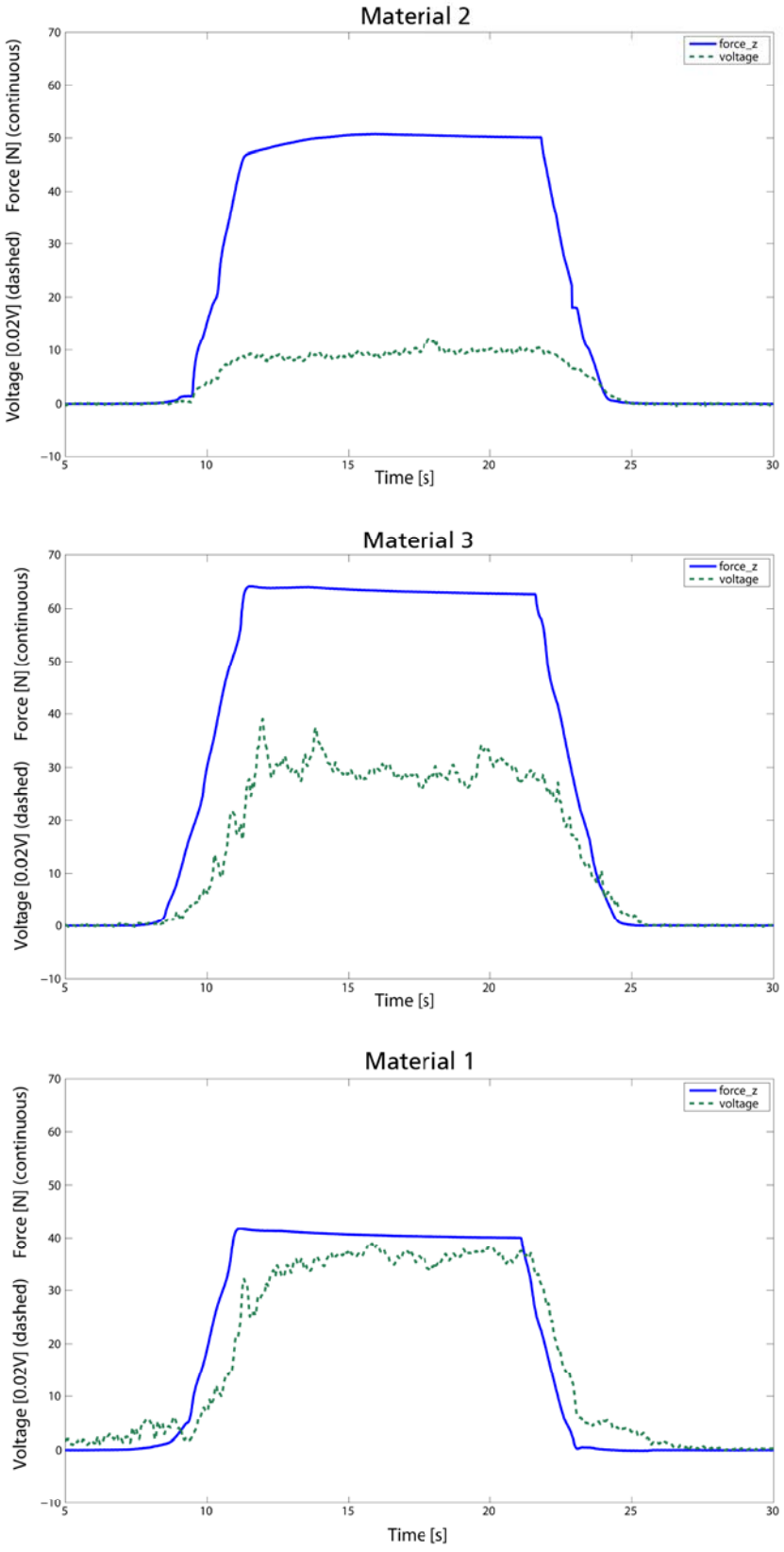

Figure 40: Piezoresistive behavior of the basis materials

Materials 2 and 3 exhibit a higher reset force as they are apparently harder than material 1 (Shore A 40), which is still to hard for the application as matrix material for the "dermal" sensor. The low change of voltage indicates that all materials exhibit a filler content outside the percolative area. Therefore the basis-materials have to be blended with softer non-conductive additives to meet both, a satisfying softness and a high sensitivity to pressure. The content of conductive filler of material 1 apparently is closest to the percolative area, therefore the material exhibits the greatest change in resistance. Another advantage of material 1 is the fact, that the material is jet commercialized and thus will be available for future sensor production. Hence material 1 is a good starting position and will be examined in further tests. As the future availability of the laboratory materials 2 and 3 is not assured, the materials will not be utilized for the further development of the "dermal" sensor.

6.3 Optimization

To be able to manufacture a valuable "dermal" sensor the provided basis material has to be tuned. Following the challenge of the optimization, shown in figure 41 is described. The first challenge is to find a solution that enables both, a pressure-sensitive behavior,

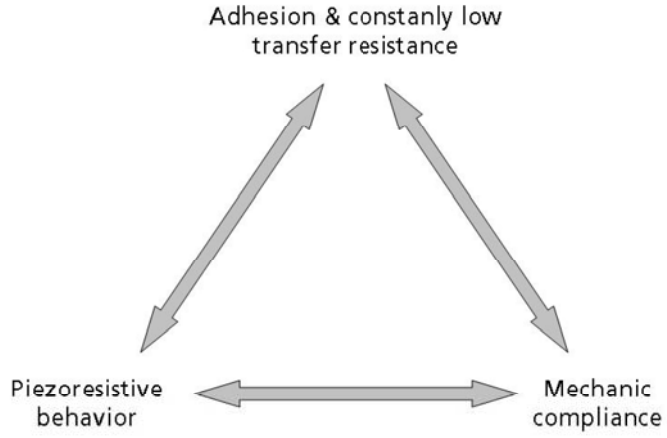

Figure 41: Optimization challenge

ranging about $10k\Omega$ *to* $100k\Omega$, and a compliance comparable to that of the human

fingertip. The second challenge, arises form the results of the preliminary tests of the SEBS patches, that showed the importance of the adhesion between wires and matrix material for a monotonic sensor output. The means to tune the basis material towards a desired property affect the other properties, e.g., the fraction of the carbon black filler affects the compliance, while additives, that help to increase the compliance, do reduce the conductivity. Whereas adhesives enabling a satisfying adhesion affect the measurable resistance. Following the experiments for the optimization of the basis material towards the three desired properties are shown.

6.3.1 Pressure dependent conductivity

To tackle the challenge of the optimization of the piezoresistivity and the softness the provided basis material is blended with different soft, non-conductive materials.

Materials and Methods

The liquid components of the basis material are weighed using a laboratory precision balance (Sartorius Competence CP423S). As recommended by the manufacturer the components A and B are weighed in the ratio 1 : 1 and poured into a mixing pot. Subsequently the components of the additive are weighed and added to a mixing pot. For the blending a simple kitchen mixer is used. To ensure uniform distribution all components are mixed at top speed of the mixer for 90s per 100g silicone. The mixing time has to be limited as otherwise the curing starts resulting to the applied heat that results from the internal friction in the uncured silicone. For the adjustment of the mechanical properties of the sensitive matrix material the following, non-conductive silicone is evaluated in blending tests:

Material 4 with a hardness of Shore $A20$. Moreover the silicone oil (material 5) is tested regarding its influence to the mechanical properties of the sensor material. The mixed silicone blend is poured into a $40mm \cdot 40mm \cdot 1mm$ steel mould. Applying the same process as shown in 6.2.2, blends with different allowance of additives are manufactured.

To be able to determine the influence of the additives to the piezoresistive behavior the silicone patches are tested on the testbed.

Experiments

The mixed silicone patches are loaded with a trapezoid indentation path, see 6.1.2. For every mixing ratio a patch is tested with the following parameters:

- indentation depth $500\mu m$
- indentation speed $100\frac{\mu m}{s}$
- maximum indentation force $35N$
- hold time $10s$
- release speed $100\frac{\mu m}{s}$

For every allowance of additive three patches are mechanically loaded on the testbed and the resulting voltage is recorded. For the assessment of the piezoresistive behavior the maximum upstroke of the measured voltage at a defined load is utilized as a measure of the sensitivity. Therefore the curves of the resulting voltage are compared, 42 and the mean value of the maximum upstroke is calculated. Following the maximum upstroke is plotted over the allowance of the additive.

Results

As figure 43 shows, for the unmixed patch and the allowance of $5w/w$ additive the maximum upstroke is limited by the operational amplifier. Although the other recorded values show a high variance a non-monotonic correlation between the maximum upstroke and the allowance of the additive is observable. The allowance of the additive exhibits a high influence to the resulting maximum upstroke. A higher allowance of additive tends to result in a lower maximum upstroke, but the correlation is not strictly monotonic decreasing. The curve shows a local minimum at $20w/w$ additive. Thus

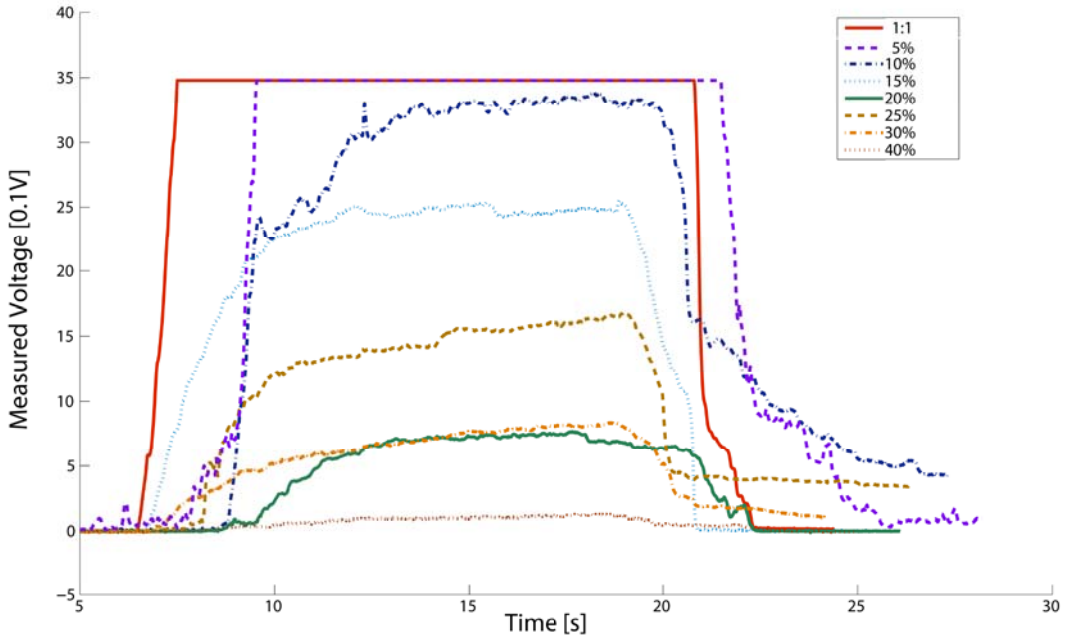

Figure 42: Piezoresistive behavior for different allowance of additive

a allowance of additive between $15w/w$ and $25w/w$ disproportionately decreases the maximum upstroke, i.e., at a allowance of $20w/w$ the maximum upstroke is as low as at a allowance of $30w/w$ additive.

Discussion

A possible cause for the non-monotonic curve progression could be the superposition of two opposing effects. While the decreasing maximum upstroke is likely to be caused by the disturbance of the conductive pathways by the non-conducting additive. The sharp increase of the maximum upstroke at a allowance of $25w/w$ might result from the precipitation of the conductive particles at the phase interfaces of the two blended silicones. Although the allowance of the non-conductive additive is increased the conductivity of the blend increases, especially when the non-conductive silicone percolates, and thus forms a scaffold of phase interfaces loaded with a high fraction of conductive particles. For a further increasing allowance the effect of the disturbance of the conductive pathways outweighs, as more and more conductive pathway end in cul-de-sacs within the growing cluster of the non-conductive additive. For the optimization of the

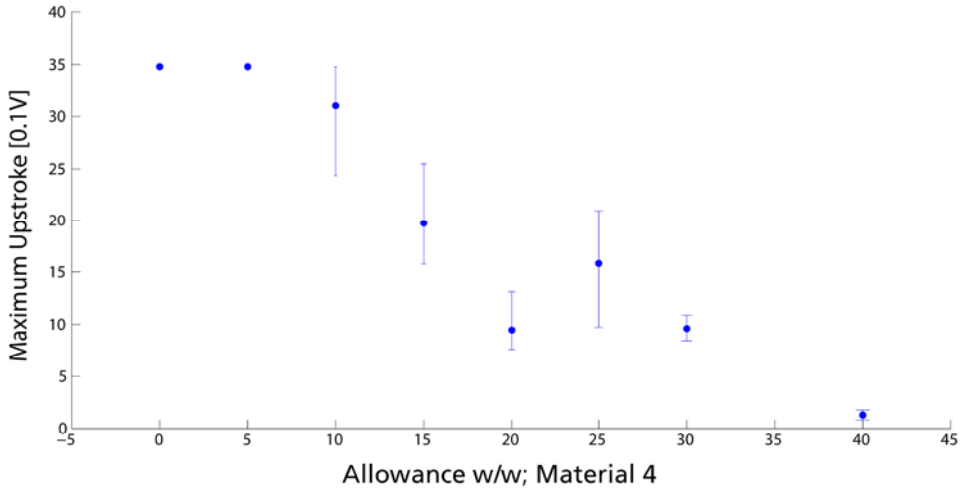

Figure 43: Maximum upstroke for different allowance of additive

material towards a high pressure sensitivity the non-monotonic correlation has to be considered, and if possible, allowances near the local minimum should be avoided.

6.3.2 Mechanical properties

To enable a compliance of the conductive matrix material the basis material is blended with a soft, non-conductive material.

Materials and Methods

The silicone patches, manufactured for the experiments concerning the piezoresistive properties, are utilized for the evaluation of the dependency of the mechanical properties from the additive. To be able to determine the influence of the additives to the mechanical properties the patches are tested on a Zwick/Roell $Z2.5$ tension/pressure testing machine. As for the pressure sensor especially the behavior of the material under pressure is interesting the patches are tested in pressing modus.

Experiments

One by one the $40mm \cdot 40mm \cdot 1mm$ patches are loaded using a cylindric indentation probe with a surface of $315mm^2$. The resulting force/strain characteristic curves are recorded, see figure 44. To enable a comparison of the softness of the manufactured

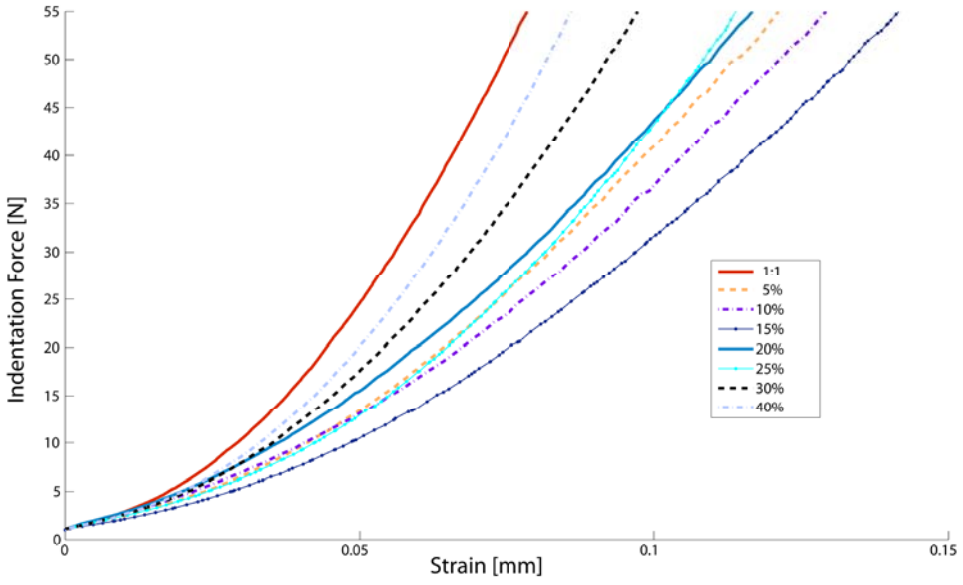

Figure 44: Force/Strain characteristic curves

silicone patches the slope of the recorded curves is approximated as linear between $20N$ and $50N$. Following the slopes are plotted over the allowance of the additive, figure 45.

Results

The mixing of the basis material with a highly compliant additive affects the softness of the resulting blend, represented by the slope of the force/strain curve. While the addition of small fractions ($5w/w$ *to* $15w/w$) decreases the slope by almost 50%, a further increasing of the allowance of the additive results in an increasing slope, see figure 45.

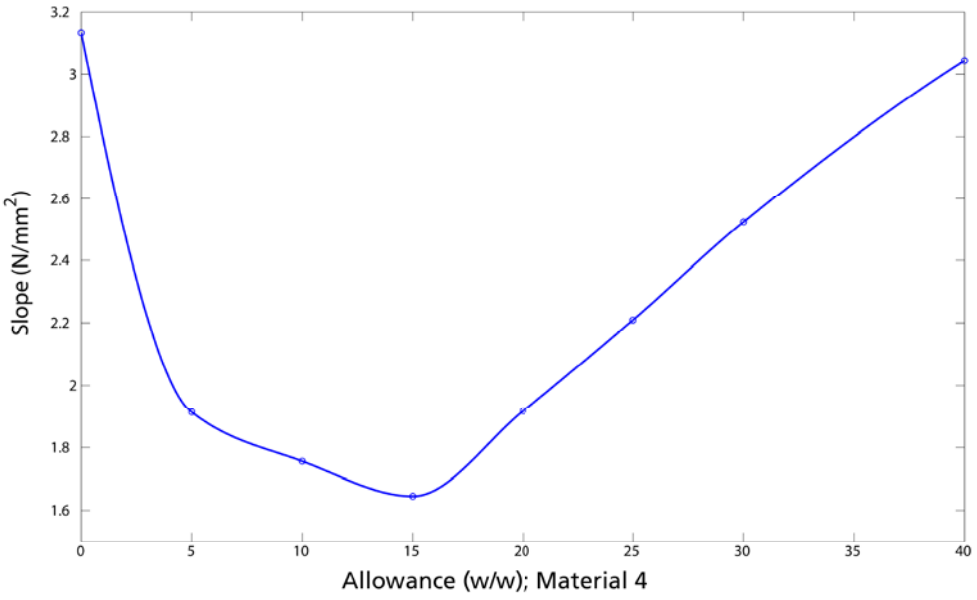

Figure 45: Slope for different allowance of additive

Discussion

A possible cause for the non-monotonic correlation of the allowance of the additive and the compliance of the blend is an assumed immiscibility of the two silicones, i.e., component A of the basis material only cures with its dedicated component B, and not with component B of the additive and vice versa. Thus, at low allowances, the curing additive forms isolated clusters within the basis material. These clusters disturb the formation of the silicone chains forming the basis material. Therefore the resulting blend exhibits a higher compliance than the unmixed basis material. From a allowance of $15w/w$ the clusters of the additive percolate and form a structure within the basis material, which results in increasing rigidity and an increasing slope. To enable a high compliance of the "dermal" sensor the blend will be tuned to the minimum slope at the determined allowance of $15w/w$.

6.3.3 Adhesion & Transfer resistance

To enable a monotonic sensor output a sufficient adhesion of the matrix material on the cast-in wires is necessary. As silicone does not self-adhere on metal, the surface of the wires has to be specially treated before they are cast-in. Therefore different means of pre-treatment are evaluated.

Materials and Methods

Three different approaches to the enhancement of the adhesion are investigated: The mechanical keying of the surface, the surface-activation applying plasma, and the utilization of a special primer. Preliminary tests of different wire materials showed that the adhesion is not affected by the material. Therefore the possible means for the enhancement of the adhesion are conducted with mechanically robust steel wires (diameter $0.2mm$). To enable the keying of the surface the wires are grid blasted. As

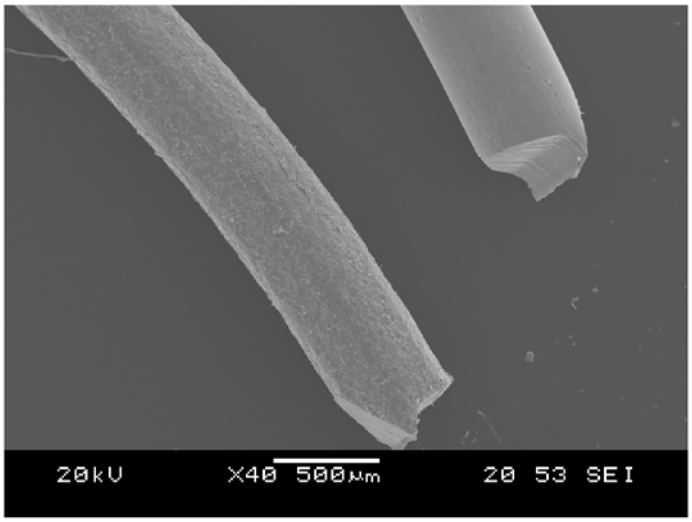

Figure 46: SEM of the grid blasted wires

shown in figure 46, the grid blasted wires exhibit a structured surface that might help to increase the adhesion. An other means to enhance the adhesion of the silicone on the wires is the activation of the wire surface applying plasma. For the activation of the wires a Tetra 30 LF PC plasma plant from Diener Electronic is utilized. The plant

is operated with the following parameters: $600W$ power provided by a low frequency generator, applied at the distance between cathode and anode of $60mm$. As processing gas oxygen is provided at $0.5mbar$. Before the activation the wires are cleaned with benzine, dried and put to the plasma plant where they are processed for 30min. The third examined possibility is the application of special primers. For the following experiments a primer (material 6) was applied. As recommended by the manufacturer the wires are dipped into the primer. Subsequently the wires are dried at room temperature for 10min in upright position to enable for a homogenous distribution of the primer over the surface of the wire. Afterwards the primer is burned-in at $100°C$ for 10 min in the conditioning cabinet.

To enable the assessment of the adhesion the pre-treated wires are cast into a silicone patch. For the testpatch the previously determined allowance of $15w/w$ is applied to enable for a maximum upstroke of the readout signal. The prepared wires are fixed in a semi-filled $80mm \cdot 80mm \cdot 6mm$ steel mould, leaving enough space for later clamping of the patch in the tension testing machine. Then the mould is over-filled ($20Vol\%$) with silicone and put into the Collin $P300P$ press. Applying the standard parameters, the silicone is cured at $200°C$ and $50bar$ for $600s$ and post-cured at $200°C$ for four hours. Following the patch is cooled and the top ends of the wires are laid open with a scalpel, leaving $55mm$ of cast-in wires.

Experiments

The different approaches are evaluated regarding the effect to the adhesion and the influence to the transition resistance between wire and matrix material as well as a possible constriction of the piezoresistive behavior. Therefore the resistance of the different wires to a reference electrode is measured. Subsequently the patch is mechanically loaded on the testbed and the change of the resistance between the different wires and the reference electrode is recorded. Finally the cast-in wires are pulled out of the testpach on the Zwick/Roell $Z2.5$ tension testing machine to determine the influence on the adhesion. First the transition resistance is measured using the readout facility

of the testbed. For it the wires are one by one connected and the resulting transition resistance is measured to a equidistant reference electrode. Following the testpatch is loaded with a trapezoid indentation path with the following parameters:

- indentation depth $650\mu m$
- indentation speed $100\frac{\mu m}{s}$
- maximum indentation force $22N$
- hold time $10s$
- release speed $100\frac{\mu m}{s}$

During the indentation the course of the resistance is measured. As the final experiment the adhesion between the wires and the silicone is testes in a pull-out test. Therefore the prepared testpatch with the cast-in wires is clamped into the lower acceptance of the Zwick $Z2.5$ tension testing machine. While the free end of one wire is clamped into the top acceptance. With this setup one by one the differently pre-treated wires are pulled out of the testpatch. To display the influence of the applied pre-treatment the characteristic travel/force curves are recorded. To enable an optical examination of the pulled-out wires, they are surveyed in the SEM.

Results

Within this paragraph the outcomes of the tests conducted with the testpatch are outlined. The preliminary tests of the static transition resistances revealed, that the pre-treatment has a significant influence on the static transition resistance. While grid blasting has no influence to the transition resistance, the application of the primer highly affects the resulting transition resistance. The resistance increases form $16k\Omega$ of the untreated wire to $206.1k\Omega$ for the wire coated with primer. Whereas the resistance for the wire activated with plasma is increased to $22k\Omega$. In the next paragraph the results of the indentation tests of the differently pre-treated cast-in wires are presented.

Firstly the results of the tests of the plain wire are outlined. The description refers to the labelled sections in figure 47. The decrease of the measured voltage in section A

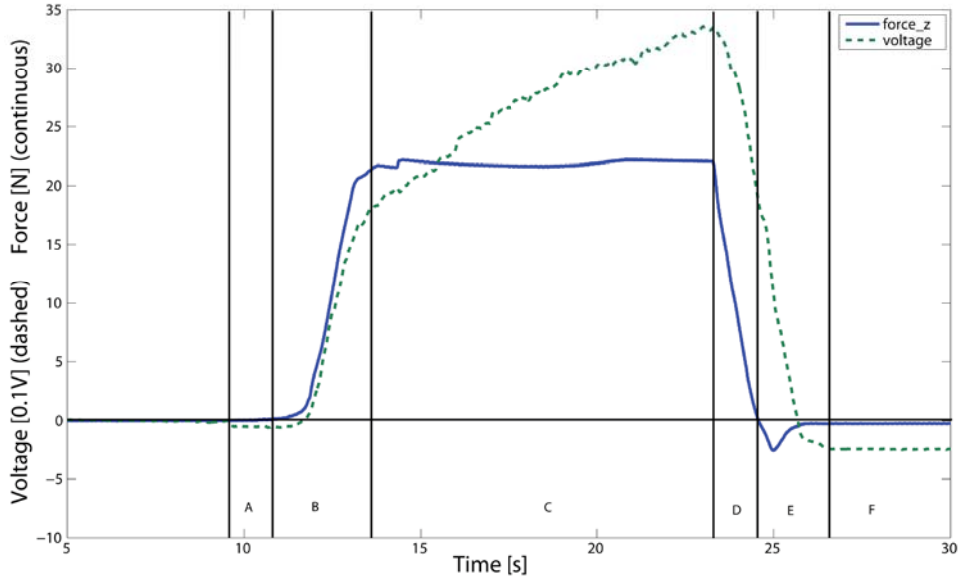

Figure 47: Behavior of the untreated wire

is likely to result from a change of the contacting surface of the reference electrode. In section B the voltage linearly increases with the applied force. While the force is maintained in section C the voltage increases further due to the formation of additional conductive pathways. During the release of the patch (section D) the voltage decreases proportional to the applied force. The dip to negative values of the force in section E results from the linear motor that pulls the OFTS against the force that is exhibited by the slowly relaxing patch. The force is transmitted to the OTFS because the patch self-adheres to the indentation probe and to the support under the applied load. Although the force converges to zero the resulting voltage decreases further and maintains a constant deviation resulting from a persistent change of the transition resistance (section F).

Secondly the results of the indentation tests of the plasma-activated wire are described, see figure 48. In contrast to the behavior of the plain wire the plasma-activated wire exhibits a non-linear increase of the resulting voltage while the force increases in sec-

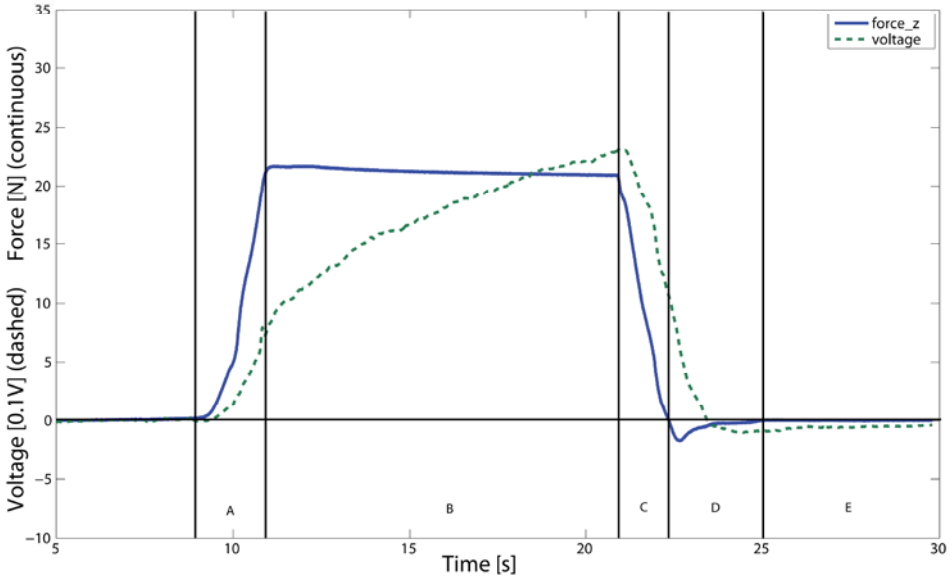

Figure 48: Behavior of the plasma-treated wire

tion A. Within section B the force gradually decreases while the voltage increases further as more and more conductive pathways are formed within the loaded material. As the patch is released the measured voltage decreases along with the force (section C). The overshoot of the measured voltage in section D is induced by the applied negative force. The convergence of the measured voltage towards its initial value in sections D and E which is likely to result from relaxation processes of the material.

Thirdly the behavior of the wire treated with the primer is described, the sections refer to figure 49. Although the force starts to increase at the end of section A the measured voltage decreases. As the applied force exceeds $2N$ the measured voltage increases with the force (section B). Although the resulting upstroke of the voltage is significantly lower, the course of the voltage exhibits the same behavior as for the other patches in sections C, D and E. But in section F the wire coated with primer features a large overshoot induced by the applied negative force. At the end of section F a slow convergence towards the initial value can be observed. This behavior hints at a high strain sensitivity of the material. Lastly the results of the pull-out tests are delineated in figure 50. The maximum pull-out force indicates the adhesion of the silicone to

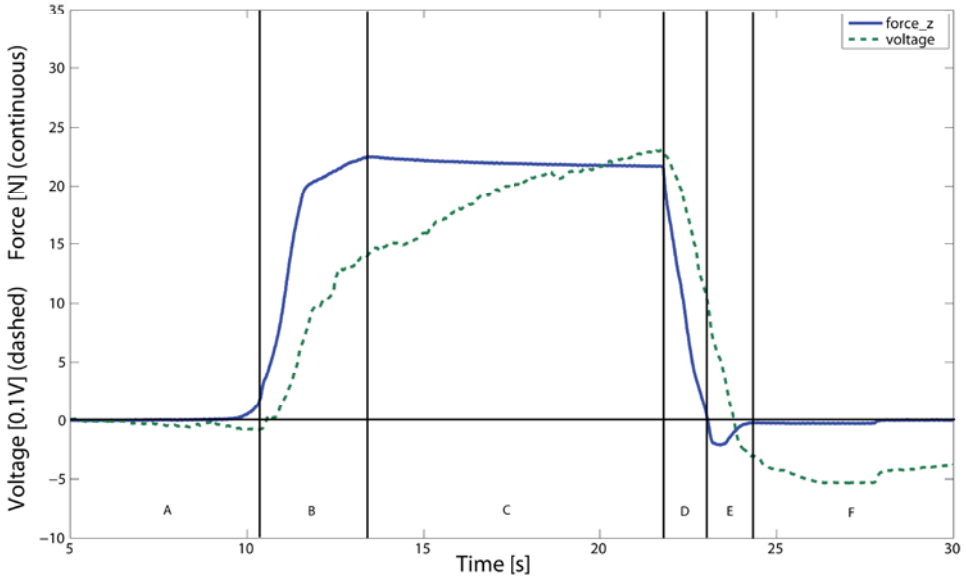

Figure 49: Behavior of the primer-coated wire

the wire. For the plain wire a maximum pull-out force of $31N$ is measured. While the plasma-activation results in an increase of the force to $40N$ the coating with the primer shows a maximum force of $47N$. The altering value of the curve for the wire coated with primer results from the stick-slip effect induced by the silicone that adhered to the wire. An examination of the wires under the SEM showed that only for the wire coated with primer an adherence can be obtained, see figure 51.

Discussion

The conducted tests revealed that the pre-treatment significantly influences the static transition resistance and the adhesion. While the adhesion between the wires and the matrix material can be enhanced applying plasma or primer, as a negative side effect, the transition resistance is elevated. Therefore the pressure sensitivity of the sensor is diminished. The indentation tests of the patch revealed a high influence of the pretreatment on the piezoresistive behavior. The primer forms an insulating layer around the wire which results in a high transition resistance. Therefore the relative

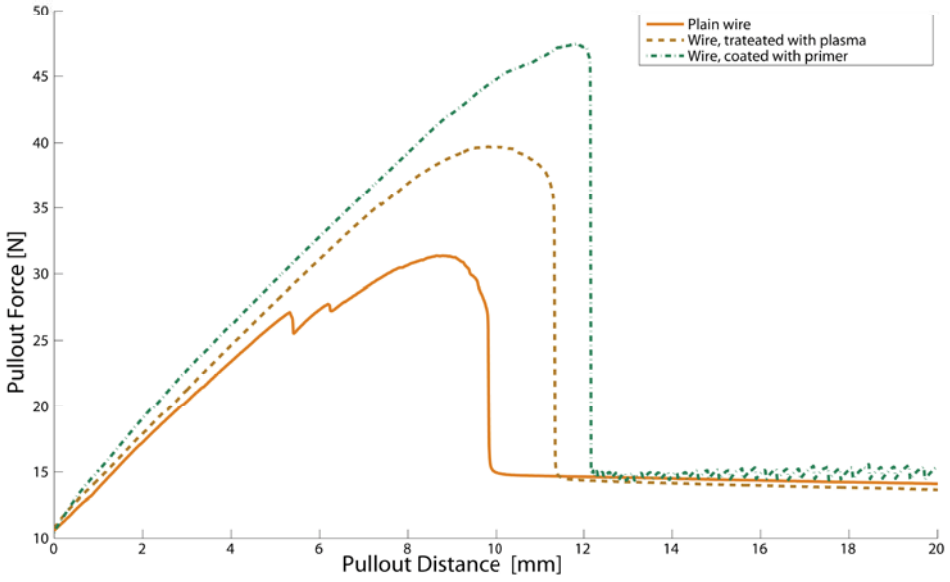

Figure 50: Pull-out test

change in the measurable resistance induced by the external load decreases. Hence the pressure sensitivity of the sensor becomes very low. Moreover the indentation tests of the primer-coated wire revealed a high sensitivity to strain of the applied piezoresistive silicone. This finding is confirmed in personal communication with experts in conductive silicones, Due to this strain sensitivity the enhanced adhesion between wire and matrix impairs the piezoresistive behavior of the sensor setup. If pressure is applied the matrix material shunnes from the load. In contrast to the wires that do not show a sufficient adhesion the matrix material can not lift of from the rigid wire. Hence local areas with high intra-matrix strain are formed that show a high resistance which affects the measurable resistance of the sensor setup. Even if a good adhesion is obtained, the sensor setup shows an unwanted behavior.

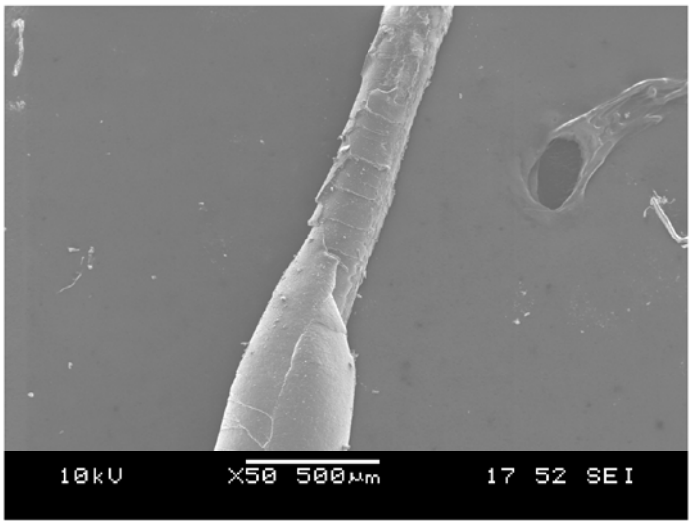

Figure 51: SEM of the pulled-out wire

6.4 Discussion

As a high compliance is crucial for the matrix material of the dermal sensor the material is optimized towards a allowance of the additive of $15w/w$. This results in a comparatively high compliance and in a maximum upstroke of about $2V$. The experiments revealed, that even if the adhesion is optimized and the transfer resistance is no longer influenced via the lift-off of the matrix material from the wire, the setup shows an unwanted behavior. A satisfactory solution of the described optimization challenge is not possible with the evaluated materials and their combination. The presented approach, combining a piezoresistive, highly compliant material with metal readout wires is not leading to a desirable overall performance of the "dermal" sensor.

Although the combination with the comparatively rigid metal wires is not applicable, the evaluated silicones show very promising properties. Therefore the application for the superficial sensor is expedient. The goal for the development of the superficial sensor is to turn the disadvantages to advantages and to apply the strain sensitivity of the investigated materials in the superficial sensor. The following chapter shows the development and realization of a prototype of the superficial sensor.

7 Realization of an artificial skin prototype

Within this chapter the realization of a prototype of the superficial sensor is described.

7.1 Sensor setup

For the superficial sensor the high strain sensitivity of the afore evaluated conductive silicone is utilized as transduction principle. The core idea is to use the gradual disturbance of conductive pathways under strain instead of the formation of pathways under pressure as transduction principle. The strain of the conductive pathways results in a measurable change of resistance. For it the sensor setup intrinsically has to transduce the external pressure into internal strain. This is realized applying the layer setup proposed in the bio-inspired sensor setup. The supporting matrix material of the future "dermal" sensor is very compliant and yields under applied external load. The covering layer, containing strain sensitive conductive pathways is stretched and the conductive pathways are elongated. Thus the applied external load is transformed into strain of the conductive pathways. For the stretchable conductive pathways the materials and the results of the evaluation in chapter 6 are used. For the evaluation of the applicability of the proposed sensor setup a prototype of the superficial sensor is manufactured. The principle of the setup is shown in figure 52. The transduction

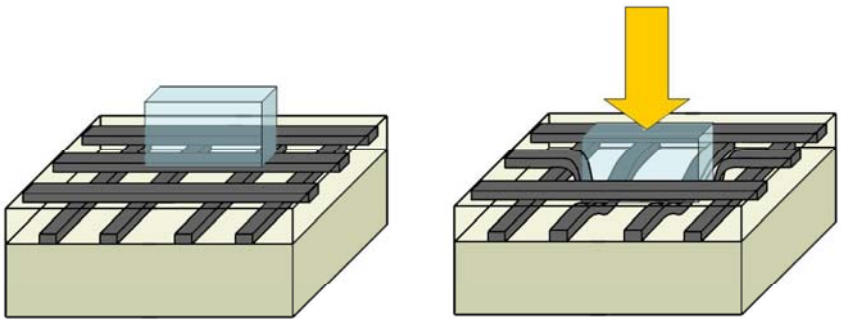

Figure 52: Setup of the superficial sensor

is based on the deformation of the stretchable conductive pathways. If the surface of the sensor is indented the supporting encapsulation gives way and the strain sensitive pathways are elongated. Especially at the edges of the indenting object areas of high strain are formed.

7.2 Materials and methods

Preliminary tests of different conductive silicones and mixing ratios are carried out with a simple test setup. To ensure that the electrical connection is not affected by the mechanical fixation the setup shown in figure 53 is used for the qualitative tests. For the tests $1mm \cdot 1mm \cdot 40mm$ bars are cut out of the testpaches manufactured in

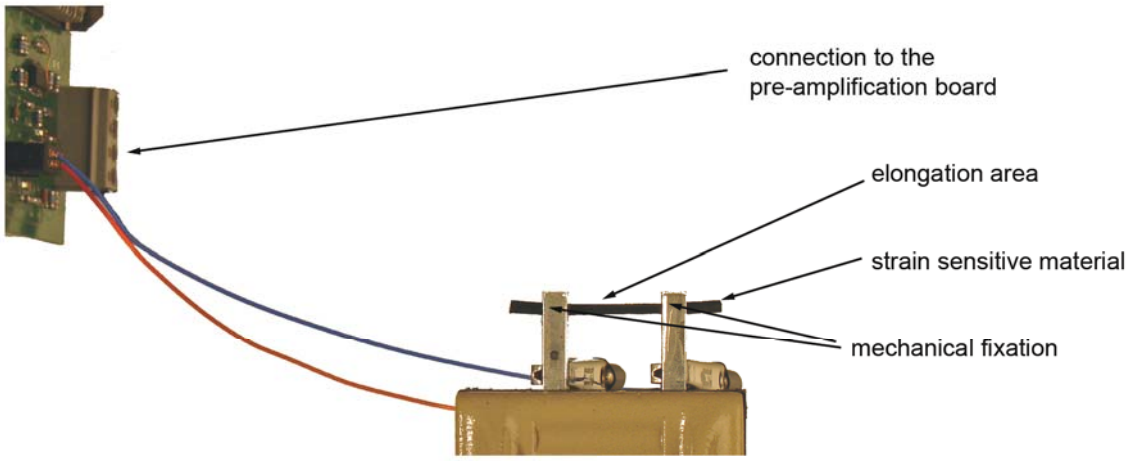

Figure 53: Setup for the evaluation of the strain sensitivity

chapter 6. The bars are fixed in the setup and connected to the readout facility of the testbed.

The major challenge of the manufacturing of the sensor prototype is the electrical connection of the stretchable conductive pathways to metal wires in a reliable setup, that is not affected by the applied pressure. Therefore the electrical connection and the mechanical fixation of the silicone pathways within a frame is proposed. To realize the sensor prototype a frame is cut out from a double sided conductor board. The $0.5mm$ conductor board is coated on both sides with a $35\mu m$ layer of copper that is

sealed with photoresist. The first step is the removal of the copper layer leaving over eight contacting plates for two silicone pathways. The dedicated contacting surfaces are freed from photoresist and coated with primer. The primer is cured at $70°C$ for 10 minutes. Due to the large surface of the contact plates the additional resisitance induced by the primer is negligible. Following, the prepared $0.5mm$ frame is cast into conducting silicone using a $40mm \cdot 40mm \cdot 1mm$ mold. For it the conductive silicone, containing the frame, is cured at $200°C$ *and* $50bar$ for ten minutes. After the cooling the patch is removed from the mold.

Using a scalpel the conductive pathways are cut out of the patch leaving only the pathways and half of the contacting plates covered with conductive silicone. The remaining contact plates are freed from photoresist and tinned. To protect the delicate silicone pathways an encapsulation is required. Therefore the whole frame and the conductive pathways are cast into a highly compliant, electrically insulating silicone (material 7), using a $80mm \cdot 80mm \cdot 6mm$ mold. The encapsulating silicone is processed according to 6.2.2. After the cooling the frame is cut out and the tinned contacting plates are laid open. The metal readout cables are soldered on the pre-tinned contacting plates of the frame. The soldering process has to be conducted very fast as the silicone can stand the applied temperatures ($340°C$) only short-time.

Subsequently the free ends of the readout cables are connected to a Datamate connector that is directly pluggable to the pre-amplification board and ensures a reliable and time-invariant electrical connection. As the final step the overall neutral resistance of the sensor prototype is tuned to suit to the pre-amplification board by the reduction of the contacting surface between the copper plates of the frame and the silicone pathways. For one of the pathway in addition the diameter of the conductive pathway is reduced to enable an amplification. Applying the presented procedure a prototype of the superficial sensor was realized, see figure 54. To enable the assessment of the proposed transduction principle the prototype is tested on the testbed.

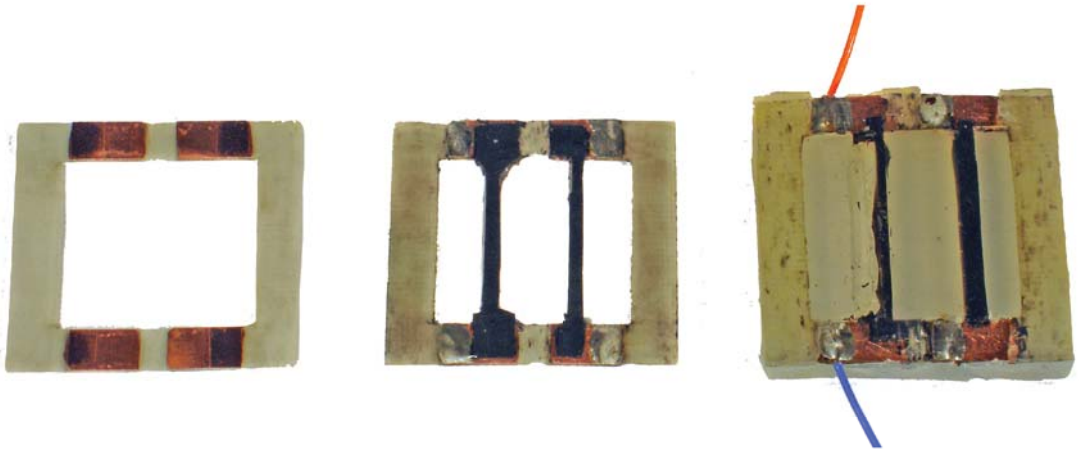

Figure 54: Prototype of the superficial sensor

7.3 Experiments

Manual indentation of the sensor showed good dynamic response of the sensor to external load. To quantify the dynamic correlation between the applied force and the resulting resistance the prototype is fixed to a $40mm \cdot 40mm$ aluminium plate attached to the indentation probe. Thus the prototype is mechanically connected to the OFTS. External load is transmitted through the sensor to the OFTS. Subsequently the prototype is manually loaded with short impulses ranging from $0N$ *to* $50N$. The force in z-axis and the resulting resistance of the silicone pathways is recorded.

7.4 Results

Figure 55 shows the response of the sensor prototype to the loading with small forces. The sensor exhibits a high sensitivity to small forces. In section A the sensor is unloaded and shows a quasi-stationary output signal. Within section B the sensor shows an output that alters almost linearly with the applied force. While the force reaches its initial value at the end of section B, the measured voltage maintains an offset. This offset decreases in section C and converges to its initial value. As shown in figure 56 the manufactured prototype shows a good dynamic behavior. The initial relaxation of the sensor from high applied forces is fast but leaves an offset voltage. The maximum

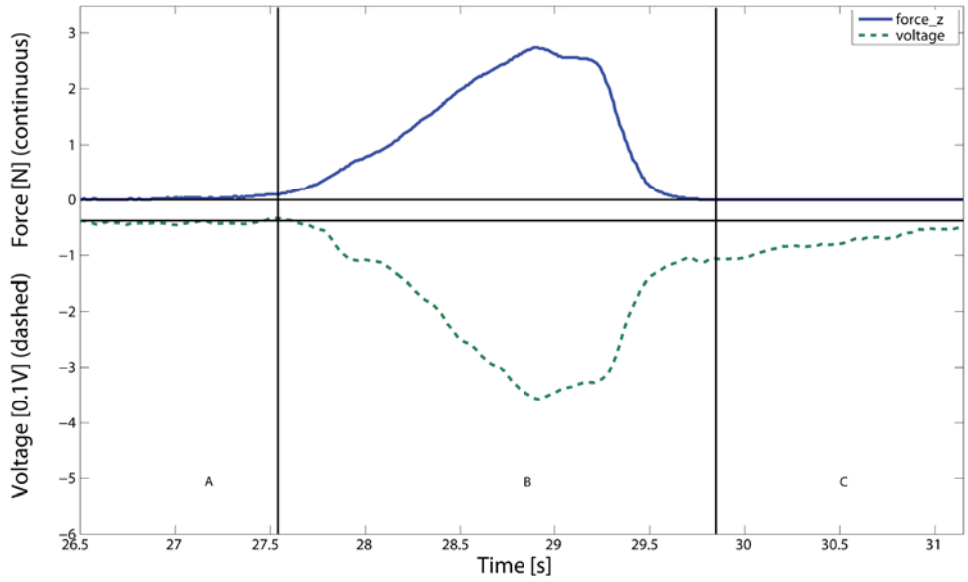

Figure 55: Behavior of the superficial sensor

upstroke of the measured voltage is $3V$ resulting from an applied force of $50N$.

7.5 Discussion

The observed behavior of the dynamic properties of the prototype is very promising. For a wide range of forces the sensor shows a quasi-linear correlation between the applied force and the measurable voltage. The only drawback of the sensor setup is the observed offset, resulting from high applied forces. A possible reason for the observed long relaxation time is the $6mm$ thick encapsulation of the sensor prototype. In contrast to the manufactured prototype the proposed, bio-inspired setup of the superficial sensor will consist of a very thin encapsulation. To enable for the evaluation of the applicability of the sensor principle future prototypes have to be equipped with a thin encapsulation.

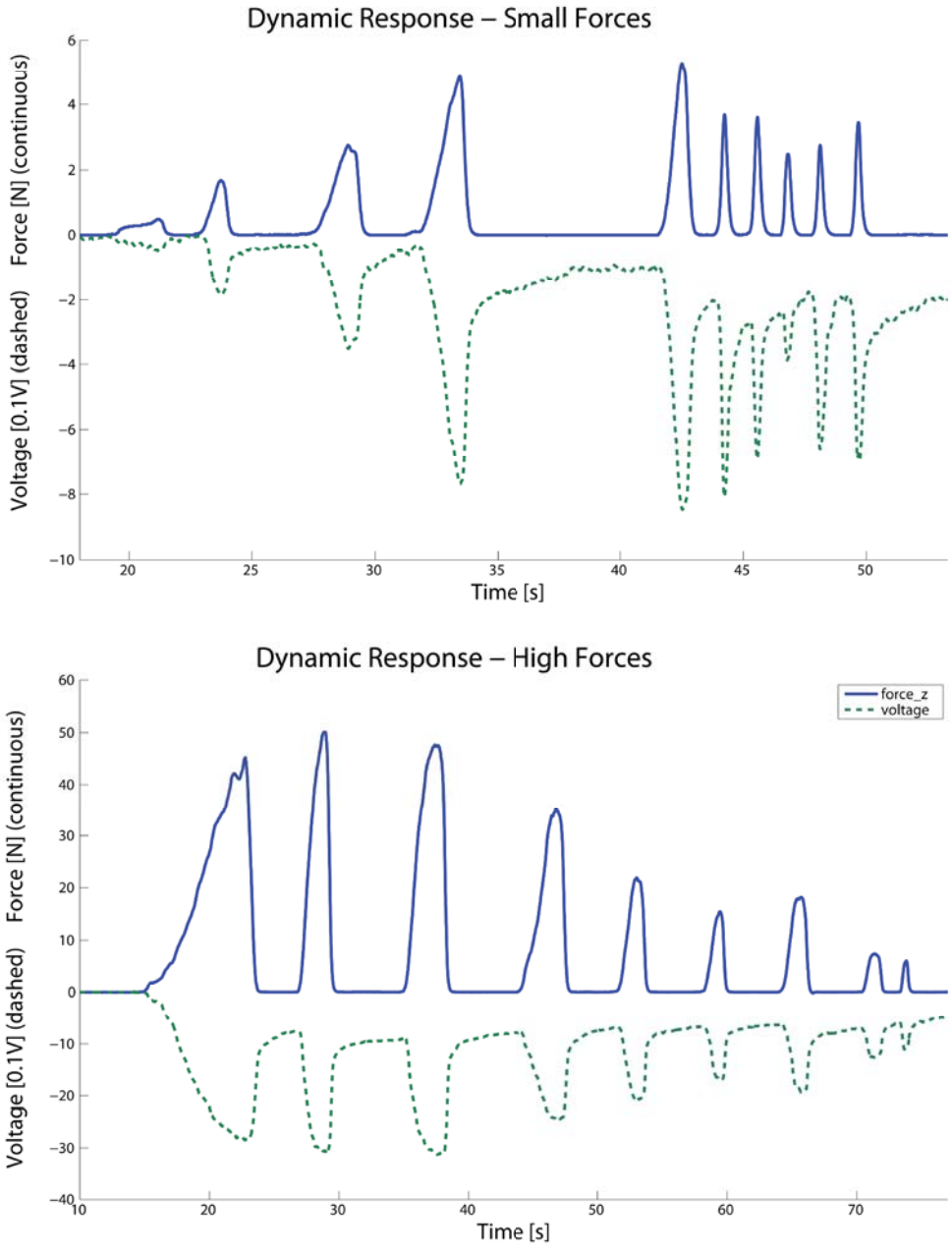

Figure 56: Dynamic loading of the superficial sensor

8 Discussion

For the deployment of robotic systems in human's environment their suitability has to be increased. Therefore robotic devices have to be equipped with dexterous robotic hands or manipulators. To enable the required dexterity a combination of sophisticated robotic hardware and a powerful sensory system is necessary. The conducted literature research showed, that to this day no such combination is available. Approaching this demand, an anthropomorphic Hand-Arm system is developed at DLR. Its desired small size and the mechatronic integration results in little designed space, preventing the application of "classical" sensor system as 6DoF load cells. Therefore this study aimed toward the development of a bio-inspired sensor setup for DLR's new Hand-Arm system. The study consists of two main parts:

The derivation of a bio-inspired sensor setup which is capable to replace the "classical" sensor systems. And the development and realization of a test facility enabling the evaluation and optimization of possible sensor materials as well as the development of a prototype of the bio-inspired sensor.

Therefore different transduction principles applied in technical tactile sensors have been reviewed, and as a result, piezoresistivity has been chosen as transduction principle. For the identification of the requirements for a valuable tactile sensor a literature research on robotic hand-hardware and tactile sensors has been conducted. For the derivation of the bio-inspired sensor setup the general requirements for valuable tactile sensors and the special requirements resulting form the anthropomorphic design approach are assessed. Hence a consistency matrix is applied to evaluate the requirements and to identify possible conflicts of goals between the requirements. For conflicts that are not directly solvable with a "classical" technical approach, bionics is applied as a method towards bio-inspired technical solutions of the conflicts. Therefore the most critical conflicts are selected and possible approaches for the avoidance of the conflicts of goals are derived. Using the human mechano-perceptive system as a source of inspiration the following method is applied:

- Abstraction of the technical challenge
- Analysis of the functionality in human tactile perception
- Abstraction of the functional principle; Nature's strategy?
- Propagation of the functional principles to a technical system
- Derivation of possible technical approaches

Thus different approaches for the solution of the conflicts of goals are derived. Following the proposed approaches are assessed using a rating matrix.

The most promising approaches are combined to a bio-inspired sensor setup for the anthropomorphic Hand-Arm system. The proposed bio-inspired sensor setup consists of a "dermal" and a superficial sensor. While the "dermal" sensor is based on metal readout wires, cast into a compliant piezoresisitive material, the superficial sensor is designed as a strain sensitive layer covering the "dermal" sensor. With the proposed sensor setup a solution was derived, that intrinsically solves the conflicts of goals by its design.

For the investigation of the proposed sensor principles a modular testbed has been designed and realized within this study. In its current version the testbed allows for automated testing of a testpatch under a pre-set force or indentation depth.

For the evaluation of different sensor materials and their combination testpatches have been manufactured and tested on the testbed as well as on a Zwick/Roell tensile testing machine. Based on the results of those tests, a particularly suitable piezoresistive silicone has been selected for the further development of the tactile sensor.

During the development of the "dermal" sensor the conducted tests revealed an optimization challenge concerning good piezoresistive behavior, high compliance and good adhesion to the cast-in metal wires. In addition the tests of the manufactured testpatches revealed a high strain sensitivity of the applied material. Therefore a satisfactory solution of the optimization challenge is not possible with the evaluated materials

and their combination. The "dermal" sensor setup, based on the combination of a piezoresistive, highly compliant material with metal readout wires is not leading to a desirable overall performance. Although the combination with metal wires is not applicable, the evaluated silicone shows very promising properties. Therefore the application for the superficial sensor is expedient.

Based on the results of the experiments for the "dermal" sensor a new transduction principle for the superficial strain sensor was developed and patented. Applying the afore investigated materials a prototype of the superficial sensor could be realized. For a wide range of forces the sensor shows a quasi-linear correlation between the applied force and the measurable voltage. The only drawback of the sensor setup is the observed offset, resulting from high applied forces.

9 Future prospects

As the approach for the "dermal" sensor was proven to be not feasible, an alternative concept for the "dermal" sensor will have to be developed. For the superficial sensor the next step is the crossing of different layers to allow for the detection of forces in multiple DoF. Further, the refinement of the processing technology and the evaluation of the applicability of alternative technologies is aspired. A future task is the propagation of the bio-inspired sensor setup to the anthropomorphic fingertip. Furthermore the extension of the testbed and the data analysis will be subject of future studies.

References

[1] Alberts, B. ; Johnson, A. ; Lewis, J. ; Raff, M. ; Roberts, K. ; Walter, P.: *Molecular Biology of the Cell.* 4. New York : Garland Science, 2002

[2] Ando, S. ; Shinoda, H. ; Yonenaga, A. ; Terao, J.: Ultrasonic six-axis deformation sensing. In: *IEEE Transactions on Ultrasonics, Ferroelectrics and Frequency Control* 48 (2001), 07, Nr. 4, S. 1031–1045

[3] Aramphongphun, C. ; Castro, J.M.: Microfluidics and rheology of carbon black suspensions for In-Mold Coating applications: some insights into the slip flow phenomena. In: *Journal of Computer-Aided Materials Design* DOI 10.1007/s 10820-006-9028-7 (2006)

[4] Bauer, F.: High pressure applications of ferroelectric polymers. In: *Proceedings of the IEEE/ISAF International Symposium on Applications of Ferroelectrics.* Penn State, PE, 1994, S. 333–336

[5] Bell, J. ; Holmes, M.: Model of the Dynamics of Receptor Potential in a Mechanoreceptor. In: *Mathematical Biosciences* (1992), Nr. 110, S. 139–174

[6] Bicchi, A. ; Kumar, V.: Robotic Grasping and Contact: A Review. In: *Proceedings of the IEEE International Conference on Robotics and Automation.* San Francisco, CA, 2000, S. 348–353

[7] Birznieks, I. ; Jenmalm, P. ; Goodwin, A.W. ; Johansson, R.S: Encoding of Direction of Fingertip Forces by Human Tacatile Afferents. In: *The Journal of Neuroscience* 21 (2001), 10, Nr. 20, S. 8222–8237

[8] Black, A.F. ; Bouez, C. ; Perrier, E. ; Schlotmann, K. ; Chapuis, F. ; Damour, O.: Optimization and Characteriszation of an Engineeres Human Skin Equivalent. In: *Tissue Engineering* 11 (2005), Nr. 5/6, S. 723–733

[9] Borst, C. ; Fischer, M. ; Haidacher, S. ; Liu, H. ; Hirzinger, G.: DLR-Hand II and Experiments and Experiences with an Antropomorphic Hand. In:

Proceedings of the IEEE International Conference on Robotics and Automation. Taipei, Taiwan, 2003, S. 702–709

[10] Butterfass, J.: *Eine hochintegrierte multisensorielle Vier-Finger-Hand für Anwendungen in der Servicerobotik.* Darmstadt, Technische Universität Darmstadt, Diss., 12 1999

[11] Charlot, B. ; Parrain, F. ; Galy, N. ; Courtois, B.: A Sweeping Mode Integrated Tactile Fingerprint Sensor. In: *Proceedings of the IEEE International Conference on Solid Slate Sensors, Actuators and Microsystems.* Boston, 2003, S. 1031–1034

[12] Chodak, I. ; Krupa, I.: Percolation Effect and Mechanical Behavior of Carbon Black Filled Polyethylene. In: *Journal of Material Science Letters* 18 (1999), S. 1457–1459

[13] Clark, J.J.: A Magnetic Field Based Compliance Matching Sensor for High Resolution, High Compliance Tactile Sensing. In: *Proceedings of the IEEE International Conference on Intelligent Robots and Systems.* Philadelphia, PE, 1988, S. 772–777

[14] Craelius, W.: The bionic Man: Restoring Mobility. In: *Science* 295 (2002), S. 1018–1021

[15] Crowder, R.: Towards Robots That Can Sense Texture by Touch. In: *Science* 312 (2006), 06, S. 1478–1479

[16] Dandekar, K. ; Raju, B.I. ; Srinivasan, M.A.: 3-D Finite-Element Models of Human and Monkey Fingertips to Investigate the Mechanics of Tactile Sensing. In: *Journal of Biomechanical Engineering* 125 (2003), 10, S. 682–691

[17] Dario, P. ; Laschi, C. ; Carozza, M. ; Guglielmelli, E. ; Teti, G. ; Massa, B. ; Zecca, M. ; Taddeucci, D. ; Leoni, F.: An Integrated Approach for the Design and Devellopment of a Grasping and Manipulation System in Humanoid

Robots. In: *Proceedings of the IEEE/RSJ International Conference on Intelligent Robots and Systems*. Takamatsu, Japan, 2000

[18] Delalleaua, A. ; Jossea, G. ; Lagardea, J.-M. ; Zahouanib, H. ; Bergheaub, J.-M.: Characterization of the mechanical properties of skin by inverse analysis combined with the indentation test. In: *Journal of Biomechanical Engineering* 39 (2006), S. 1603–1610

[19] D.Stauffer ; A.Aharony: *Introduction to Percolation Theory*. 2. London : Taylor & Francis, 1998

[20] Edin, B.B.: Quantitative Analyses of Dynamic Strain Sensitivity in Human Skin Mechanoreceptors. In: *Journal of Neurophysiology* 92 (2004), S. 3233–3243

[21] Edwards, C. ; Marks, R.: Evaluation of Biomechanical Properties of Human Skin. In: *Clinics in Dermatology* (1995), Nr. 13, S. 375–380

[22] Faller, A. ; Schünke, M.: *Der Körper des Menschen*. 14. Stuttgart : Thieme, 2004

[23] Ferrier, N.J. ; Brockett, R.W.: Reconstructing the Shape of a Deformable Membrane from Image Data. In: *The International Journal of Robotic Research* 19 (2000), 09, Nr. 9, S. 795–816

[24] Frings, S. ; (Eds.), J. B.: *Transduction Channels in Sensory Cells*. 1. Weinheim : Wiley-VCH Verlag GmbH, 2004

[25] Fuentes, O. ; Nelson, R.C.: Learning Dextrous Manipulation Skills Using Multisensory Information. In: *Proceedings of the IEEE/SICE/RSJ International Conference on Multisensor Fusion and Integration for Intelligent Systems*, 1996, S. 342–348

[26] Gao, X.H. ; Butterfass, J. ; Grebenstein, M. ; Seitz, N. ; Hirzinger, G.: The HIT/DLR Dexterous Hand: Work in Progress. In: *Proceedings of the IEEE International Conference on Robotics and Automation*. Taipei, Taiwan, 2003, S. 3164–3168

[27] Gerling, G.J. ; Thomas, G.W.: The Effect of Fingertip Microstructures on Tactile Edge Perception. In: *IEEE Virtual Reality Conference - World Haptics Symposium* - (2003), 03

[28] Goodwin, A.W. ; John, K.T. ; Sathian, K. ; Darian-Smith, I.: Spatial and Temporal Factors Determining Afferent Fiber Responses to a Grating Moving Sinusoidally Over the Monkeys Fingerpad. In: *The Journal of Neuroscience* 9 (1989), Nr. 4, S. 1280–1293

[29] Grebenstein, M. ; Smagt, P. v.d.: *Antagonism for a Highly Anthropomorphic Hand-Arm system.* 2007. – in print

[30] Guett, S.: *Rheologische in vivo-Untersuchungen an der menschlichen Haut mit nicht-invasiven Verfahren*, Universitaet Hamburg, Diss., 10 1999

[31] Haddadin, S. ; Albu-Schäffer, A. ; Hirzinger, G.: Safety Evaluation of Physical Human-Robot Interaction via Crash-Testing. In: *Robotics: Science and Systems Conference* (2007)

[32] Harmon, L.D.: Automated tactile sensing. In: *International Journal of Robotics Research* 1 (1982), Nr. 2, S. 3–31

[33] Hasegawa, Y. ; Sasaki, H. ; Shikida, M. ; Sato, K. ; Itoigawa, K.: Magnetic actuation of a micro-diaphragm structure for an active tactile sensor. In: *Proceedings of the 2004 International Symposium on Micro-Nanomechatronics and Human Science*, 2004, S. 99–104

[34] Hellard, G. ; Russell, R.A.: A Robust, Sensitive and Economical Tactile Sensor for a Robotic Manipulator. In: *Proceedings of the Australasian Conference on Robotics and Automation.* Auckland, 2002, S. 100–104

[35] Hendriks, F.M.: *Mechanical behaviour of human epidermal and dermal layers in vivo*, Technische Universiteit Eindhoven, Diss., 03 2005

[36] Hill, B.: *Innovationsquelle Natur and Naturorientierte Innovationsstrategie für Entwickler, Konstrukteure und Designer.* Aachen : Shaker, 1997

[37] Howe, R.D.: Tactile Sensing and Control of Robotic Manipulation. In: *Journal of Advanced Robotics* 8 (1994), Nr. 3, S. 245–261

[38] Hristu, D. ; Ferrier, N. ; Brockett, R.W.: The Performace of a deformable-membrabe tactile Sensor: Basic Results on Geometrically-defined Tasks. In: *Proceedings of the IEEE International Conference on Robotics and Automation*. San Francisco, CA, 2000

[39] Huang, J.-C.: Carbon Black Filled Conducting Polymers and Polymer Blends. In: *Advances in Polymer Technology* 21 (2002), 06, Nr. 4, S. 299–313

[40] Hussain, M. ; Choa, Y.-H. ; Niihara, K.: Conductive rubber materials for pressure sensors. In: *Journal of Material Science Letters* (2001), 09, Nr. 20, S. 525–527

[41] Iggo, A. ; Andres, K.H.: Morphology of cutaneous receptors. In: *Annual Reviews of Neuroscience* 5 (1982), S. 1–31

[42] Jaervilehto, T. ; Haemaelaeinen, H. ; Laurinen, P.: Characteristics of Single Mechanoreceptive Fibres Innervating Hairy Skin of the Human Hand. In: *Experimental Brain Research* 25 (1976), S. 45–61

[43] Jagur-Grodziniski, J.: Elektronically Conductive Polymers. In: *Polymers for Advanced Technilogies* 13 (2002), 04, S. 615–625

[44] Jenmalm, Per: *Dexterous Manipulation in Humans: Use of Visual and Tactile Information about Object Shape in Control of Fingertip Actions*, UmeåUniversity, Sweden, Diss., 03 2000

[45] Johansson, R.S: Tactile Sensibility in the Human Hand: Receptive Fields Characteristics of Mechanoreceptive Units in the Glabrous Skin Area. In: *Journal of Physiology* 281 (1978), S. 101–123

[46] Johansson, R.S: Sensory Input and Control of Grip. In: *Proceedings of the Sensory guidance of movement. (Novartis Foundation Symposium 218)*. Wiley, Chichester, 1998, S. 45–63

[47] Johnson, K.O. ; Hsiao, S.S.: Neural Mechanisms of Tactual Form and Testure Perception. In: *Annual Reviews of Neuroscience* 15 (1992), S. 227–250

[48] K., H. Maekawa K. T. ; Komoriya: Tactile Feedback for Multifingered Dynamic Grasping. In: *Proceedings of the IEEE International Conference on Robotics and Automation.* Minneapolis, MN, 1996, S. 63–71

[49] Kamiyama, K. ; Kajimoto, H. ; Kawakami, N. ; Tachi, S.: Evaluation of a Vision-based Tactile Sensor. In: *Proceedings of the IEEE International Conference on Robotics and Automation.* New Orleans, LA, 2004, S. 1542–1547

[50] Kandel, E.R. ; Schwartz, J.H. ; Jessell, T.M.: *Principles of Neuroscience.* 4. New York : McGraw-Hill, 2004

[51] Kane, B.J ; Cutkosky, M.R. ; Kovacs, G.T.A.: A Traction Stress Sensor Array for Use in High-Resolution Robotic Tactile Imaging. In: *Journal of Microelectromechanical Systems* 9 (2000), 12, Nr. 4, S. 425–434

[52] Katada, A. ; Buys, Y. F. ; Tominaga, Y. ; Asai, S. ; Sumita, M.: Resistivity Control in the Semiconductive Region for Carbon-black-filled Polymer Composites. In: *Colloid Polymer Science* 283 (2005), S. 367374

[53] Kawasaki, H. ; Komatsu, T. ; Uchiyama, K.: Dexterous Anthropomorphic Robot Hand With Distributed Tactile Sensor: Gifu Hand II. In: *IEEE/ASME Transactions on Mechatronics* 7 (2002), Nr. 3, S. 296–303

[54] Kerpa, O. ; Weiss, K. ; Wörn, H.: Development of a Flexible Sensor System for a Humanoid Robot. In: *Proceedings of the IEEE International Conference on Intelligent Robots and Systems.* Las Vegas, NE, 2003

[55] Kim, E.-S. ; Hun-Sik, K. ; Seong-Hun, J. ; Jin-San, Y.: Adhesion Properties and Thermal Degradation of Silicone Rubber. In: *Journal of Applied Polymer Science* 103 (2007), S. 2782–2787

[56] Ko, C.-T. ; Tseng, S.-H. ; Lu, M. S.-C.: A CMOS Micromachined Capacitive Tactile Sensor With High-Frequency Output. In: *Journal of Microelectromechanical Systems* 15 (2006), 12, Nr. 6, S. 1708–1714

[57] Kolesar, E.S. ; Dyson, C.S.: Object Imaging with a Piezoelectric Robotic Tactile Sensor. In: *Journal of Microelectromechanical Systems* 4 (1995), 06, Nr. 2, S. 87–96

[58] Korthagen, E.J.M.: Human skin in vivo: Overview of mechanical experiments and imaging techniques - A literature review. In: *KONINKLIJKE PHILIPS ELECTRONICS N.V. and Technical Note: 2003/00132* (2003)

[59] Kost, J. ; Foux, A. ; Narkis, M.: Adhesion Properties and Thermal Degradation of Silicone Rubber. In: *Journal of Applied Polymer Science* 34 (1994), 11, Nr. 21, S. 1628–1634

[60] Lacour, S.P. ; Jones, J. ; Suo, Z. ; Wagner, S.: Design and Performance of Thin Film Interconnects for Skin-Like Electronic Circuits. In: *IEEE Electron Device Letters* 25 (2004), 04, Nr. 4, S. 179–181

[61] Lang, S.B. ; Muensit, S.: Review of Some Lesser-known Applications of Piezoelectric and Pyroelectric Polymers. In: *Journal of Applied Physics A* 85 (2006), S. 125134

[62] Lee, M.H.: Tactile Sensing: New Directions, New Challenges. In: *The International Journal of Robotics Research* 19 (2000), 07, Nr. 7, S. 636–643

[63] Lee, M.H. ; Nicholls, H.R.: Tactile sensing for mechatronics - a state of the art survey. In: *Mechatronics* 9 (1999), S. 1–31

[64] Lindemann, U.: *Methodische Entwicklung technischer Produkte*. 2. Berlin, Heidelberg : Springer Verlag, 2006

[65] Lippert, H.: *Anatomie*. 4. München-Wien-Baltimore : Urban & Schwarzenberg, 1983

[66] Lovchik, C. ; Diftler, M.: A Dexterous Hand for Space. In: *Proceedings of the IEEE International Conference on Robotics and Automation.* Detroit, MI, 1999, S. 907–912

[67] Lumelsky, V. J. ; Shur, M. S. ; Wagner, S.: Sensitive Skin. In: *IEEE Sensors Journal* 1 (2001), Nr. 1, S. 41–51

[68] Maaroufi, A. ; Haboubi, K. ; Amarti, A. E. ; Carmona, F.: Electrical resistivity of polymeric matrix loaded with nickel and cobalt powders. In: *Journal of Material Science* 39 (2004), S. 265 270

[69] Maheshwari, V. ; Saraf, R.F.: High-Resolution Thin-Film Device to Sense Texture by Touch. In: *Science* 312 (2006), 06, S. 1501–1504

[70] Marieb, E.N.: *Essentials of human anatomy and physiology.* 8. San Francisco, CA94111 : Pearson Education, Inc. publishing as Benjamin Cummings, 2006

[71] M.E.H. Eltaib, J.R. H.: Tactile Sensing Technology for Minimal Access Surgery a Review. In: *Mechatronics* 13 (2003), S. 11631177

[72] Mei, T. ; Li, W.J. ; Ge, Y. ; Chen, Y. ; Ni, L. ; Chan, M.H.: An Integrated MEMS Three-Dimensional Tactile Sensor With Large Force Range. In: *Sensors and Actuators* 80 (2000), S. 155–162

[73] Nachtigall, W.: *Bionik: Grundlagen und Beispiele für Ingenieure und Naturwissenschaftler.* Berlin, Heidelberg : Springer Verlag, 1998

[74] Nachtigall, W.: *Das große Buch der Bionik. Neue Technologien nach dem Vorbild der Natur.* München : Deutsche Verlags-Anstalt DVA, 2003

[75] Neumann, D. ; Bechert, D. W. ; al. et: *Analyse und Bewertung zukuenftiger Technologien and Technologieanalyse Bionik.* VDI-Technologiezentrum, Düsseldorf, 1993

[76] Noda, K. ; Hoshino, K. ; Matsumoto, K. ; Shimoyama, I.: A Shear Stress Sensor for Tactile Sensing with the Piezoresistive Cantilever Standing in Elastic Material. In: *Sensors and Actuators* 127 (2006), 10, S. 295–301

[77] Ogawa, H.: The Merkel Cell as a Possible Mechanoreceptor Cell. In: *Progress in Neurobiology* 49 (1996), S. 317–334

[78] Okamura, A.M. ; Cutkosky, M.R.: Feature Detection for Haptic Exploration with Robotic Fingers. In: *The International Journal of Robotics Research* 20 (2001), 12, Nr. 12, S. 925–938

[79] Okamura, A.M. ; Smaby, N. ; Cutkosky, M.R.: An Overview of Dexterous Manipulation. In: *Proceedings of the IEEE International Conference on Robotics and Automation.* San Francisco, CA, 2000, S. 255–262

[80] Okamura, A.M. ; Turner, M.L. ; Cutkosky, M.R.: Haptic Exploration of Objects with Rolling and Sliding. In: *Proceedings of the IEEE International Conference on Robotics and Automation.* Albuquerque, NM, 1997, S. 2485–2490

[81] Pocock, G. ; Richards, C.D.: *Human Physiology.* 2. New York : Oxford University Press, 2004

[82] Potdar, A.: *Modeling and Design of Soft Fingertips of a Dexterous Robot Hand.* Duisburg, University of Duisburg Essen, Diplomarbeit, 03 2007

[83] Pramanik, P.K. ; Khastagir, D. ; Saha, T.N.: Effect of extensional strain on the resistivity of electrically conductive nitrile-rubber composites filled with carbon filler. In: *Journal of Material Science* 28 (1993), S. 3539–3546

[84] Princy, K.G. ; Joseph, R. ; Kartha, C.S.: Studies on Conductive Silicone Rubber Compounds. In: *Journal of Applied Polymer Science* 69 (1998), S. 10431050

[85] Qian, K. ; Chen, T. ; Yan, B. ; Lin, Y. ; Xu, D. ; Sun, Z. ; Cai, B.: Simulation and fabrication of carbon nanotubes field emission pressure sensors. In: *Journal of Applied Surface Science* 255 (2005), 08, S. 4198–4201

[86] Rocha, J.G. ; Santos, C. ; Cabral, J.M. ; Lanceros-Mendezt, S.: 3 Axis Capacitive Tactile Sensor and Readout Electronics. In: *Proceedings of the International Smposium on Industrial Electronics 2006.* Montreal, Quebec, Canada, 2006, S. 2767–2772

[87] Rossi, D. D. ; Carpi, F. ; Scilingo, E.P.: Polymer Based Interfaces as Bioinspired Smart Skins. In: *Advances in Colloid and Interface Science* 116 (2005), S. 165–178

[88] Ruschau, G.R. ; Yoshikawa, S. ; Newnham, R.E.: Resistivities of conductive composites. In: *Journal of Applied Physics* 72 (1992), 08, Nr. 3, S. 953–959

[89] Saal, H. *Artificial Skin: Final Report, internal DLR report.* 08 2006

[90] Sau, K.P. ; Khastgir, D. ; Chaki, T.K.: Electrical Conductivity of Carbon Black and Carbon Fibre Filled Silicone Rubber Composites. In: *Die Angewandte Makromolekulare Chemie* 258 (1998), S. 11–17

[91] Sau, K.P. ; T.K. Chaki, D. K.: Conductive rubber composites from different blends of ethylenepropylenediene rubber and nitrile rubber. In: *Journal of Material Science* 32 (1997), S. 5717–5724

[92] Schmidt, R.F. ; (Eds.), H.G. S.: *Neuro- und Sinnesphysiologie.* 5. Heidelberg : Springer Medizin Verlag, 2006

[93] Schulz, S.: *Konzept einer neuen Adaptiv-Hand-Prothese auf der Basis flexibler Fluidaktoren*, Universitaet Karlsruhe and Germany, Diss., 2003

[94] Shinoda, H. ; Matsumoto, K. ; Ando, S.: Tactile sensing based on acoustic resonance tensor cell. In: *Proceedings of International Conference on Solid State Sensors and Actuators.* Chicago, 1997, S. 129–132

[95] Silbernagel, S. ; Despopoulos, A.: *Taschenatlas der Physiologie.* 5. Stuttgart : Georg Thieme Verlag, 2001

[96] Soares, B.G. ; Gubbels, F. ; Jerome, R. ; Teyssie, P. ; Vanlathem, E. ; Deltour, R.: Electrical conductivity in carbon black-loaded polystyrene-polyisoprene blends. Selective localization of carbon black at the interface. In: *Polymer Bulletin* 35 (1995), S. 223–228

[97] Someya, T. ; Sekitani, T. ; Iba, S. ; Kato, Y. ; Kawaguchi, H. ; Sakurai, T.: A Large Area, Flexible Pressure Sensor Matrix with Organic Field-Effect-Transistors for Artificial Skin Applications. In: *Proceedings of the National Academy of Sciences of the USA* (2004), 12

[98] Stricker, H.: *Bionik in der Produktentwicklung unter Berücksichtigung menschlichen Verhaltens*, Technische Universität München, Germany, Diss., 03 2006

[99] Struempler, R. ; Glatz-Reichenbach, J.: FEATURE ARTICLE - Conducting Polymer Composites. In: *Journal of Electroceramics* 3/4 (1999), S. 329–346

[100] Tada, Y. ; Hasoda, K. ; Yamasaki, Y. ; Asada, M.: Sensing the Texture of Surfaces by Anthropomorphic Soft Fingertips with Multi-Modal Sensors. In: *Proceedings of the IEEE International Conference Intelligent Robots and Systems.* Las Vegas, NE, 2003, S. 31–35

[101] Tegin, J. ; Wikander, J.: Tactile Sensing in Intelligent Robotic Manipulation - A Review. In: *Industrial Robot: An International Journal* 32 (2005), Nr. 1, S. 64–70

[102] Tiezzi, P. ; Vassura, G. ; Biagiotti, L. ; Melchiorri, C.: Nonlinear Modeling and Identification of Hemispherical Soft Pads for Robotic Manipulators. In: *Proceedings of IDETC/CIE.* Long Beach, CA, 2005, S. 1–10

[103] Tomanek, A.: *Silicone & Technik.* 1. Munich, Viena : Carl Hanser Verlag, 1990

[104] Trulsson, M.: Mechanoreceptive Afferents in the Human Sural Nerve. In: *Experimental Brain Research* 137 (2001), S. 111–116

[105] Ueda, J. ; Ishida, Y. ; Kondo, M. ; Ogasawara, T.: Development of the NAIST-Hand with Vision-based Tactile Fingertip Sensor. In: *Proceedings of the IEEE International Conference on Robotics and Automation.* Barcelona, Spain, 2005, S. 2343–2348

[106] Utracki, L.A.: *Polymer Alloys and Blends.* 1. Munich, Viena : Carl Hanser Verlag, 1990

[107] Vaccaro, M. ; Pergolizzi, S. ; Mondello, M.R. ; Santoro, G. ; Cannavò, S.P. ; Guarneri, B. ; Magaudda, L.: The Dermoepidermal Junction in Psoriatic Skin as Revealed by Scanning Electron Microscopy. In: *Arch Dermatological Research* 291 (1999), 03, S. 396 399

[108] Weddell, G. ; Miller, S: Cutaneous Sensibility. In: *Annual Reviews of Neuroscience* 24 (1962), S. 199–222

[109] Weiss, K. ; Wörn, H.: The Working Principle of Resistive Tactile Sensor Cells. In: *Proceedings of the IEEE International Conference on Mechatronics and Automation 2005.* Niagara Falls, Canada, 2005, S. 471–476

[110] Wessling, B.: Electrical Conductivity in Heterogeneous Polymer Systems: Further Experimental Evidence for a Phase Transition at the Critical Volume Concentration. In: *Polymer Engineering and Science* 31 (1991), 08, Nr. 16, S. 1200–1206

[111] Westling, G. ; Johansson, R.S.: Responses in Glabrous Skin Mechanoreceptors During Precision Grip in Humans. In: *Experimental Brain Research* 66 (1987), S. 128–140

[112] Wintermantel, E. ; Ha, S.-W.: *Medizintechnik mit biokompatiblen Werkstoffen und Verfahren.* 3. Berlin : Springer, 2002

[113] Wisitsoraat, A. ; Patthanasetakul, V. ; Lomas, T. ; Tuantranont, A.: Low Cost Thin Film Based Piezoresistive MEMS Tactile Sensor. In: *Sensors and Actuators A* (2006), 10

[114] Yamada, K. ; Cutkosky, M.R.: A Sensor Skin Using Wire-Free Tactile Sensing Elements Based on Optical Connection. In: *IEEE, 1050-4729/94* (1994), S. 3550–3557

[115] Yamada, K. ; Goto, K. ; Nakajima, Y. ; Koshida, N.: A Sensor Skin Using Wire-Free Tactile Sensing Elements Based on Optical Connection. In: *Science* 233 (2002), 08, S. 131–134

[116] Zacchi, V. ; Soranzo, C. ; Cortivo, R. ; Radice, M. ; Brun, P. ; Abatangelo, G.: In vitro engineering of human skin-like tissue. In: *Journal of Biomedical Material Research* 40 (1997), S. 187–194

[117] Zerbst, E.: *Bionik: Biologische Funktionsprinzipien und ihre technische Anwendung.* Stuttgart : Teubner, 1987

[118] Zhang, J. ; Feng, S.: Effect of Crosslinking on the Conductivity of Conductive Silicone Rubber. In: *Journal of Applied Polymer Science* 89 (2003), S. 3471–3475

[119] Zhang, J. ; Feng, S. ; Ma, Q.: Kinetics of the Thermal Degradation and Thermal Stability of Conductive Silicone Rubber Filled with Conductive Carbon Black. In: *Journal of Applied Polymer Science* 89 (2002), S. 1548–1554

[120] Zucolotto, V. ; Avlyanov, J. ; Mattoso, L.H.C.: Elastomeric Conductive Composites Based on Conducting PolymerModified Carbon Black. In: *Polymer Composites* 25 (2004), 12, Nr. 6, S. 617–621

List of Figures

10 Appendix

The mathematical model of [88] is presented in abbreviated form:

According to this model the resulting resistance consists of constriction resistivity, tunnelling resistivity and the resistivity resulting from the varying contact spot area. The constriction resistivity R_{cr} describes the effects at the contact point if two conductive spheres meet. Contrary to the expectation, that R_{cr} is proportional to the area of the contact spot, it has been shown that R_{cr} is inversely proportional to the diameter d of the contact area:

$$R_{cr} = \frac{\rho_i}{d} \tag{4}$$

where ρ_i represents the intrinsic resistivity and d the diameter of the contact spot. This relation results from the superposition of effects of ohmic conduction and electric fields. Important for the constriction resistance is the size of the conductive particles D and the relationship of

$$\frac{D}{d} \tag{5}$$

For ratios > 10 very high R_{cr} result even if physical contact between the particles is maintained. But the resistivity is not only determined by the aforementioned resistances but also by effects like quantum tunnelling. The cast in carbon black particles can be surrounded completely with a thin layer of insulation polymer matrix material. Thus two neighboring conductive spheres are separated by an insulating layer of varying thickness. According to classical mechanics the altering of conductive particles and surrounding insulating matrix material can be referred to as serial connection of conductors with high and low resistance. As the single resistances of the matrix layers are high a resulting very high resistivity between the surfaces would be expected. This is not observed in real polymers filled with conductive particles. A possible reason could be the effect of quantum-mechanical tunnelling. If the separating layer shows a thickness of $100\mathring{A}$ or less quantum-mechanical tunnelling becomes possible. The probability that an electron does not surmount but tunnel through a potential barrier is proportional to the thickness, and the relative dielectric permittivity of the separating

film and the work function of the conductor. Surprisingly the resistance of the separating film is of no influence to the probability of quantum-tunnelling. It has been shown that the tunnelling resistance is inversely proportional to the contact area a.

$$R_t = \frac{\rho_t}{a} \tag{6}$$

Therefore the resistance of a contact R_c between neighboring particles is the sum of constriction resistance R_{cr} and the tunnelling resistance R_t:

$$R_c = \frac{\rho_i}{d} + \frac{\rho_t}{a} \tag{7}$$

As, for spherical particles and circular contact areas,

$$a = \frac{d^{\,2} \cdot \pi}{4} \tag{8}$$

both R_{cr} and R_t depend on the contact spot area, which itself depends on the applied external force. As the conductive filler particles are not to be treated as rigid, their deformation under external force is taken into account in the mathematical model.
Two types of deformation are possible: elastic (reversible) and plastic (irreversible). Former studies have shown that the strains required for significant reduction of the constriction resistance are higher than the elastic yield strain, and thus both, elastic and plastic deformation of the filler particles are expected [88].
For a certain force F the plastic deformation is limited by the contact hardness H

$$a = \frac{F}{H} \tag{9}$$

For elastic deformation the contact surface is approximated as:

$$a = 2.43 \left(\frac{F \cdot D}{E} \right)^{\frac{2}{3}} \tag{10}$$

Where E represents the elastic modulus of the particles. As the different types of deformation do not occur independently within the presented model this is mapped via an empirical term ξ ranging from 0.2 (only elastic deformation) to 0.7 (only plastic deformation). According to the authors $\xi = 0.7$ is applicable for the combined deformation in most systems. Thus the contact area can be described as:

$$a = \frac{\xi \cdot F}{H} \tag{11}$$

With this assumption the contact resistance can be represented by

$$R_{c\ (plastic)} = 0.89 \cdot \rho_i \left(\frac{\xi \cdot H}{F} \right)^{\frac{1}{2}} + \rho_t \cdot \xi \frac{H}{F} \tag{12}$$

$$R_{c\ (elastic)} = 0.57 \cdot \rho_i \left(\frac{E}{F \cdot D} \right)^{\frac{1}{3}} + 0.26 \cdot \rho_t \left(\frac{E}{F \cdot D} \right)^{\frac{2}{3}} \tag{13}$$

Figure 57: Collin twin screw extruder

Figure 58: Battenfeld MicroSystem 50

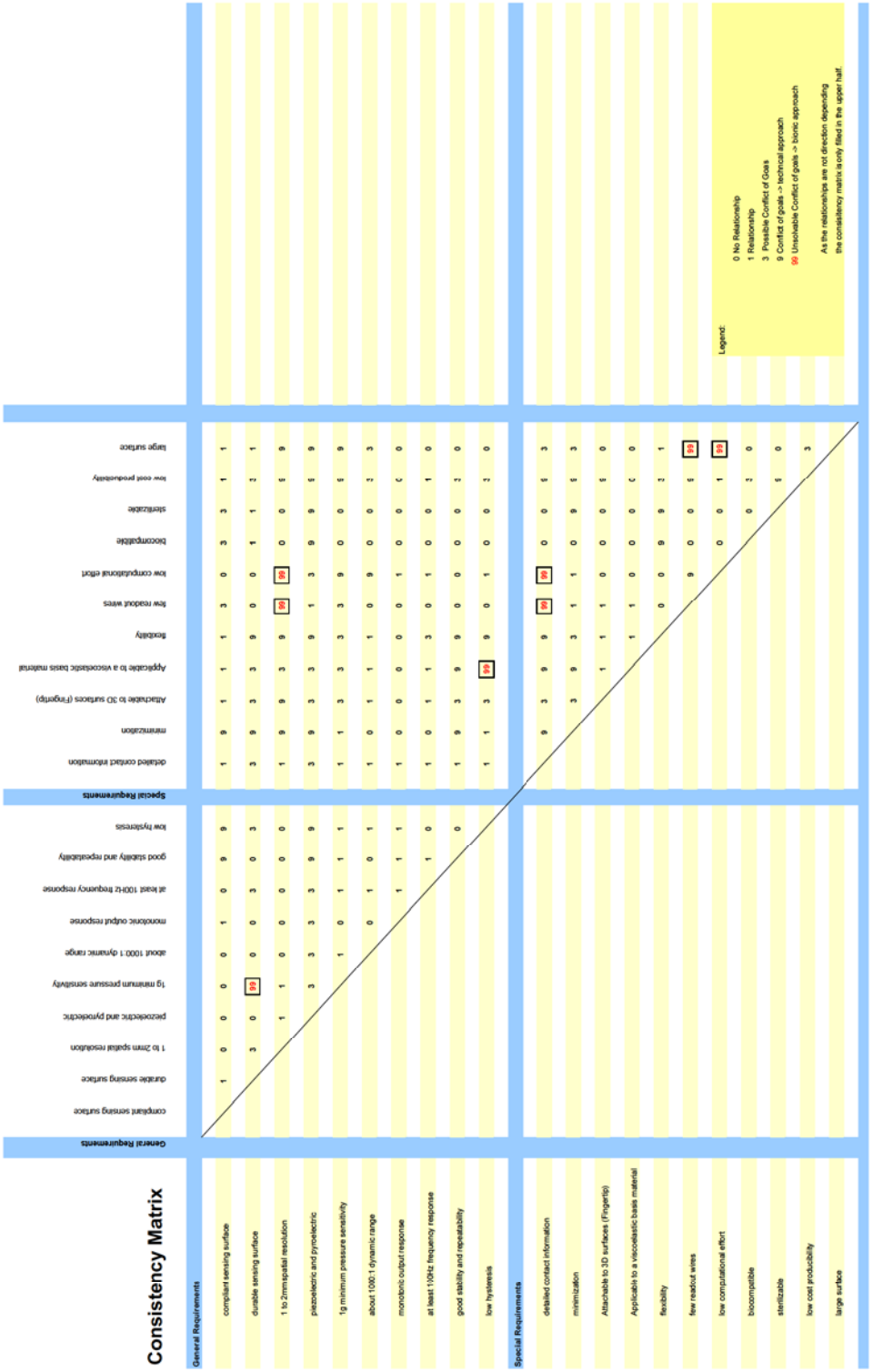

Figure 59: Consistency matrix

Rating Matrix	Rating	Technical Feasibility	weighting	Weighted Feasibility	Benefit	weighting	Weighted benefit	Effort	weighting	Weighted effort	Time frame, short-term, long-term	Sum	Realization
Bioinspired approaches													
exchangeable protective layer		3	4	12	3	3	9	3	2	6	9	36	9
multi-layer composition		1	4	4	9	3	27	1	2	2	3	36	3
combination of different sensor types		1	4	4	9	3	27	1	2	2	3	36	9
anisotropic sensing properties		1	4	4	3	3	9	1	2	2	1	16	1
arrangement of sensors in different depth		1	4	4	9	3	27	1	2	2	3	36	9
measurement of pressure and strain		1	4	4	9	3	27	1	2	2	3	36	9
generation of an proportional electrical signal		1	4	4	1	3	3	1	2	2	3	12	3
encoding of the signal to a frequency signal		1	4	4	3	3	9	1	2	2	1	16	3
artificial papillary structure		1	4	4	3	3	9	1	2	2	1	16	1
overlapping receptive fields		3	4	12	3	3	9	3	2	6	3	30	9
labeling of the sensory channel		1	4	4	3	3	9	1	2	2	1	16	1
convergence		1	4	4	9	3	27	1	2	2	1	34	3
divergence		1	4	4	3	3	9	1	2	2	1	16	3
virtual clusters of sensory cells		1	4	4	9	3	27	3	2	6	9	46	9
distributed artificial nerve fibers		1	4	4	9	3	27	1	2	2	9	42	9
superficial sensor		1	4	4	9	3	27	1	2	2	1	34	9
"dermal" sensor		1	4	4	9	3	27	1	2	2	1	34	9

Legend:

Feasibility
- 0 No technical feasibility
- 1 Sphisticated
- 3 State of the art
- 9 Trivial

Benefit
- 0 No benefit
- 1 Low benefit
- 3 considerable benefit
- 9 High benefit

Effort
- 0 Disproportional effort
- 1 Considerable effort
- 3 Low effort
- 9 No effort

Time frame
- 0 Infinite
- 1 Long-term, 5 years
- 3 Medium-term, 2 years
- 9 Short-term, 3 month

Realization
- 0 No
- 1 Long-term, 5 years
- 3 Medium-term, 2 years
- 9 Within this study

Figure 60: Rating matrix

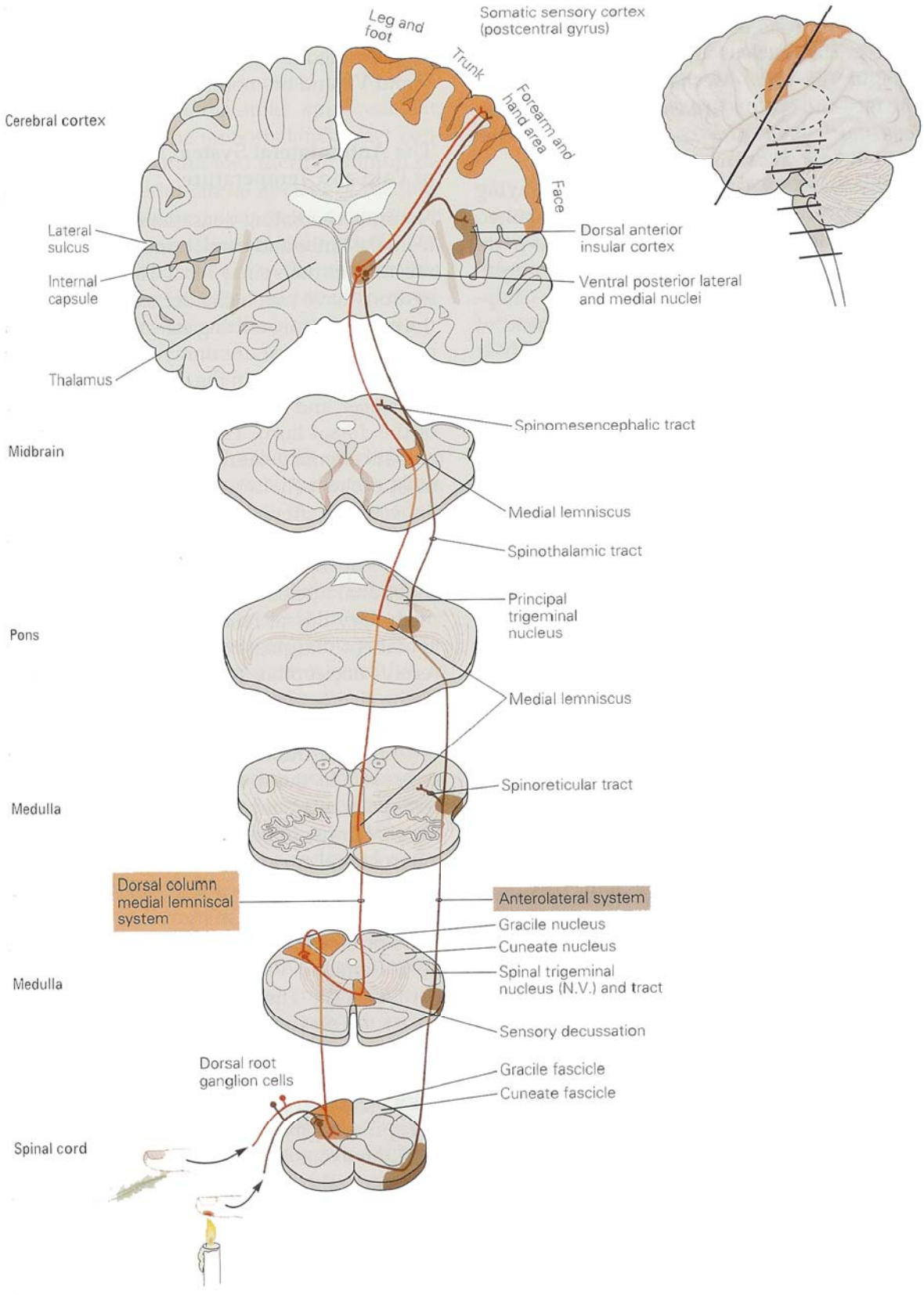

Figure 61: Signal propagation from skin to cortex

Figure 62: Framework

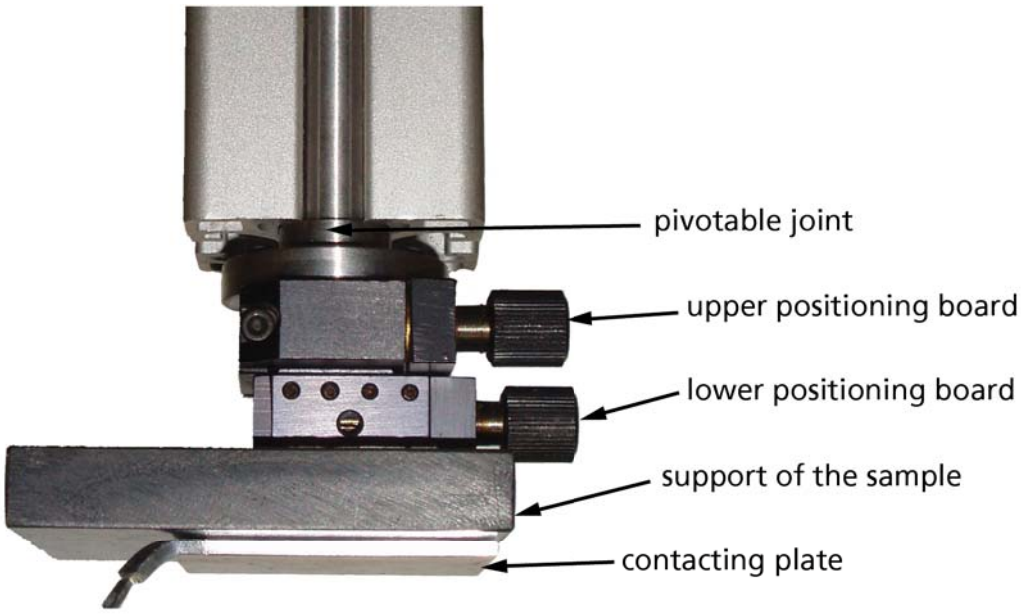

Figure 63: Support of the sample

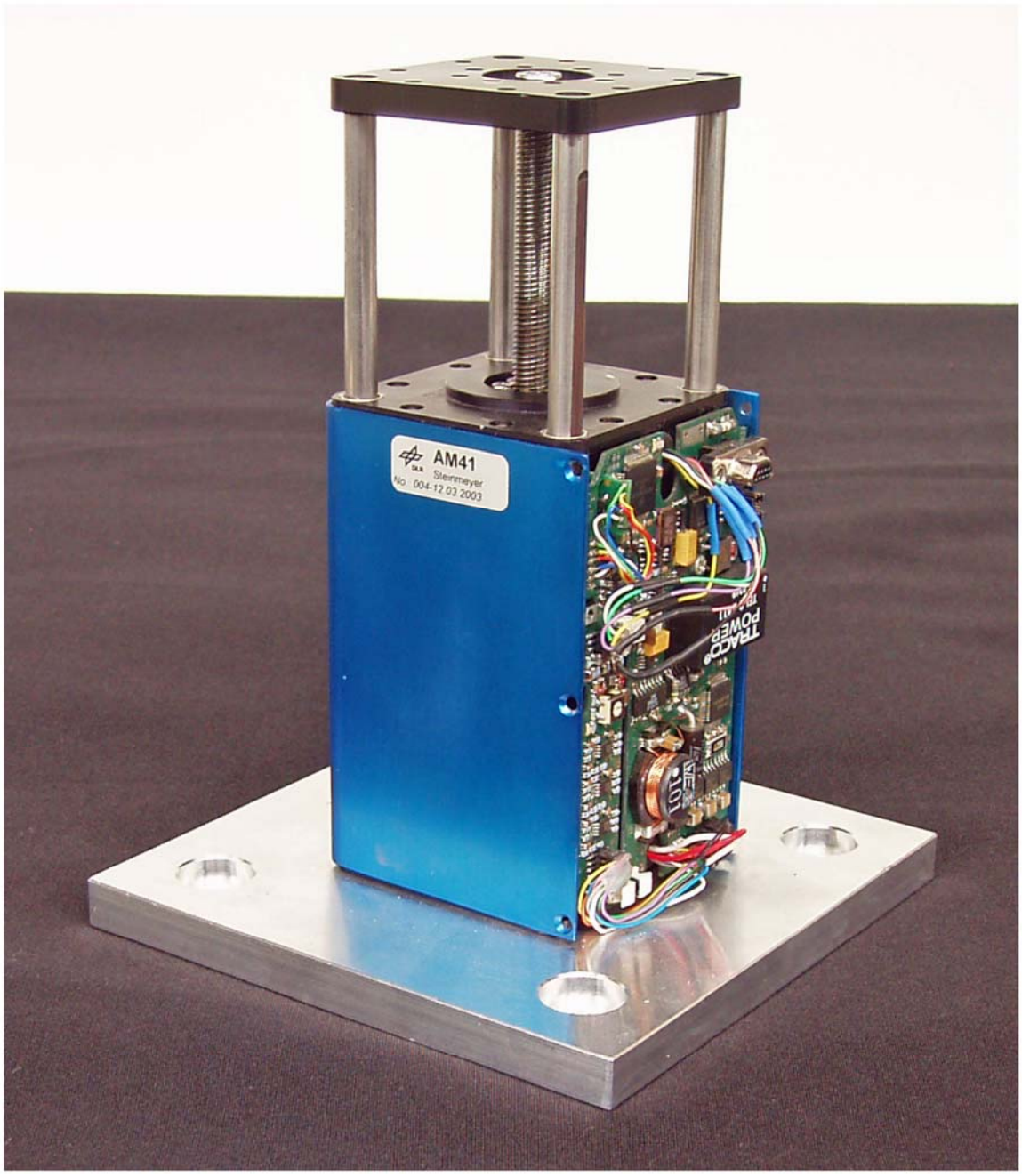

Figure 64: Linear motor

Figure 65: Optical force torque sensor